UNIVERSIDADE ESTADUAL DE
CAMPINAS

Instituto de Física
“Gleb Wataghin”

MELISSA MENDES SILVA

A cosmological model inspired on a quark-gluon plasma

Um modelo cosmológico inspirado em um plasma de quark-gluons

Campinas
2017

Melissa Mendes Silva

A cosmological model inspired on a quark-gluon plasma

Um modelo cosmológico inspirado em um plasma de quark-gluons

Dissertação apresentada ao Instituto de Física "Gleb Wataghin" da Universidade Estadual de Campinas como parte dos requisitos exigidos para a obtenção do título de Mestra em Física.

Dissertation presented to the Institute of Physics "Gleb Wataghin" of the University of Campinas in partial fulfillment of the requirements for the degree of Master in Physics.

Supervisor/Orientador: Prof. Dr. Donato Giorgio Torrieri

Este exemplar corresponde à versão final da Dissertação defendida pela aluna Melissa Mendes Silva e orientada pelo Prof. Dr. Donato Giorgio Torrieri.

Campinas

2017

Agência(s) de fomento e nº(s) de processo(s): CNPq, 132657/2015-5; ELAP
ORCID: https://orcid.org/0000-0002-5250-0723

Ficha catalográfica
Universidade Estadual de Campinas
Biblioteca do Instituto de Física Gleb Wataghin
Lucimeire de Oliveira Silva da Rocha - CRB 8/9174

Mendes, Melissa, 1994-
M522c A cosmological model inspired on a quark-gluon plasma / Melissa Mendes Silva. – Campinas, SP : [s.n.], 2018.

Orientador: Donato Giorgio Torrieri.
Dissertação (mestrado) – Universidade Estadual de Campinas, Instituto de Física Gleb Wataghin.

1. Yang-Mills, Teoria de. 2. Universo inflacionário. 3. Transição de deconfinamento. I. Torrieri, Donato Giorgio, 1975-. II. Universidade Estadual de Campinas. Instituto de Física Gleb Wataghin. III. Título.

Informações para Biblioteca Digital

Título em outro idioma: Um modelo cosmológico inspirado em um plasma de quark-gluons
Palavras-chave em inglês:
Yang-Mills theory
Inflationary universe
Deconfinement transition
Área de concentração: Física
Titulação: Mestra em Física
Banca examinadora:
Donato Giorgio Torrieri [Orientador]
José Ademir Sales de Lima
Pedro Cunha de Holanda
Data de defesa: 27-02-2018
Programa de Pós-Graduação: Física

MEMBROS DA COMISSÃO JULGADORA DA DISSERTAÇÃO DE MESTRADO DE **MELISSA MENDES SILVA – RA 118166** APRESENTADA E APROVADA AO INSTITUTO DE FÍSICA "GLEB WATAGHIN", DA UNIVERSIDADE ESTADUAL DE CAMPINAS, EM 27 / 02 / 2018.

COMISSÃO JULGADORA:

- Prof. Dr. Donato Giorgio Torrieri – Orientador – IFGW/UNICAMP
- Prof. Dr. José Ademir Sales de Lima – IAG/USP
- Prof. Dr. Pedro Cunha de Holanda – IFGW/UNICAMP

OBS.: Informo que as assinaturas dos respectivos professores membros da banca constam na ata de defesa já juntada no processo vida acadêmica do aluno.

CAMPINAS
2018

To my past self, for all the time and energy invested and the hard decisions made.
To my future self, for the constant motivation and kind dreams. But mainly for my present self.
I am proud of us.

Acknowledgements

We acknowledge the support from the Brazilian federal agency CNPq, by the process $132657/2015-5$, that financed this research from March 2015 to October 2016. We also acknowledge the support from the Canadian agency Global Affairs Canada through its legal title: the Department of Foreign Affairs, Trade and Development (DFATD), by the concession of an ELAP scholarship that financed this research from October 2016 to February 2017. The institutions University of Campinas (Campinas/BR) and McGill Univeristy (Montreal/CA), that hosted this student and her supervisors, are also to be thanked.

For the trust, teachings, utter support and access to his vast network of researchers, I thank my Master's supervisor, prof. Giorgio Torrieri. I also thank prof. Charles Gale and prof. Sangyong Jeon for the warm welcome to a very cold country.

No thanks will ever be enough for the unconditional support, love and understanding provided by my family and friends. Being physically present or not, you are all always with me and all my achievements are also yours. For lack of space I refrain from writing your names but as my heart knows no limits, the memories of interminable phone calls, wild dancing in the kitchen, a five-hour-long kiss and an extraordinary trip to China shall remain with me forever. I feel enormously blessed for having you in my life.

Il y a quelque chose de plus puissant
que la force brutale des baïonettes: c'est
l'idée dont le temps est venu et l'heure est sonée

Gustave Aimard. Les Francs Tireurs. Paris: Amyot. pp. 68.

Resumo

Nós mostramos que diversos ingredientes cruciais para o Modelo Padrão Cosmológico, como Inflação e Matéria Escura, podem ter uma origem comum em uma teoria de Yang-Mills desacoplada do Modelo Padrão das Partículas Elementares. Vários aspectos da teoria de Yang-Mills em temperatura finita, em particular o comportamento não-trivial da viscosidade volumétrica com a temperatura, têm o potencial de fornecer um candidato para a matéria escura, na forma de partículas de glueballs, e de gerar Inflação com uma transição de deconfinamento.

Nessa dissertação, nós resolvemos as equações de Friedmann utilizando a equação de estado de Yang-Mills $SU(N_c)$ e o comportamento conjecturado da viscosidade volumétrica, com parâmetro de quebra de simetria conforme e número de cores genéricos. Nós calculamos o número de efoldings produzido nos cenários investigados e checamos a existência de uma transição suave no fim do período Inflacionário. Um caso viável é detalhado.

Palavras-chave: Teoria de Yang-Mills, Universo inflacionário, Transição de deconfinamento.

Abstract

We show that several ingredients crucial to the Standard Cosmological Model, such as Inflation and Dark Matter, could have a common origin in a Yang-Mills theory decoupled from the Standard Model of Particle Physics. Several aspects of finite temperature Yang-Mills theory, in particular the non-trivial behavior of bulk viscosity with temperature, have the potential to provide a candidate for dark matter, in the form of glueball particles, and to generate Inflation with a deconfinement transition.

In this thesis, we solve the Friedmann equations using the $SU(N_c)$ Yang-Mills equation of state and conjectured bulk viscosity behaviour, with generic conformal symmetry breaking parameter and number of colors. We calculate the number of efoldings generated in the scenarios investigated and we check the existence of a smooth transition at the end of the Inflationary period. A viable case is detailed.

Keywords: Yang-Mills theorie, Inflationary universe, Deconfinement transition.

Contents

Introduction

The Standard Model of Particle Physics describes all elementary particles and their interactions through the Strong, Weak and Electromagnetic forces. It has been extremely successful in explaining phenomena from the microscopical to the galatic scales, from the Early times, few seconds after the Big Bang, to nowadays. However, the recent discoveries of dark matter and dark energy, unpredicted and unexplained by the Standard Model, have led to the suspicion that a more fundamental theory of Particle Physics is yet to be discovered.

Many theories beyond the Standard Model have been proposed aiming to complete our picture of the understanding of nature. Although many of these theories dedicate themselves to the proposal of candidates for dark matter and the unification of the gravitation with the remaining forces, few theories attempt to address another important issue of the Standard Model: the elusive nature of the Inflaton. The Inflaton is a scalar field assumed to permeate the whole Universe and be responsible for the Inflationary period in the Early Universe. Later, its oscillations accounted for the production of all barionic matter in the Universe, in a process known as *reheating*. Despite its predictions having been indirectly confirmed through observational data, many open questions remain for this model, for example, the exact format of this field or how to falsify this theory.

In this work, we present an extension to the Standard Model of Particle Physics that explains the Inflationary period of the Early Universe without recurring to a scalar field. We hypothesize the existence of a Yang-Mills $SU(N_c)$ fluid, non-coupled to the standard matter, whose deconfinement transition at a critical temperature T_c generates this exponential expansion of the scale factor of the Universe. Yang-Mills theories are generalizations of the mathematical formulation of the *Quantum Chromodynamics*, or QCD, the theory of the strong forces. This theory presents several distinguished proprieties, such as color confinement and asymptotic freedom. In particular, at the deconfinement transition, a plasma of free elementary particles, such as quarks and gluons, transforms into a hadronic gas of composed particles, such as protons and neutrons. It is our hypothesis that a transition like this could generate the Inflationary period of the universe and the hadronic $SU(N_c)$ particles formed could be the dark matter particles.

In chapter 1, we introduce some useful results from General Relativity to derive the Friedmann equations, that determine the evolution of the universe with time. We study their formulation with perfect and imperfect fluids and we detail the Inflationary model, its justification and current formulation. In chapter 2, we review Yang-Mills theories starting from QCD and we introduce techniques such as lattice QCD and the large-N limit to study their non-perturbative limit. This is the basis for our inflationary model, introduced in chapter 3. In this chapter we motivate our model, describe it and find the new equations of state for the primordial plasma of

the Early Universe. We also solve the Friedmann equations and calculate the number of efolds for some configurations of the free parameters of the model. A viable scenario for the description of our universe is found and discussed.

1 Understanding Friedmann's equations

In this chapter, we derive Friedmann's equations from Einstein's equations and a specific metric, one that describes an isotropic and homogeneous universe. We start with a generic energy-momentum tensor and then analyze the specific cases where this tensor represents an ideal fluid (section 1.1) and a non-ideal fluid (section 1.2). We interpret how these scenarios differ in determining the evolution of the universe with time and introduce the principal features of the ΛCDM model, the *Standard Cosmological Model*, specially its inflationary period. We assume the reader is familiarized with Lorentzian Geometry, General Relativity and Fluid Mechanics.

We start by introducing some useful quantities. Given that:

$$ds^2 = g_{\mu\nu}dx^\mu dx^\nu \quad \text{and} \quad g^{\mu\nu}g_{\nu\sigma} = \delta^\mu_\sigma, \tag{1.1}$$

we have the Christoffel symbols $\Gamma^\lambda_{\mu\nu}$, determined from the metric $g_{\mu\nu}$ by:

$$\Gamma^\lambda_{\mu\nu} = \frac{1}{2}g^{\lambda\sigma}(\partial_\mu g_{\nu\sigma} + \partial_\nu g_{\sigma\mu} - \partial_\sigma g_{\mu\nu}) \tag{1.2}$$

They help us to find the Ricci tensor $R_{\mu\nu}$ from the connection $R^\rho_{\sigma\mu\nu}$ (the Riemann tensor). The Ricci tensor, in turn, determines the Ricci scalar R:

$$\begin{aligned} R^\rho_{\sigma\mu\nu} &= \partial_\mu\Gamma^\rho_{\nu\sigma} - \partial_\nu\Gamma^\rho_{\mu\sigma} + \Gamma^\rho_{\mu\lambda}\Gamma^\lambda_{\nu\sigma} - \Gamma^\rho_{\nu\lambda}\Gamma^\lambda_{\mu\sigma}, \\ R^\lambda_{\mu\lambda\nu} &= R_{\mu\nu}, \\ R &= g^{\mu\nu}R_{\mu\nu} \end{aligned} \tag{1.3}$$

Having all these quantities for a specific metric in a determined set of coordinates, one can solve Einstein's equations:

$$R_{\mu\nu} - \frac{1}{2}Rg_{\mu\nu} + \Lambda g_{\mu\nu} = 8\pi G T_{\mu\nu}, \tag{1.4}$$

where Λ represents a cosmological constant and $T_{\mu\nu}$ stands for the energy-momentum tensor. Here G is the gravitational constant and we're using units such that $\hbar = c = k_b = 1$.

The following metric in spherical coordinates was proposed by Friedmann and Lemaître independently and then further studied by Robertson and Walker. Its model is constantly referred to by the FRLW metric:

$$ds^2 = -dt^2 + a^2(t)\left[\frac{dr^2}{1-kr^2} + r^2\left(d\theta^2 + \sin^2\theta d\phi^2\right)\right] \tag{1.5}$$

This represents a space-time where the time coordinate is t and the space coordinates are r, θ and ϕ. The term $a(t)$, also called the *scale factor*, determines how these three last coordinates change with time. Their evolution is completely specified by this quantity and the curvature of the manifold k, therefore, this space-time is spatially isotropic and homogeneous.

This structure reflects our universe's and among several experiments that investigated this, we highlight the Planck telescope, which measured CMB (cosmic microwave background) radiation from 2009 to 2013. It was able to determine the degree of isotropy and homogeneity of the early universe with accuracy of 0.1 percent as well as its flatness, with accuracy of 0.5 percent [1].

Because this space-time evolves with time, it does not represent a maximally symmetric universe, but one that can be decomposed in 3D space-like slices, each one maximally symmetric. This immensely simplifies the calculations of the quantities defined above. To find them, we first identify the metric tensor.

From equation (1.1) and remembering Einstein's sum convention (repeated indexes on top and bottom of a expression are to be summed), we identify:

$$g_{\mu\nu} = \begin{pmatrix} -1 & 0 & 0 & 0 \\ 0 & \dfrac{a^2}{1-kr^2} & 0 & 0 \\ 0 & 0 & a^2r^2 & 0 \\ 0 & 0 & 0 & a^2r^2\sin^2\theta \end{pmatrix}$$

Then, we find, from equation (1.2), all non-zero Christoffel symbols. Due to symmetry properties (such as $\Gamma^{\alpha}_{\beta\gamma} = \Gamma^{\alpha}_{\gamma\beta}$), they can all be found from this list:

$$\begin{aligned}
\Gamma^0_{11} &= \frac{a\dot{a}}{1-kr^2} & \Gamma^2_{12} &= \frac{1}{r} \\
\Gamma^0_{22} &= a\dot{a}r^2 & \Gamma^2_{33} &= -\sin\theta\cos\theta \\
\Gamma^0_{33} &= a\dot{a}r^2\sin^2\theta & \Gamma^3_{23} &= \cot\theta \\
\Gamma^1_{11} &= \frac{kr}{1-kr^2} & \Gamma^1_{01} &= \Gamma^2_{02} = \Gamma^3_{03} = \frac{\dot{a}}{a} \\
\Gamma^1_{22} &= -r(1-kr^2) & \Gamma^3_{13} &= \frac{1}{r} \\
\Gamma^1_{33} &= -r(1-kr^2)\sin^2\theta
\end{aligned}$$

We then find the Ricci tensor:

$$R_{\mu\nu} = \begin{pmatrix} -\frac{3\ddot{a}}{a} & 0 & 0 & 0 \\ 0 & \frac{a\ddot{a} + 2\dot{a}^2 + 2k}{1 - kr^2} & 0 & 0 \\ 0 & 0 & r^2(a\ddot{a} + 2\dot{a}^2 + 2k) & 0 \\ 0 & 0 & 0 & r^2(a\ddot{a} + 2\dot{a}^2 + 2k)\sin^2\theta \end{pmatrix}$$

As well as the Ricci scalar, both from the equations (1.3) :

$$R = g^{00}R_{00} + g^{11}R_{11} + g^{22}R_{22} + g^{33}R_{33} = 6\left(\frac{\ddot{a}}{a} + \frac{\dot{a}^2}{a^2} + \frac{k}{a^2}\right)$$

Plugging this in the expression of the Einstein's tensor,

$$G_{\mu\nu} = R_{\mu\nu} - \frac{1}{2}Rg_{\mu\nu}, \tag{1.6}$$

$$G_{\mu\nu} = \begin{pmatrix} 3\left(\frac{\dot{a}}{a}\right)^2 + 3\frac{k}{a^2} & 0 & 0 & 0 \\ 0 & \frac{-2a\ddot{a} - \dot{a}^2 - k}{1 - kr^2} & 0 & 0 \\ 0 & 0 & r^2(-2a\ddot{a} - \dot{a}^2 - k) & 0 \\ 0 & 0 & 0 & r^2\sin^2\theta(-2a\ddot{a} - \dot{a}^2 - k) \end{pmatrix}$$

Because we want this metric to solve Einstein's equations (1.4) and assuming, for now, that there's no cosmological constant, we find the energy-momentum tensor in terms of the Einstein's tensor:

$$T_{\mu\nu} = \frac{G_{\mu\nu}}{8\pi G} \tag{1.7}$$

Thus, for the metric (1.5), we have found an expression for the energy-momentum tensor without special considerations for its format. There's one other important generic relation we can find for this tensor. The energy-momentum tensor describes the energy content of the universe, therefore, it's reasonable to ask for its conservation. As we are in a Lorentzian manifold, we write this requirement as:

$$\nabla_\mu T^{\mu\nu} = 0, \tag{1.8}$$

where ∇_μ stands for a covariant derivative. Thus:

$$\nabla_\mu T^{\mu\nu} = \partial_\mu T^{\mu\nu} + \Gamma^\mu_{\mu\sigma}T^{\sigma\nu} + \Gamma^\nu_{\mu\sigma}T^{\mu\sigma} = 0 \tag{1.9}$$

The equality $\nabla_\mu G^{\mu\nu} = 0$ is equivalent to the above for a universe without cosmological constant. It is a rewritten Bianchi identity ($\nabla_\lambda R_{\rho\sigma\mu\nu} + \nabla_\rho R_{\sigma\lambda\mu\nu} + \nabla_\sigma R_{\lambda\rho\mu\nu} = 0$). Because this identity describes intrinsic symmetries of the Riemann tensor, we know it is already satisfied by the metric. However, it's interesting to explicitly state it and contrast it against this equation for a Euclidean space-time: $\partial_\mu T^{\mu\nu} = 0$.

Later, we will show how this expression (1.9) can be rewritten in terms of the components of the energy-momentum tensor. This will clarify its interpretation.

1.1 Perfect fluid energy-momentum tensor

The homogeneity and isotropy of the FLRW metric require the energy-momentum tensor to be form-invariant with respect to coordinate transformations that leave the metric form-invariant [2], equation (1.10). Therefore, T^{00} must transform as a three-scalar, T^{i0} as a three-vector and T^{ij} as a three-tensor, where we used the indexes i and j to represent spatial coordinates, thus running from 1 to 3.

$$T_{\mu\nu}(y) = T'_{\mu\nu}(y) \tag{1.10}$$

This implies that the energy-momentum tensor must have the form of:

$$T_{00} = \alpha(t) \quad T_{i0} = 0 \quad T_{ij} = g^3_{ij}\,\beta(t) \tag{1.11}$$

where $\alpha(t)$ and $\beta(t)$ are unknown functions that must depend only on t and g^3_{ij} represents the spatial part of the metric tensor. This tensor can be conveniently written as:

$$T_{\mu\nu} = (\alpha + \beta)U_\mu U_\nu + \beta g_{\mu\nu} \tag{1.12}$$

with $U^0 = 1$ and $U^i = 0$. If we take $\alpha = \rho =$ energy density and $\beta = p =$ pressure, we find that this tensor takes the form of a perfect fluid: $T_{\mu\nu} = (\rho + p)U_\mu U_\nu + p g_{\mu\nu}$. Therefore, the symmetry properties of the FLRW metric only allow energy-momentum tensors that can be written like this.

Regarding the vector $U^\mu = (1, 0, 0, 0)$, one can interpret it as follows: an isotropic and homogeneous metric in a certain reference frame gives rise to a tensor in the form of an isotropic and homogeneous fluid in a certain reference frame, thus, the reference frame of the metric and the fluid must be the same. This information is encoded in the vector U^μ, as it represents the fluid at rest in relation to those coordinates.

These specific coordinates are called comoving coordinates and the vector U^μ is the velocity four-vector. It is normalized such that:

$$g_{\mu\nu}U^\mu U^\nu = -1 \tag{1.13}$$

Replacing the energy-momentum tensor of a perfect fluid in equation (1.7) and having (1), one can find relations between the scale factor $a(t)$ and $\rho(t), p(t)$. These relations are called the Friedmann equations:

$$\begin{cases} 3\left(\dfrac{\dot{a}}{a}\right)^2 + 3\dfrac{k}{a^2} = 8\pi G\rho(t) \\ \dfrac{-2a\ddot{a} - \dot{a}^2 - k}{1-kr^2} = 8\pi G p(t)\dfrac{a^2}{1-kr^2} \\ r^2(-2a\ddot{a} - \dot{a}^2 - k) = 8\pi G p(t) a^2 r^2 \\ r^2\sin^2\theta(-2a\ddot{a} - \dot{a}^2 - k) = 8\pi G p(t) a^2 r^2 \sin^2\theta \end{cases} \tag{1.14}$$

They can be resumed to two equations, more commonly written as:

$$\begin{aligned} \left(\frac{\dot{a}}{a}\right)^2 &= \frac{8\pi G\rho(t)}{3} - \frac{k}{a^2}, \\ \frac{\ddot{a}}{a} &= -\frac{4\pi G}{3}\left(\rho(t) + 3p(t)\right) \end{aligned} \tag{1.15}$$

From those equations, one can find the evolution of the scale factor $a(t)$ with time, depending only on the energy density $\rho(t)$, pressure $p(t)$ and curvature k. It's possible to choose a normalization where $a(t)$ is dimensionless or where it has dimension of length. This happens because the metric (1.5) is invariant to transformations as:

$$\begin{aligned} a &\to \lambda^{-1}a \\ r &\to \lambda r \\ k &\to \lambda^{-2}k \end{aligned} \tag{1.16}$$

In this work, we chose to use a dimensionless scale factor, thus, r has dimensions of distance and k has dimensions of $(\text{length})^{-2}$.

Plugging the perfect fluid energy-momentum tensor in equation (1.9), we find, for $\nu = 0$, the conservation of energy equation (1.17). We keep from writing this expression for $\nu = (1, 2, 3)$, which represents the conservation of momentum equations, because those explicit equations are not very clarifying.

$$\partial_\mu T^{\mu 0} + \Gamma^\mu_{\mu\sigma}T^{\sigma 0} + \Gamma^0_{\mu\sigma}T^{\mu\sigma} = 0 \to \dot{\rho} + 3\frac{\dot{a}}{a}(\rho(t) + p(t)) = 0 \tag{1.17}$$

In most studied cases, it's possible to write $p(t) = w\rho(t)$, where w is a function that doesn't depend on time. This is called the equation of state. Note that equations (1.15 and 1.17) are not independent, they're related by Bianchi's identity. Therefore, to solve for a specific scenario (a specific w), we don't need all three equations, as they get redundant. Specially for simple cases, it suffices to solve the first equation in (1.15), also known as the first Friedmann equation. Some examples will be given later in section (1.3), where we solve Friedmann equations for matter, radiation and vacuum dominated scenarios.

1.2 Imperfect fluid energy-momentum tensor

Different from perfect fluids, imperfect fluids exhibit pressure, density and/or velocity varying considerably in distances of the order of the mean free path or times of the order of the mean free time [2]. In other words, they represent fluids whose constituents interact with each other. Thus, the easiest way to write an energy-momentum tensor for this configuration is to add a correction in the perfect fluid energy-momentum tensor, to account for the interactions:

$$T^{\mu\nu} = pg^{\mu\nu} + (p+\rho)U^\mu U^\nu + \Delta T^{\mu\nu} \tag{1.18}$$

We can model the internal structure of those fluids as blocks of particles moving in a certain direction with a specific velocity. Therefore, we expect that the correction will quantify the possibility of particles moving between blocks and of their kinetic energy being dissipated in this process. It can be shown [2] that the most generic way of writing this correction in a Lorentzian manifold is:

$$\Delta T^{\mu\nu} = -\eta H^{\mu\gamma}H^{\nu\sigma}W_{\gamma\sigma} - \chi\left(H^{\mu\gamma}U^\nu + H^{\nu\gamma}U^\mu\right)Q_\gamma - \zeta H^{\mu\nu}\frac{\partial U^\gamma}{\partial x^\gamma} \tag{1.19}$$

where

$$\begin{aligned} H^{\mu\nu} &= g^{\mu\nu} + U^\mu U^\nu, \\ W^{\mu\nu} &= \frac{\partial U^\mu}{\partial x_\nu} + \frac{\partial U^\nu}{\partial x_\mu} - \frac{2}{3}g^{\mu\nu}\frac{\partial U^\gamma}{\partial x^\gamma}, \\ Q^\mu &= \frac{\partial T}{\partial x_\mu} + T\frac{\partial U^\mu}{\partial x^\gamma}U^\gamma \end{aligned} \tag{1.20}$$

for $\chi, \eta, \zeta \geqslant 0$ and T is the temperature per particle. χ is called the coefficient of heat conduction; η is the shear viscosity coefficient, accounting for the fluid's resistance to adjacent parallel layers of fluid at different speeds; and ζ is the bulk viscosity coefficient, expressing the resistance of the

fluid to be compressed or expanded evenly. Following the same logic, $W^{\mu\nu}$ is called the shear tensor and Q^{μ} is the heat-flow vector. $H^{\mu\nu}$ is a projector tensor on the hyperplane normal to U_{μ}.

For a FLRW metric, two of the three terms in the correction are annulled. Also, because in this metric $\frac{\partial U^{\gamma}}{\partial x^{\gamma}} = 3\frac{\dot{a}}{a}$, we can rewrite equation (1.19) as:

$$\Delta T^{\mu\nu} = -\zeta H^{\mu\nu}\frac{\partial U^{\gamma}}{\partial x^{\gamma}} = -3\zeta\left(g^{\mu\nu} + U^{\mu}U^{\nu}\right)\frac{\dot{a}}{a} \tag{1.21}$$

Therefore, the complete energy-momentum tensor is:

$$T^{\mu\nu} = pg^{\mu\nu} + (p+\rho)U^{\mu}U^{\nu} - 3\zeta\frac{\dot{a}}{a}\left(g^{\mu\nu} + U^{\mu}U^{\nu}\right) = \left(p - 3\zeta\frac{\dot{a}}{a}\right)g^{\mu\nu} + \left(p - 3\zeta\frac{\dot{a}}{a} + \rho\right)U^{\mu}U^{\nu} \tag{1.22}$$

Note that it has the same form of the perfect fluid energy-momentum tensor. In fact, we can rewrite it as that tensor if we replace the original pressure for an effective pressure $p^{*} = \left(p - 3\zeta\frac{\dot{a}}{a}\right)$.

We proved in the previous section (1.2) that only tensors that can be written as (1.12) originate Friedmann equations. Thus, these equations can only be solved for the perfect fluid energy-momentum tensor and the imperfect fluid with bulk viscosity energy-momentum tensor.

All expressions we found previously, such as equations (1.15 and 1.17), remain valid if instead of writing pressure p, we use effective pressure p^{*}. So, for example, equation (1.17) becomes:

$$\partial_{\mu}T^{\mu 0} + \Gamma^{\mu}_{\mu\sigma}T^{\sigma 0} + \Gamma^{0}_{\mu\sigma}T^{\mu\sigma} = 0 \rightarrow \dot{\rho} + 3\frac{\dot{a}}{a}\left(\rho(t) + \left(p(t) - 3\zeta\frac{\dot{a}}{a}\right)\right) = 0 \tag{1.23}$$

Using the first Friedmann equation, we can replace the term $\left(\frac{\dot{a}}{a}\right)^{2}$ and rewrite equation (1.23) as:

$$\dot{\rho} + 3\rho\left(\frac{\dot{a}}{a} - 8\pi G\zeta\right) + 3p\frac{\dot{a}}{a} + 9\zeta\frac{k}{a^{2}} = 0 \tag{1.24}$$

This poses a restriction on the $a(t)$ we can have when $\zeta \neq 0$. It also highlights that, for the limit where $\zeta = 0$, $a(t)$ should behave as if it's immersed in a perfect fluid, because we recover equation (1.17). Finally, one should note that, as we are dealing with imperfect fluids, equation (1.23) doesn't represent the conservation of energy equation anymore. When $\zeta \neq 0$, we should expect dissipation of energy generated by viscosity, therefore, equation (1.23) is only one of the four expressions of Bianchi's identity, a restriction imposed on the metric tensor due to symmetries of the Riemann tensor.

1.3 Possible solutions for Friedmann equations

Let's now attempt to solve equations (1.15) assuming the universe is filled with a perfect fluid and that we can write its equation of state: $p(t) = w\rho(t)$. Thus, we have the set of equations:

$$\begin{aligned} \left(\frac{\dot{a}}{a}\right)^2 &= \frac{8\pi G\rho(t)}{3} - \frac{k}{a^2}, \\ \frac{\ddot{a}}{a} &= -\frac{4\pi G}{3}\rho(t)(1+3w), \\ 0 &= \dot{\rho} + 3\rho(t)\frac{\dot{a}}{a}(1+w) \end{aligned} \tag{1.25}$$

Integrating in time the final equation of this set, we find that:

$$\rho(t) = \rho_c \left(\frac{a}{a_c}\right)^{-3(1+w)} \Rightarrow p(t) = w\rho_c \left(\frac{a}{a_c}\right)^{-3(1+w)} \tag{1.26}$$

where ρ_c is a constant with dimension of energy density and a_c is a dimensionless constant. Note that since we chose $\hbar = c = k_b = 1$, $p(t)$ and $\rho(t)$ have the same units. With the information in (1.26), we only need a value for k to find $a(t)$, the evolution of the scale factor with time. To simplify its calculation, let's put $k = 0$, an experimentally confirmed value, as discussed in (1.1). Then, by solving the first equation of the set (1.25), we find:

$$\frac{a^{3/2(1+w)}}{\frac{3}{2}(1+w)} - \frac{a_{c_2}^{3/2(1+w)}}{\frac{3}{2}(1+w)} = \left(\frac{8\pi G}{3}\rho_c a_c^{3(1+w)}\right)^{1/2} t - \left(\frac{8\pi G}{3}\rho_c a_c^{3(1+w)}\right)^{1/2} t_c \tag{1.27}$$

where a_{c_2} and t_c are integration constants. Choosing $t_c = 0$,

$$a(t) = \left[\left(\frac{8\pi G}{3}\rho_c a_c^{3(1+w)}\right)^{1/2} \frac{3}{2}(1+w)t + a_{c_2}^{3/2(1+w)}\right]^{\frac{2}{3(1+w)}} \tag{1.28}$$

Thus, we can see that for fluids with this simple equation of state it's relatively easy to find analytic solutions for the Friedmann equations. Before exploring some fluids that satisfy this condition, let's define a very useful quantity: the number of efoldings, N. It is given by:

$$N = \int_{t_i}^{t_f} \frac{\dot{a}}{a} dt \tag{1.29}$$

It quantifies how much the scale factor varies for a given time interval. According to inflationary theories, the size of the observable universe nowadays pose an inferior limit on

this number. We will discuss this in section (1.4), for now let's find its generic expression for a perfect fluid and its equation of state. Replacing equation (1.28) in (1.29), we find:

$$\frac{\dot{a}}{a} = \frac{\frac{2}{3(1+w)} t^{-\frac{(1+3w)}{3(1+w)}}}{t^{\frac{2}{3(1+w)}}} \Rightarrow e^N = \left(\frac{t_f}{t_i}\right)^{\frac{2}{3(1+w)}} \tag{1.30}$$

Note that we put $a_{c_2} = 0$ to make the calculation easy, which represents a normalization such that $a(t = 0) = 0$. If necessary, this can be changed to more convenient values without modifying the power of t in the expression above.

Matter dominated universe

In a matter dominated universe, the fluid is collisionless and the particles are non-relativistic. Thus, $p(t) = 0 \Rightarrow w = 0$. We have, then:

$$\begin{aligned} \rho(t) &= \rho_c \left(\frac{a}{a_c}\right)^{-3}, \\ a(t) &= \left[\left(\frac{8\pi G}{3}\rho_c a_c^3\right)^{1/2} \frac{3}{2} t\right]^{\frac{2}{3}}, \\ e^N &= \left(\frac{t_f}{t_i}\right)^{\frac{2}{3}} \end{aligned} \tag{1.31}$$

The energy density $\rho(t)$ falls as a^{-3}, which suggests that the energy decreases as the number of particles is being diluted with the expansion of the universe.

Radiation dominated universe

A fluid composed mainly of radiation is formed by relativistic particles, such as photons or anything massive moving at $v \approx c$. Following the derivation of [3], an isotropic gas of those particles will behave as a perfect fluid and it will also obey:

$$T^{\mu\nu} = F^{\mu\lambda} F^{\nu}_{\lambda} - \frac{1}{4} g^{\mu\nu} F^{\lambda\sigma} F_{\lambda\sigma} \tag{1.32}$$

where $F^{\mu\nu}$ represents the electromagnetic field strength. But the trace of this tensor is null, $T^{\mu}_{\mu} = 0$, while the trace of the perfect fluid energy-momentum tensor is $T^{\mu}_{\mu} = -\rho + 3p$. Thus,

$p = \rho/3 \Rightarrow w = 1/3$. Therefore, we have:

$$\begin{aligned} \rho(t) &= \rho_c \left(\frac{a}{a_c}\right)^{-4}, \\ a(t) &= \left[\left(\frac{8\pi G}{3}\rho_c a_c^4\right)^{1/2} 2t\right]^{\frac{1}{2}}, \\ e^N &= \left(\frac{t_f}{t_i}\right)^{\frac{1}{2}} \end{aligned} \tag{1.33}$$

We are interested in these two scenarios because they provide scale factors that grow with time, thus, they are mathematically fit to describe the early universe, which is expected to expand. Although both of these scenarios could generate an expansion, it is believed that the universe after the Big Bang could not be matter dominated because of its high temperature and density. Besides, for reasons that will be discussed in section (1.4), an exponential expansion is expected, not a power law expansion. So, we present one other scenario that provide us that.

Vacuum dominated universe

In a vacuum dominated universe, we assume there is an energy that fills the empty space. Because this energy is expected to be isotropic, then the energy-momentum tensor corresponding to it must be proportional to the metric. The simplest tensor we can build in this condition is $T^{\mu\nu} = -\rho g^{\mu\nu}$.

Comparing to the perfect fluid energy-momentum tensor, $T^{\mu\nu} = pg^{\mu\nu} + (p+\rho)U^\mu U^\nu$, we must have that $p(t) = -\rho(t) \Rightarrow w = -1$. Therefore, we will have:

$$\begin{aligned} \rho(t) &= \rho_c \\ a(t) &= a_c e^{\left(\sqrt{\rho_c \frac{8\pi G}{3}} t\right)} \\ N &= \sqrt{\rho_c \frac{8\pi G}{3}}(t_f - t_i) \quad \Rightarrow e^N = e^{\left(\sqrt{\rho_c \frac{8\pi G}{3}}(t_f - t_i)\right)} \end{aligned} \tag{1.34}$$

Note that, for a perfect fluid with equation of state, this is the only case where an exponential expansion is possible. This inspired us to look for negative pressure in non-perfect fluids and check if that is a sufficient condition for this kind of evolution.

1.4 The inflationary model

The current accepted model to describe the evolution of the universe is called the *Standard Cosmological Model* or ΛCDM. Based on General Relativity and the *Standard Model*

of Particle Physics, it describes the synthesis of light elements, the formation of atoms and nuclei and the origin of CMB (cosmic microwave background) radiation, among other things. It assumes the universe was originated at the Big Bang, an event where the space-time structure was created. In this work, we're interested in the period right after the Big Bang called the "inflationary period".

Redshift measuring detected that the majority of the galaxies are receding from us, an indication that the universe is expanding. This reinforced the belief that the young universe was smaller than today's and that it began expanding right after the Big Bang. This allowed for several different scenarios, as we showed in section (1.3), that could present an expansion of some sort. Later, satellites measurements of the CMB radiation indicated that, in large scales, the early universe was extremely isotropic and homogeneous, a result also confirmed by galaxy counts measurements.

This pointed to a perfect-fluid universe from the beginning, because inhomogeneities cannot be dissolved through a power law expansion, according to General Relativity [4]. However, this assumption wasn't enough to explain why non-causal regions (regions far enough that light going from one of them wouldn't have time to reach the other one) had the same temperature to one part in 10^{-4}. This is known as the *horizon problem*.

The horizon problem

Following [4], we can estimate the number of causally disconnected regions that had to agree in temperature to generate the universe today, if the scale factor grows as a power law. We know the universe today remains highly isotropic and homogeneous, at least until the particle horizon scale $l_0 = ct_0 \approx 10^{28}$ cm. But the original size of this domain was $l_i \approx ct_0 \frac{a_i}{a_0}$, also assumed to be isotropic and homogeneous. Comparing this to the initial causal region $l_c = ct_i$,

$$\frac{l_i}{l_c} \approx \frac{t_0}{t_i}\frac{a_i}{a_0} \approx \frac{\dot{a_i}}{\dot{a_0}} \tag{1.35}$$

Estimating the initial time as Planck's time $t_p = 10^{-43}$ s, and that $a(T) \propto 1/T$, then,

$$\frac{l_i}{l_c} \approx \frac{t_0}{10^{-43}}\frac{T_0}{T_i} \approx \frac{10^{17}}{10^{-43}}\frac{1}{10^{32}} \approx 10^{28} \tag{1.36}$$

where we used that today's time $t_0 \approx 10^{17}$s and today's temperature of the CMB radiation $T_0 \approx 1$K. In estimating initial temperature, we assumed the universe was radiation dominated.

Thus, we found that $l_i \approx 10^{28} l_c$, therefore, the initial horizon was 28 orders of magnitude bigger than the initial causal horizon. Since no information travels faster than light, this means that no physical process could have occurred to smooth the temperatures in all those regions. Also, if we assume that the scale factor grows as a power law with time and that gravity

was always attractive, thus decelerating this expansion, since the Big Bang the causal horizon was always smaller than the homogeneous horizon. On the other hand, to assume all regions in the homogeneous horizon coincidentally had the same temperature to a degree of 10^{-4} seems fine-tuned.

There is still another problem with this scenario, called the flatness problem.

The flatness problem

The distribution of matter plays an important role in the evolution of the universe. Because we're assuming gravity is always attractive, the initial distribution of velocities of matter particles can determine the curvature of the universe. Again following [4], for a large spherically symmetric cloud of matter, its total energy is:

$$E^T = E_i^k + E_i^p = E_0^k + E_0^p \tag{1.37}$$

where E^k stands for kinetic energy and E^p, for potential energy. Note that the total energy is conserved. We assume the velocity of the particles is proportional to $\dot{a}$, otherwise the homogeneity of the universe would be quickly spoiled. Then,

$$E_i^k = E_0^k \left(\frac{\dot{a}_i}{\dot{a}_0}\right)^2 \Rightarrow \frac{E^T}{E_i^k} = \frac{E_0^k + E_0^p}{E_0^k}\left(\frac{\dot{a}_0}{\dot{a}_i}\right)^2 \tag{1.38}$$

For $E^k \approx |E^p|$ and, using a result from the previous subsection $\frac{\dot{a}_0}{\dot{a}_i} \approx 10^{-28}$, we find that:

$$\frac{E^T}{E_i^k} \leqslant 10^{-56} \tag{1.39}$$

this means that the kinetic and potential energies of the matter particles in the early universe should be balanced to a factor of 10^{-56}. Also, it can be shown that $\Omega = |E^p|/E^k$. Thus,

$$\frac{E^T}{E_i^k} = (\Omega_0 - 1)\left(\frac{\dot{a}_0}{\dot{a}_i}\right)^2 \leqslant 10^{-56} \tag{1.40}$$

Because $\Omega_0 = \rho_0 \frac{8\pi G}{3}\frac{1}{\left(\frac{\dot{a}}{a}\right)^2}$, the second Friedmann equation can be written as $\Omega_0 - 1 = \frac{k}{\dot{a}^2}$. Therefore, we found that the curvature of the universe must be extremely close to zero, which again seems fine-tuned.

The horizon problem and the flatness problem expose the fact that, from all possible configurations of energy density, pressure and distribution of velocities the particles at the early universe could have, they presented incredibly specific values. In order to explain those values

(and the density of particles nowadays), another explanation was provided [4, 5]. They postulated the universe (or at least the universe contained in the event horizon) was entirely generated from a causal part of the early universe. This could only be possible if the scale factor expanded exponentially instead of according to a power law, or, in other words, if gravity acted repulsively instead of attractively for a period of time. As we saw in section (1.3), this is only possible when $p < 0$.

It can be shown [4] that the causal part from which the universe originated does not need to be homogeneous and isotropic. Inflation can expand the universe enough to dilute possible initial anisotropies. According to the inflationary model, this expansion was generated by a scalar field that encompasses all causal early universe. Its format would be the simplest possible to present negative pressure, generate the minimum necessary number of efoldings and have a smooth transition to a Friedmann expansion, where the scale factor grows as a power law.

1.4.1 The *slow-roll* scalar field

Let's consider the energy-momentum tensor of a scalar field. In a Minkovski manifold, it can be written as [4]:

$$T^{\alpha}_{\beta} = g^{\alpha\gamma}\frac{\partial\phi}{\partial x^{\gamma}}\frac{\partial\phi}{\partial x^{\beta}} - \left(\frac{1}{2}g^{\gamma\delta}\frac{\partial\phi}{\partial x^{\delta}}\frac{\partial\phi}{\partial x^{\gamma}} - V(\phi)\right)\delta^{\alpha}_{\beta} \tag{1.41}$$

Comparing it with the energy-momentum tensor of a perfect fluid (1.12), we can identify energy density and pressure as:

$$p = \frac{1}{2}g^{\gamma\delta}\frac{\partial\phi}{\partial x^{\delta}}\frac{\partial\phi}{\partial x^{\gamma}} - V(\phi) \qquad \rho = \frac{1}{2}g^{\gamma\delta}\frac{\partial\phi}{\partial x^{\delta}}\frac{\partial\phi}{\partial x^{\gamma}} + V(\phi) \tag{1.42}$$

If the scalar field ϕ is homogeneous, that is, $\frac{\partial\phi}{\partial x^{i}} = 0$, then,

$$p = \frac{1}{2}\left(\frac{\partial\phi}{\partial t}\right)^{2} - V(\phi) \qquad \rho = \frac{1}{2}\left(\frac{\partial\phi}{\partial t}\right)^{2} + V(\phi) \tag{1.43}$$

But, as shown previously (section 1.3), we need $p = -\rho$ to generate an exponential expansion. Thus, we need:

$$|V(\phi)| \geqslant \left(\frac{\partial\phi}{\partial t}\right)^{2} \tag{1.44}$$

This is known as the first *slow roll* condition. It is a basic condition an homogeneous scalar field has to fulfill to produce an expansion faster than a power law. We also know this field

has to obey the conservation law (1.17), this is,

$$\frac{\partial\phi}{\partial t}\frac{\partial^2\phi}{\partial t^2} + \frac{\partial V}{\partial\phi}\frac{\partial\phi}{\partial t} = -3\frac{\dot{a}}{a}\left(\frac{\partial\phi}{\partial t}\right)^2 \tag{1.45}$$

This equation is most commonly written as:

$$\frac{\partial^2\phi}{\partial t^2} + 3\frac{\dot{a}}{a}\frac{\partial\phi}{\partial t} + \frac{\partial V}{\partial\phi} = 0 \tag{1.46}$$

Note that it resembles the movement equation for a damped harmonic oscillator. As previously mentioned, in addition to an exponential expansion, we need a smooth transition from this regime to a power-law-expansion regime. This can be accomplished by demanding that:

$$3\frac{\dot{a}}{a}\frac{\partial\phi}{\partial t} \gg \left|\frac{\partial^2\phi}{\partial t^2}\right| \tag{1.47}$$

This is the second *slow roll* condition.

Initially, it was expected that experimental evidences would be able to determine the shape of the scalar field, but there have been some claims that any ϕ obeying those conditions would provide a viable universe in this context. Other critic to this model is that the scalar field cannot be explained from first principles using particle theory. Given this situation, many proposals started to emerge recently, attempting to answer these questions with or without scalar fields.

We conclude this chapter by pointing out that the ΛCDM model has this name to emphasize the presence of cold dark matter (CDM) representing $\approx 26\%$ of the energetic content of the universe and the presence of dark energy, treated as a cosmological constant (Λ), representing 70% of this content. Although the model did not predict these quantities or even the existence of the dark sector, it was able to incorporate them. This is a very active area of both theoretical and experimental research, to find the constituents of dark matter and the nature of dark energy.

Our cosmological model proposes a candidate for dark matter and sheds some light on its interactions while at the same time providing a more physical origin to the inflationary period, without a scalar field. In chapter 3, we will present its details along with a highlight of the most relevant experimentally found characteristics of dark matter. But first let's make a quick review of SU(N) theories.

2 Some results of non-perturbative QCD

In this chapter we introduce the theory that describes the strong force, Quantum Chromodynamics. We highlight techniques to study its non-perturbative limit, such as lattice QCD and the large-N limit and we present their most important findings for our research. We also present the results of a research internship period, at McGill University, dedicated to provide an alternative view on the importance of viscous coefficients in the description of the quark-gluon plasma.

2.1 Quantum Chromodynamics

Up until now, only four forces have been necessary to explain all known phenomena in physics, from the subatomic to the extragalatic level: the gravitational force, the electromagnetic force, the weak force and the strong force. While the gravitational force can be explained by Einstein's theory of General Relativity, all other three forces are described by the *Standard Model of Particle Physics* as quantum field theories. In this section, we focus on the strong force and its formalization, the theory of *Quantum Chromodynamics*, QCD.

The strong force describes the interactions between all particles with color charge, this is, quarks and gluons (the elementary particles that form protons, neutrons, etc). Gluons are the mediators of this force, but because they have color charge as well, they feel the force by self-interacting. Following [6], we present an heuristic derivation of the mathematical formalism behind this theory.

Quarks have spin $1/2$, thus, if they were free particles in a relativistic quantum scenario, they would obey Dirac's equation, that can be deducted from the Lagrangian (2.1):

$$\mathcal{L}(x) = \bar{\psi}_j(x)(i\partial\!\!\!/ - m)\psi_j(x) \tag{2.1}$$

Here, $\partial\!\!\!/ = \gamma^\mu \partial_\mu$ where γ^μ are Dirac matrices; j is an index that stands for color; ψ is a 4-dimensional spinor and m represents quarks' masses, if quarks were free particles. We demand this Lagrangian to be invariant to the transformation:

$$\psi'(x) \to U\psi(x) \tag{2.2}$$

where U is a 3x3 unitary matrix acting on the color index. Because U has a real determinant that obeys $|\text{Det } U| = 1$, this matrix is part of a group called $SU(3)$, a subgroup of $U(3)$ - the group of

unitary matrices. Matrices obeying these conditions depend only on 8 real free parameters, which is another way of saying that there are 8 generators for the $SU(3)$ group. Generally speaking, the generators for the $SU(N_c)$ groups are $N_c^2 - 1$ gauge bosons.

We chose the matrix U to have these characteristics because we know quarks present themselves in three colors: red, blue or green. $SU(3)$ is the symmetry group that represents the Lagragian invariance to these colors (as well as the 3 anticolors for the antiquarks). In other words, these three color states form a basis in the quark's color vector space.

The fact that gluons are the mediators of this interaction can be shown by identifying them as the gauge fields introduced for the demanded invariance in the Lagrangian [6]. In other words, to be invariant to (2.2), the Lagrangian (2.1) has to be modified such that it doesn't represent quarks as free particles anymore, but as particles coupled with gauge fields, the gluons. Thus, the Lagrangian (2.1) $\mathcal{L}(x)$ corresponds only to $\mathcal{L}_{\text{quarks}}$ and the Lagragian representing QCD will now be called $\mathcal{L}_{QCD}$.

Because gluons also have energy and momentum, these additional degrees of freedom must be accounted for in an extra term ($\mathcal{L}_{\text{gluons}}$) in the Lagrangian $\mathcal{L}_{QCD}$, so that $\mathcal{L}_{QCD} = \mathcal{L}_{\text{quarks}} + \mathcal{L}_{\text{gluons}}$. Demanding this extra term to be invariant to the transformation (2.2) as well, we find that it depends on non-linear terms in the gauge fields. In other words, color rotations don't commute, for $SU(3)$ is a non-abelian group. Physically, this translates as self-interacting gluons. Because the modified Lagrangian L_{QCD} accounts for all the experimentally observed characteristics of the strong force, we conclude it's an accurate description. It's worth mentioning that quarks are organized by flavours, to represent their different quantum numbers, as charge and mass. Until now, six flavours have been found: up(u), down(d), charm(c), strange(s), top(t) and bottom(b). This was the final information missing in our Lagrangian, so now we can explicitly write it:

$$\mathcal{L}_{QCD} = -\frac{1}{4} F^a_{\mu\nu} F^{\mu\nu}_a - \sum_f \bar{\psi}^f_\alpha (i\gamma_u \partial^u + m_f - g\gamma_\mu A^\mu)^{\alpha\beta} \psi^f_\beta \tag{2.3}$$

$$F^a_{\mu\nu} = \partial_\mu A^a_\nu - \partial_\nu A^a_\mu - g f^a_{bc} A^b_\mu A^c_\nu \tag{2.4}$$

A^a_μ stands for the gluon field of color a and ψ^f_α, the quark field of colour α and flavour f. The effective quark masses are represented by m_f, g is the coupling constant for this interaction and f^a_{bc} are the structure constants of $SU(3)$, which tell us each component of the $SU(3)$ generators as well as their commutative relations.

The procedure of imposing local symmetries of compact Lie groups (such as U(N) and SU(N)) to a Lagrangian, as we just did, originated the *Yang-Mills theories*. Those theories describe non-linear gauge fields, self-interacting particles, thus, they were used to formalize QCD and the electroweak theory. Note that this gauge symmetry does not imply new symmetries in nature, they only represent a constrain in the action that generates the Lagrangian. Therefore,

one can interpret gauge symmetries as a specification in the form of the interaction felt by the particles [7].

Gluons' self-interaction is responsible for many characteristics exclusive to the strong force, such as the phenomena of asymptotic freedom and color confinement. Asymptotic freedom is the fact that the coupling between quarks and gluons becomes smaller as the distance between the interacting quarks gets shorter. This is also known as the anti-screening effect. Therefore, at small distances of the order of 0.8fm, one can study quarks interactions using perturbative techniques (pQCD) [7].

Color confinement stands for the experimental fact that isolated free quarks were never detected in nature. One can extend the reasoning of asymptotic freedom and conclude that as the interacting quarks get distant, the coupling between quarks and gluons gets bigger, thus it becomes energetically unfavourable to isolate one quark. Although this has not been mathematically proved yet, this energetic limit could not be described by a perturbative treatment, indicating that we entered the regime of strong coupling.

2.1.1 Lattice QCD

One of the techniques to further our understanding of QCD in the non-perturbative limit is *lattice QCD*. Within this technique, one studies the action that generated the Lagrangian by calculating Feynman's integrals in a finite lattice. Each vertex of the lattice represents a quark and each edge, a gluon. To get physically valid behaviours in this configuration, one extrapolates its results to zero lattice spacing, which is the continuum limit. This procedure works well for baryochemical potential $\mu = 0$ but technical difficulties arise as one tries to investigate $\mu > 0$. Lattice QCD is an active area of research, of which we will summarize here only its most relevant findings for our work.

There are strong indications that a deconfinement transition takes place for certain values of temperature and baryon density. This means that hadrons (particles composed of quarks) become a fluid of deconfined quarks and gluons at a given region of the phase diagram [8]. This fluid is called the *quark-gluon plasma*. For $\mu = 0$, the transition is a cross-over that happens at $T_c \approx 170$ MeV. For $\mu \neq 0$, it is believed that, above a critical point in temperature and baryon density, the transition becomes first-order. A sketch of this phase diagram is shown in Figure 1.

We are specially interested in the quark-gluon plasma and its transition to a hadronic phase, thus, we illustrate the behaviour of the energy density of this fluid near deconfinement in Figure 2a. There's a clear distinction in the values of energy density for the fluid and for the hadronic gas. In particular, the sudden jump in energy density at T_c is proportional to the latent heat of deconfinement [9]. Note also that all values are below the Stefan-Boltzmann limit - the expected value for an ideal gas of massless quarks and gluons - which highlights the

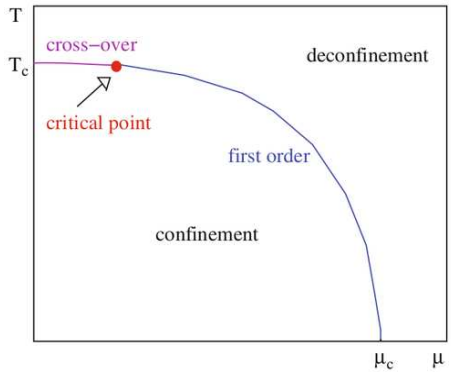

Figure 1 – Sketch of the phase diagram of nuclear matter when $\mu \neq 0$. From [9].

importance of quarks' mass in this simulation. This result was obtained by lattice simulations of [10], considering two and three flavours of quarks with $\mu = 0$.

Other useful quantity to analyze is the expectation value for the trace of the energy-momentum tensor, $\Delta = (\rho - 3p)/T^4$. It measures the degree of interaction of the constituents of a fluid, such that, for example, for an ideal gas of massless particles, that behaves as radiation, $p = \rho/3 \Rightarrow \Delta = 0$. In the Figure 2b, from the same simulations of [10], we can see that the strong interaction effects, expected to vanish at $T = T_c$, remain for $T_c < T < 2T_c$, which is evident from the peak's considerable width. This can be an indication that during the deconfinement transition there's a mixed phase of deconfined plasma and hadron gas [9].

Finally, we highlight the result that, for lattice QCD simulations with varied number of flavours, the deconfinement transition is always present, although the critical temperature may vary with the parameters considered.

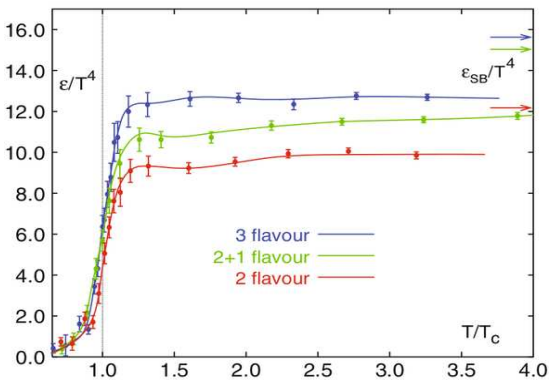

(a) Energy density over temperature T^4 in terms of temperature over critical temperature for different flavour configurations.

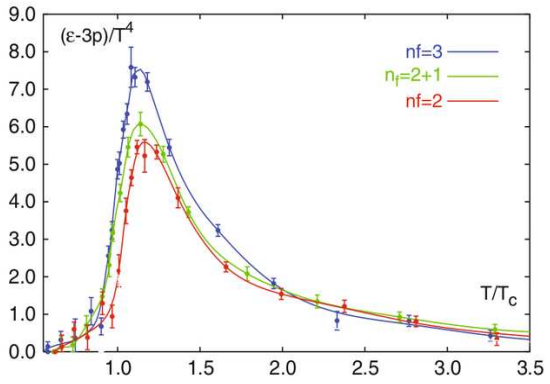

(b) Δ, defined in the main text, in terms of temperature over critical temperature for different flavour configurations.

Figure 2 – Simulations in the lattice for two $(n_f = 2)$ and three $(n_f = 3)$ flavours of light quarks and two flavours of light quarks plus one flavour of heavy quark $(n_f = 2 + 1)$ with $\mu = 0$. Results from [10] and adapted figures from [9].

2.2 Bulk viscosity in the quark-gluon plasma

A parallel study, under the supervision of Professor Charles Gale and Professor Sangyong Jeon at McGill university, was performed to further our understanding of the quark-gluon plasma and the role of bulk viscosity therein. This aggregated on the mathematical description of viscous coefficients, explicit in the previous chapter 1, to provide physical intuition.

Several experiments on heavy-ion collisions have shown that, soon after the event for a short period of time in a localized region, the formation of a quark-gluon plasma occurs. Although the evolution of this plasma can be well described by ideal hydrodynamics and the experimentally found factor $\frac{\eta}{s}$ (shear viscosity over entropy) seems to be very small - pointing that the plasma behaves very closely to an ideal fluid - there's still room for small viscous corrections. Those corrections provide better agreement of the rates of photon production with data [11].

In our work, we extended the approach of [11, 12] to dilepton (lepton-antilepton pairs) production. We understand that dileptons, as photons, are good probes for the properties and evolution of the quark-gluon plasma because they do not interact strongly. Thus, as they are produced, they are naturally transparent to the strong interactions of the medium, keeping a memory of instants after the collision and providing a clearer picture of that environment.

2.2.1 Dilepton emission rate

We start by deriving an expression for the dilepton emission rate without viscous corrections. Following the approach of [13], we study the reaction $q^+ + q^- \to l^+ + l^-$, where q represents a quark and l, a lepton.

But for the similar reaction $e^+ + e^- \to \mu^+ + \mu^-$, from Quantum Electrodynamics (QED), we know that the cross-section σ is:

$$\sigma(M) = \frac{4\pi}{3}\frac{\alpha^2}{M^2}\left(1 + \frac{2m_l^2}{M^2}\right)\left(1 - \frac{4m_l^2}{M^2}\right)^{1/2} \tag{2.5}$$

where m_l represents the dilepton mass, M, the center-of-mass energy and α stands for the coupling constant of QED. Because we want to deal with quarks instead of electrons, we must modify the expression above to account for colour effects. Thus,

$$\sigma_q(M) = F_q\sigma(M) \qquad F_q = N_c(2s+1)^2\sum_f e_f^2 \tag{2.6}$$

The factor F_q accounts for all missing degrees of freedom in the previous expression. N_c represents the number of colours; s, the spin and e_f, the fractional electric charges of each flavour. Considering only two flavours of massless quarks (u, d), we use that $N_c = 3$, $(2s+1)^2 = 4$ and $\sum_f e_f^2 = \frac{5}{9}$, therefore this factor is numerically equal to $F_q = \frac{20}{3}$.

From kinetic theory, the number of dileptons produced per unit time per unit volume is:

$$dN/d^4x = R(q^+q^- \to l^+l^-) = \int \frac{d^3p_1}{(2\pi)^3} f(\vec{p_1}) \frac{d^3p_2}{(2\pi)^3} f(\vec{p_2}) \sigma(q^+q^- \to l^+l^-; \vec{p_1}, \vec{p_2}) v_{rel}$$

$$v_{rel} = \frac{[(p_1 \cdot p_2)^2 - m_q^4]^{1/2}}{E_1 E_2} \tag{2.7}$$

Note that p_1 and p_2 are the relativistic four-momenta and $f(\vec{p_1})/f(\vec{p_2})$ are the occupation probabilities in the momentum space. Because quantum effects are not important, we use the relativistic energy and the Boltzmann distribution:

$$E^2 = \vec{p}^2 + m_q^2 \qquad f(\vec{p}) = e^{-E/T} = e^{-\frac{\left(\vec{p}^2 + m_q^2\right)^{1/2}}{T}} \tag{2.8}$$

To evaluate this integral, one can analytically integrate in five of the six variables and, assuming massless quarks, get the simplified temperature-dependent expression:

$$R(T) = \frac{T^6}{(2\pi)^4} \int_{2m_l/T}^{\infty} \sigma(z) z^4 K_1(z) dz \qquad z = M/T \tag{2.9}$$

Note that $K_1(z)$ stands for the modified Bessel function of the second kind. Although the rate of production is not experimentally accessible, it is the basis to calculate the quantities $\frac{dN}{dydM^2}$ - the number of particles produced per unit rapidity per unity center-of-mass energy squared - and $\frac{dN}{dydM^2dE_T}$ - the number of particles produced per unit rapidity per unity center-of-mass energy squared per unit total energy - which are more convenient and experimentally available. The rapidity y is defined by $y = \frac{1}{2} \ln \left(\frac{E + p_z}{E - p_z} \right)$ where p_z stands for momentum in the z direction, along the beam line of the accelerator.

2.2.2 Dilepton emission rate with bulk viscosity correction

To account for bulk viscous corrections in this scenario, we follow the approach of [11], so that the corrections are represented by an additional term in the occupation probability:

$$f(\vec{p}) = f^{(0)}(\vec{p}) + \delta f(\vec{p}) \tag{2.10}$$

Thus, from:

$$R(q^+q^- \to l^+l^-) = \frac{1}{2(2\pi)^3}\int \frac{d^3p_1}{2E_1(2\pi)^3}\frac{d^3p_2}{2E_2(2\pi)^3}\frac{d^3p_3}{2E_3(2\pi)^3}(2\pi)^4 \delta^4(P_1+P_2-P_3-P_4)|\mathcal{M}|^2 f(\vec{p_1})f(\vec{p_2}) \tag{2.11}$$

That is the same of equation (2.7), considering the following identity, for a generic reaction $1+2 \to 3+4$ [14],

$$d\sigma = \frac{(2\pi)^4|\mathcal{M}|^2}{4\sqrt{(p_1\cdot p_2)^2 - m_1^2m_2^2}}\delta^4(P_1+P_2-P_3-P_4)\frac{d^3p_3}{2E_3(2\pi)^3}\frac{d^3p_4}{2E_4(2\pi)^3} \tag{2.12}$$

Different physical processes are represented by the different cross sections (σ) or, equivalently, by the different scattering matrices $(\mathcal{M})$. We assume that $f(\vec{p_1}) = f^{(0)}(\vec{p_1}) + \delta f(\vec{p_1})$ and $f(\vec{p_2}) = f^{(0)}(\vec{p_2}) + \delta f(\vec{p_2})$, such that, in first order,

$$R_{l^+l^-} = R^{(0)}_{l^+l^-} + \frac{1}{2(2\pi)^3}\int \frac{d^3p_1}{2E_1(2\pi)^3}\frac{d^3p_2}{2E_2(2\pi)^3}\frac{d^3p_3}{2E_3(2\pi)^3}(2\pi)^4\delta^4(P_1+P_2-P_3-P_4)|\mathcal{M}|^2 \left[f^{(0)}(\vec{p_1})\delta f(\vec{p_2}) + f^{(0)}(\vec{p_2})\delta f(\vec{p_1})\right] \tag{2.13}$$

$R^{(0)}_{l^+l^-}$ stands for the dilepton production rate without corrections. Taking in account only bulk viscous corrections,

$$\delta f(P,X) = \Pi(X)\sum_j B^j_X(X)B^j_M(P,T) \tag{2.14}$$

$\Pi(X)$ represents the bulk pressure, defined as $\Pi = -\zeta\nabla_\mu u^\mu$ where ζ is the bulk viscosity and u^μ is the fluid four-velocity. $B^j_X(X)$ and $B^j_M(P,T)$ are functions that depend, respectively, on space-time position X, four-momentum P and temperature T. Thus,

$$R_{l^+l^-} = R^{(0)}_{l^+l^-} + \Pi(X)\sum_j B^j_X(X)\left[\frac{1}{2(2\pi)^3}\int \frac{d^3p_1}{2E_1(2\pi)^3}\frac{d^3p_2}{2E_2(2\pi)^3}\frac{d^3p_3}{2E_3(2\pi)^3}(2\pi)^4 \delta^4(P_1+P_2-P_3-P_4)|\mathcal{M}|^2\left(f^{(0)}(\vec{p_1})B^j_M(P_2,T) + f^{(0)}(\vec{p_2})B^j_M(P_1,T)\right)\right] \tag{2.15}$$

From [11],

$$\begin{aligned} B_X^1(X) &= -\frac{\tau_\Pi}{\zeta} & B_M^1(P,T) &= f^{(0)}(P)\frac{1}{3}\frac{m^2}{T^2}\frac{1}{P\cdot u/T} \\ B_X^2(X) &= -\frac{\tau_\Pi}{\zeta}\left(\frac{1}{3}-c_s^2\right) & B_M^2(P,T) &= f^{(0)}(P)\left(\frac{-P\cdot u}{T}\right) \end{aligned} \tag{2.16}$$

where c_s is the velocity of sound and τ_Π is the relaxation time, a transport coefficient related to the bulk viscosity. Therefore, we can explicitly write the modified rate of dilepton production as:

$$\begin{aligned} R_{l^+l^-} &= R_{l^+l^-}^{(0)} + \frac{1}{2(2\pi)^3}\int \frac{d^3p_1}{2E_1(2\pi)^3}\frac{d^3p_2}{2E_2(2\pi)^3}\frac{d^3p_3}{2E_3(2\pi)^3}(2\pi)^4\delta^4(P_1+P_2-P_3-P_4)|\mathcal{M}|^2 \\ &\quad \Pi(X)\left(\frac{-\tau_\Pi}{\zeta}\right)f^{(0)}(\vec{p_1})f^{(0)}(\vec{p_2})\left[\frac{1}{3}\frac{m^2}{T^2}\left(\frac{T}{P_2\cdot u}+\frac{T}{P_1\cdot u}\right)+\right. \\ &\quad \left.\left(\frac{1}{3}-c_s^2\right)\left(-\frac{P_2\cdot u}{T}-\frac{P_1\cdot u}{T}\right)\right] \end{aligned} \tag{2.17}$$

Note that the only dependence in the fluid velocity is in the term $P\cdot u$, a scalar. Because scalars are invariant quantities, we can choose to calculate this term in the rest referential, thus, $P\cdot u = P_0 = E$. As before, the occupation probabilities are Boltzmann distributions $f(\vec{p}) = e^{-E/T} = e^{-\frac{\left(\vec{p}^2+m_q^2\right)^{1/2}}{T}}$.

To compare the importance of this correction with the former value of the dilepton production rate, we need more realistic estimates for the transport coefficients and bulk pressure. Also, an extra effort will need to be made to find experimentally accessible quantities from this rate.

A non-zero bulk viscosity in the quark-gluon plasma represents that this fluid is not as ideal as previously thought. In other words, microscopic inelastic collisions are taking place inside it. We show in the next section how this phenomenon also happens during the deconfinement transition and its microscopical explanation. Before that, we introduce another approach in the non-perturbative study of QCD: the large-N limit.

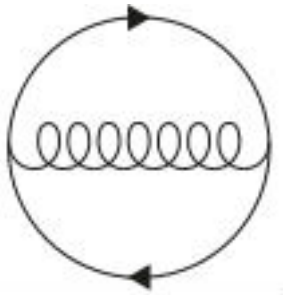

Figure 3 – An example of a Feynmann diagram illustrating a strong interaction. Adapted figure from [16].

2.3 The large-N limit

Although lattice QCD was a breakthrough in the study of non-perturbative QCD, its limitations, such as the increasing need of computational power to perform intricate calculations, stimulated the utilization of other approaches in this problem.

One of them is the *Large-N limit*. Within this technique, we consider the number of colors N_c as an arbitrary value in the Lagrangian (2.3). Then, we take the limit $N_c \to \infty$ at the same time that the coupling constant $g \to 0$, such that the quantity $\lambda = g^2 N_c$ remains finite. This guarantees that observables that grow with N_c do not diverge in this limit [15]. The term λ is called the 't Hooft coupling, after Gerard 't Hooft, who proposed this technique and proved that the finiteness of λ suffices to guarantee reasonable results in the calculations. He also fixed the number of flavours n_f, which is called the 't Hooft limit. Instead, one can choose to hold the quantity n_f/N_c finite, the Veneziano limit. This also produces finite calculations but its properties are more complex [15], so here we focus on the results of the former limit.

The greatest contribution of the large-N limit to the study of non-perturbative QCD was the finding that, in this regime, the calculations of the amplitudes of the processes become easier. Remember that particle physics reactions can be graphically represented by Feynmann diagrams (for example, Figure 3), allowing for their clear and concise visualization and simplifying the calculations of their probabilities. For any given reaction, a multitude of Feynmann diagrams can be drawn, representing multiple interactions that participate in that specific process. Quantifying the probability that a particular reaction occurs, this is, calculating its amplitude, is an intricate procedure that, in principle, demands the consideration of all related Feynmann diagrams.

However, it was shown that, for $N_c \to \infty$, only a small class of Feynmann diagrams gives a non-negligible contribution to the calculation of the amplitude of a reaction [15]. This happens because, for each diagram, there are effects proportional to N_c, that grow as $N_c \to \infty$, and effects proportional to g, that diminish as $g \to 0$. Even so, it's not possible to calculate all those contributions exactly because the number of diagrams that should be taken in account grows exponentially with the power of the coupling to which they correspond [15]. Thus, to

take valid results from this approach, one needs to appeal to the lattice technique. Note that due to the reduced number of Feynmann diagrams that must be considered in one reaction, the computational power demanded from lattice simulations is considerably lessened, despite the increase on degrees of freedom at larger N_c [16].

The lattice description in subsection (2.1.1) remains valid, but now, instead of investigating in the lattice the action that generates QCD, one shall use it to study the action that generates a $SU(N_c)$ theory. This is also an active area of research, so, in this thesis, we limit ourselves to the summary of some results that will be important for us in the next chapters.

For lattices with $4 = (3 \text{ spatial dimensions } + 1 \text{ temporal dimension })$ and $3 = (2 \text{ spatial dimensions } + 1 \text{ temporal dimension })$ Euclidean spacetime dimensions, $SU(N_c)$ Yang-Mills theories were proved to be confining [15]. This means that they were able to describe quarks and gluons confined within particles, outside the limit of asymptotic freedom. Although this is a first step to describe experimentally accessible quantities (like the mass of hadrons, for example), it should be remarked that this conclusion is valid for big lattice spaces, thus, it is not obvious that they will hold in the continuum limit, even though there are indications in this direction [15].

Those theories were also proved to generate finite mass for the lightest physical state in the spectrum. In the case of a pure Yang-Mills theory - this is, a theory without quarks, such that $n_f = 0$ - the lightest stable state are glueballs. This is an hypothetical particle, composed only of gluons. According to lattice simulations for $N_c \geqslant 2$, their masses, $m_{0^{++}}$, exhibit a mild dependence on the number of colours, such that the following relation is obeyed for any N_c [17]:

$$\frac{m_{0^{++}}}{\sqrt{\sigma}} = 3.37(15) + \frac{1.93(85)}{N_c^2} \tag{2.18}$$

This quantity is normalized by the string tension σ, a parameter for lattice calculations and the numbers in parenthesis represent simulations' uncertainties. For lattice studies including temperature through Monte-Carlo simulations, it has been proved that all $SU(N_c)$ Yang-Mills theories undergo a physical deconfining transition at a critical temperature T_c [15]. Also, for $N_c > 3$, this transition is of first order, which is associated to the finiteness of the latent heat L_h, that grows like [18]:

$$\frac{L_h^{1/4}}{N_c^{1/2} T_c} = 0.766(40) - \frac{0.34(1.60)}{N_c^2} \tag{2.19}$$

The critical temperature T_c has a small dependence on the number of colours N_c such that [19]:

$$\frac{T_c}{\sqrt{\sigma}} = 0.5949(17) + \frac{0.458(18)}{N_c^2} \tag{2.20}$$

Also, it has been verified that the thermodynamic quantities (pressure p, energy density ρ, entropy s and the trace of the energy-moment tensor Δ) present the same behaviour for $T > T_c$ in all $SU(N_c)$ theories with $N_c \geqslant 3$. Some results are shown in Figures 4 and 5, product of simulations from [20] and [21].

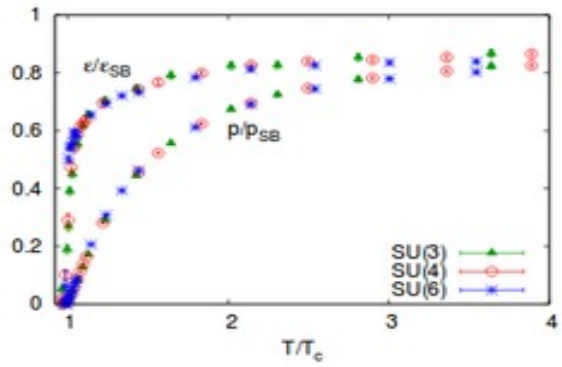

(a) Energy density and pressure normalized by their respective Steffan-Boltzmann limits in terms of temperature over critical temperature for different colour configurations. Results and figure from [20].

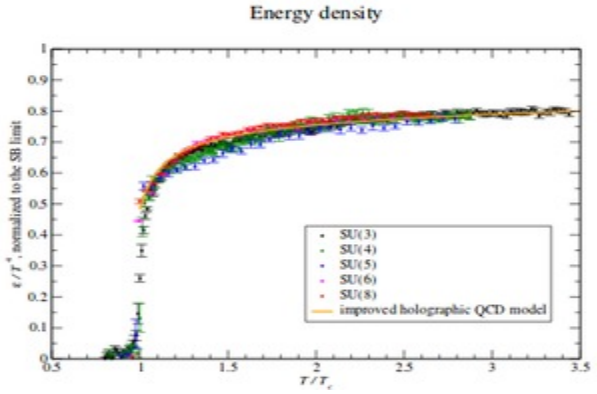

(b) Energy density over temperature T^4 normalized by its Steffan-Boltzmann limit in terms of temperature over critical temperature for different colour configurations. A comparison with an holografic model is performed. Results and figure from [21].

Figure 4 – Simulations in the lattice for energy density and pressure in several colour configurations with $n_f = 0$. Results and figures from [20, 21].

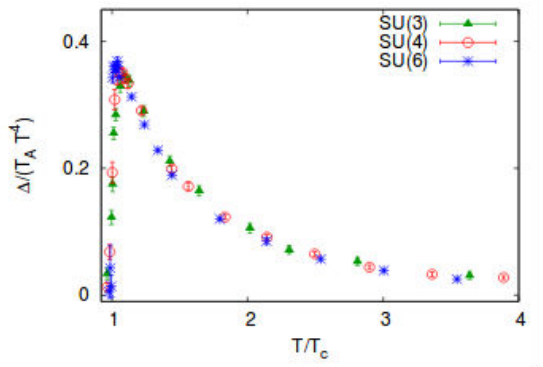

(a) Trace of the energy-momentum tensor normalized by the quantity $T_A = N_c^2 - 1$ over temperature T^4 in terms of temperature over critical temperature for different colour configurations. Results and figure from [20].

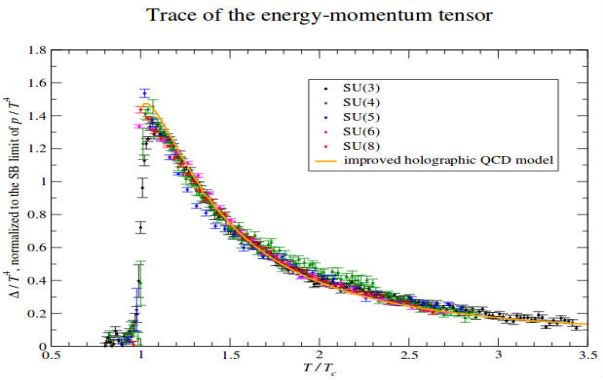

(b) Trace of the energy-momentum tensor normalized by the Steffan-Boltzmann limit of p/T^4 over temperature T^4 in terms of temperature over critical temperature for different colour configurations. A comparison with an holografic model is performed. Results and figure from [21].

Figure 5 – Simulations in the lattice for the trace of the energy-momentum tensor in several colour configurations with $n_f = 0$. Results and figures from [20, 21].

The existence of those patterns is an indication that the large-N limit can generate results valid for $N_c = 3$, describing QCD. It also suggests that the conclusions obtained with these simulations may remain valid for $N_c \to \infty$. In particular, one interested in studying the $SU(N_c)$ theories when $N_c > 3$ may grow on the knowledge obtained for QCD. For example, the

physical explanations of the features demonstrated here for $N_c > 3$ -like the peak in the energy density - are probably the same as QCD - in this example, the finiteness of the latent heat.

This extension, however, has to be cautious, for some experimental results of QCD fail to match the predictions from the large-N limit, which may be explained by non-trivial dynamics in QCD [15]. Also, the lattice presents several technical subtleties which may compromise the generalization of some results, specially regarding the continuum limit. Nonetheless, the large-N limit has proven to be a valuable technique in the study of $SU(N_c)$ Yang-Mills theories.

One final result we want to highlight is the bulk viscosity peak. Numerical estimates [22] and lattice simulations [23] for $SU(3)$ prove that, close to the deconfinement transition ($T \approx T_c$), the bulk viscosity coefficient ζ presents a non-negligible value. For temperatures $T > 2T_c$, however, it becomes almost zero. This is shown in Figure 6 below.

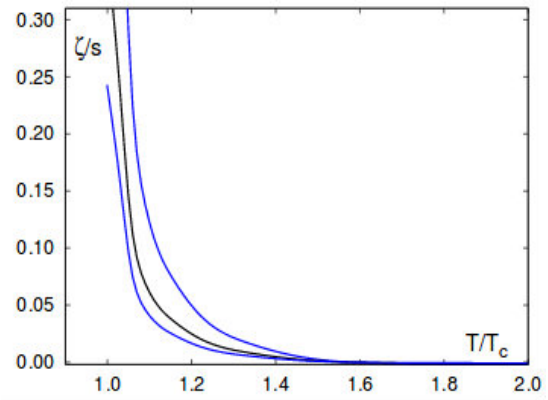

(a) The quantity ζ/s in terms of temperature over critical temperature for different *ansatz* in the estimates. Results and figure from [22].

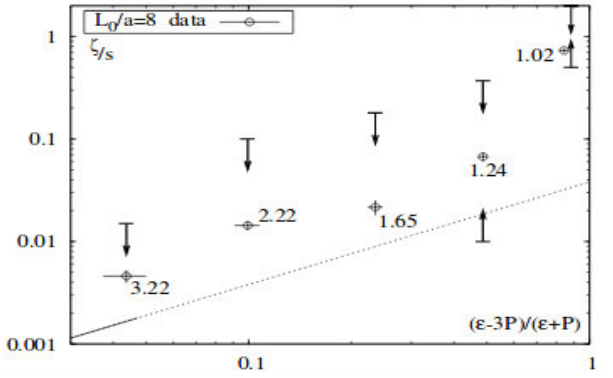

(b) The quantity ζ/s in terms of $(\epsilon - 3P)/(\epsilon + P)$, which measures the system's interaction. Uncertainties and bounds shown. The line represents a perturbative prediction. Results and figure from [23].

Figure 6 – Bulk viscosity ζ over entropy density s for estimates (Figure 6a) and lattice simulation (Figure 6b) in $SU(3)$. Results and figures respectively from [22, 23].

It is believed that this phenomenon is directly related to the peak in the trace of the energy-momentum tensor [22, 23, 24], thus, it is reasonable to assume that it happens for $SU(N_c)$ theories [24] as well. Microscopically speaking, this generalization is justified by the following explanation: considering that the bulk viscosity peak happens at a deconfinement transition region, one can interpret it as a change in the degrees of freedom of the substance [25]. During deconfinement, there is a mixed phase of a plasma of quark-gluons and a gas of hadrons, such that inelastic collisions are expected to happen. Those collisions are quantified by the bulk viscosity coefficient. Because deconfinement transitions happen for all $SU(N_c)$ theories, it is expected that in all of them a bulk viscosity peak around $T = T_c$ will be present.

It is important to note that the study of viscous coefficients in Yang-Mills theories is very recent, partially due to the difficulty of simulating these quantities in the lattice [23, 26]. Also, there are many uncertainties in their calculation, such that the exact shape of the peak ζ/s, for example, is still unknown. For completeness, we briefly mention that lattice simulations of

shear viscosity, η, for $SU(3)$, have obtained a small value for $T \geqslant 2T_c$ which grows increasingly important as the temperature approaches the critical temperature [26, 27]. This is an indication of the strong interacting nature of the system.

3 Our cosmological model

In this chapter, we will motivate and describe a cosmological model pictured by us. It provides a microscopical explanation to the inflationary period of the Universe as well as a candidate for dark matter, while being heavily based on pure Yang-Mills theories, described in chapter 2.

3.1 Motivation

As mentioned in section 1.4, at early times the Universe went through a phase of exponential expansion called Inflation. According to the Standard Cosmological Model, this was generated by a scalar field. However, as already mentioned, there is no consensus in the scientific community that this field is the most plausible way to generate this phenomenon. In addition, there have been claims that, once a scalar field obeys the *slow roll* conditions, it becomes impossible to find its exact format experimentally. From a microscopical point of view, the scalar field explanation is not a complete one either. In particular, in the Standard Model of Particle Physics, there is no prediction of its properties.

Addressing this issue was one of our motivations to propose a cosmological model. Within our model, we intended to propose a mechanism for inflation that did not rely on a scalar field. In particular, we wanted particle interactions to account for this phenomenon. The natural candidate in this case are dark matter particles because we know Standard particles' interactions could not mimic a repulsive effect at the energy range inflation is expected to happen (around 10^{16} GeV) [5].

This perspective allowed us to investigate another interesting open question: the nature of dark matter. Ever since its first experimental evidence of existence, all efforts to directly detect it have been in vain. Within our model, we propose a candidate for this matter whose only interaction with the particles of the Standard Model is through the gravitational force, therefore, explaining the lack of direct detection.

Proposing a candidate for dark matter and describing its interactions whilst microscopically explaining the inflationary model was our main motivation and goal in this project. Before describing our model in details, we will explicit some restrictions to which we've been submitted in its construction in the next section.

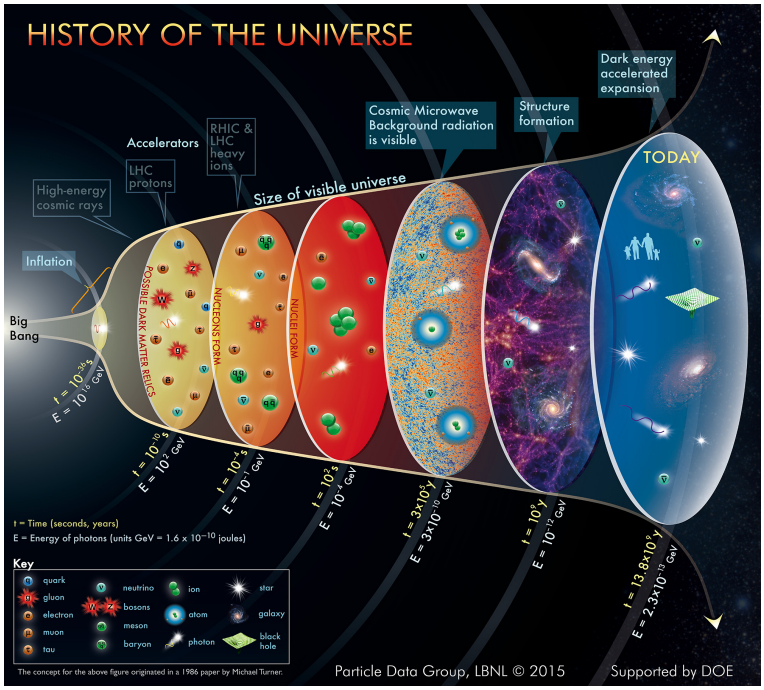

Figure 7 – Pictorial representation of the evolution of our Universe, explicitly showing the energy scales involved. Image by the Particle Data Group at Lawrence Berkeley National Lab, 2015.

3.2 Restrictions

3.2.1 Inflationary period

All information we have on the inflationary period of our Universe was obtained indirectly. The oldest register of the Early Universe available to us nowadays is the CMB radiation, which was freed long after the inflationary period had finished (see Figure 7 for an idea of the time scales involved). However, based on models of the thermal history of the Universe and structure formation simulations, we can estimate some characteristics of this period.

In specific, to account for the high degrees of homogeneity, isotropy and flatness of the universe measured by CMB radiation, there is an inferior limit in the amount of time this expansion must last. This can be translated in an inferior limit in the number of efoldings N.

Note that we can rewrite equation 1.29 as:

$$N = \int_{a_i}^{a_f} \frac{1}{a} da = \ln\left(\frac{a_f}{a_i}\right) \Rightarrow e^N = \left(\frac{a_f}{a_i}\right) \tag{3.1}$$

Also, let's introduce the Hubble factor $H = \dot{a}/a$. The very least we can demand of the observable universe today is that it fits the Hubble radius of the universe at the beginning of inflation, $(a_0 H_0)^{-1} < (a_i H_i)^{-1}$. Assuming, just for estimation purposes, that after the end of

inflation until now the universe was radiation dominated,

$$\frac{a_0 H_0}{a_e H_e} \approx \frac{a_e}{a_0} \approx \frac{T_0}{T_e} \approx 10^{-28} \tag{3.2}$$

Because, for this scenario $a(t) \propto t^{1/2}$, as demonstrated in section 1.3, then $H \propto a^{-2}$. As before, we assumed that $a(T) \propto T^{-1}$, $T_0 \approx 1$K and $T_e \approx 10^{15}$ GeV. Thus,

$$(a_i H_i)^{-1} > 10^{28} (a_e H_e)^{-1} \tag{3.3}$$

For H constant during inflation, $H_i = H_e$, therefore $a_e/a_i > 10^{28}$. This implies that $e^N > 10^{28} \rightarrow N > 64$. This derivation followed [28] and represented only one possible reasoning. Other derivations with other estimates can arrive at slightly smaller or bigger number of efoldings, but all agree that $N \approx \mathcal{O}(10)$. This represents the minimum amount of time inflation is expected to last.

Besides that, we also have an expectation on how much time after the Big Bang inflation ended, t_f. It comes from the expected durations of the reheating period and of the Friedmann expansion period of the universe. The reheating period is an hypothesized phase, to happen shortly after Inflation. It is responsible for the baryonic abundance and entropy generation, both phenomena being a result of the scalar field's oscillations at its point of minimal energy in the potential $V(\phi)$. The Friedmann expansion corresponds to a period when the universe was primarily composed of radiation, thus it expanded and cooled at a slower rate than in the inflationary period. It accounts for the production of atoms and light elements. Based on evidences from this period, it is estimated that $t_f \approx 10^{-34} - 10^{-36}$s [4].

Although these resources provide a reasonable estimate for the final time of inflation, there's no tool for the estimation of the initial time, t_i. This is a consequence of our ignorance of the mechanism of the Big Bang, which is believed to have happened in the regime of quantum gravity, starting around the Planck scale ($t \approx 10^{-43}$ s, when the Big Bang is set $t_{\text{Big Bang}} = 0$). Inflation is outside this regime, however their proximity and the lack of direct experimental data from this period turn any estimates of the initial time of inflation into speculation. Therefore, despite this quantity being related to N and t_f through equation 1.29, it is normally considered a free parameter in any inflationary model. Usually, it is set to be at the limit of the Planckian scale, thus, $t_i = 10^{-43}$ s.

The last restriction one can take from indirect evidences of the inflationary period is the fact that it ended smoothly. In other words, the transition from an exponential expansion to a power law expansion must have happened continuously, otherwise the homogeneity of the universe would be spoiled [4]. As described in section 1.4, the *slow roll* scalar field model guarantees this restriction by its second condition, equation 1.47.

3.2.2 Dark matter characteristics

Over 85 years have passed since the first experimental hint of the existence of dark matter [29]. Although we still have not directly detected the particle that composes this substance, we can infer some of its characteristics. First, let's clarify that we are referring here to cold dark matter instead of hot dark matter. The latter is assumed to be relativistic and it can be part of this matter, but not its major component because, if this was the case, no galaxies would be able to form [14].

It is believed that initial quantum fluctuations on the primordial plasma of the universe were amplified by Inflation and, later, further increased as dark matter particles agglutinated there. At this stage, these particles must have been non-relativistic and they must have had decoupled from the primordial plasma of the Early Universe much sooner than everything else. As the other components of the plasma decoupled, they were gravitationally attracted to dark matter rich regions, which became even bigger with the aggregation of matter. They became proto-galaxies that eventually grew to be galaxies. This picture is a result of simulations of structure formation and data from galaxy surveys [29] and it justified the search for cold dark matter (CDM).

The lack of direct detection of this matter from astrophysical observations implies that it is non-luminous and non-absorbing, in other words, it does not emit or absorb light. This raised the hypothesis that it could be Massive Astrophysical Compact Halo Objects, or MACHOs. This denomination represents non-relativistic, non-luminous, baryonic matter such as black holes, neutron stars or planets. These objects can account for as most as 8% of the mass of the galatic halo of a galaxy [14], according to the EROS collaboration, so they certainly do not represent CDM's main component. This directed the searches for non-baryonic cold dark matter.

As the laboratory search for these particles proceeds, more limits on their properties can be set. For example, we know that non-baryonic cold dark matter particles must be stable or long-lived, otherwise the products of their decay would have already been detected - as an excess of gamma rays or charged cosmic rays, for instance [30]. Following the same argument, these particles must be neutral of electromagnetic charge and their most important -maybe unique- interaction with other particles of the Standard Model is gravitational. Finally, from collisions of galaxies and their resultant distribution of matter and dark matter, it can be concluded that cold dark matter particles do not self-interact or they self-interact very weakly. Candidates with these characteristics are known as Weakly Interacting Massive Particles (WIMPs).

The last model-independent characteristics of dark matter we can take from experiments are its distribution in a galaxy and its abundance in the universe. The latter can be found through CMB radiation to be, according to Planck data [1], $\Omega_c h^2 = 0.1199 \pm 0.0027$ where $\Omega_c h^2$ stands for cold dark matter density today. In this expression, $h = H/100$ km s^{-1} Mpc^{-1}, H being the Hubble constant, $H_0 = (67.3 \pm 1.2)$ km s^{-1} Mpc^{-1}.

A WIMP candidate for dark matter must have all the characteristics highlighted in

this section. In addition, its mechanism of production must account for its density in the universe and galaxy distribution today, and finally, its thermal history must be compatible with structure formation models.

3.3 Description and qualitative behaviour

Inspired by Yang-Mills theories, we propose an extension to the Standard Model of Particle Physics by a $SU(N_c)$ flavourless group not coupled to the Standard Model. This extension provides a WIMP candidate for dark matter whose phase transition can generate a mechanism for Inflation in the Early Universe.

As seen in section 2.3, $SU(N_c)$ groups represent quarks and gluons that self-interact through the strong force, with N_c number of colours. Their Lagrangian is analogous to the QCD Lagrangian, where $N_c = 3$, but, within our model, N_c is a free parameter. As a flavourless -without quarks- group, we expect that its lightest stable bosonic states are glueball particles. This particle is our candidate for dark matter, having all characteristics a WIMP must possess: it is stable, it does not interact with photons - being non-luminous, non-absorbing and electrically neutral - and it does not self-interact. Also, our assumption that this particle does not interact with standard matter except gravitationally can explain the lack of direct detection of dark matter.

Our $SU(N_c)$ extension presents a deconfinement transition, as all Yang-Mills theories. As described in section 2.1, at a specific critical temperature and barionic density, free quarks and gluons -in our case, only gluons-, that composed a plasma, condensate into particles -in our case, glueballs. This dramatically changes the equation of state of the fluid, as its degrees of freedom are reduced and the bulk viscosity peaks. It is our hypothesis that this phenomenon produces a negative pressure in the equation of state of the early Universe which is responsible for its exponential expansion, the Inflationary period.

To successfully explain Inflation through this mechanism we also have to find that this expansion lasted enough to produce an isotropic and homogeneous universe, in other words, that it generated a reasonable number of efoldings. In addition, the transition from this regime to a decelerated Friedmann expansion must happen and it must be smooth. We highlight that, within this scenario, there is no scalar field and, therefore, no reheating period in the Early Universe. Consequently, all baryonic production and entropy generation must take place at the Big Bang, being diluted later by Inflation to the values known nowadays.

It is also crucial that the phase transition takes place at very high energies, of the order of 10^{16} GeV. Otherwise, this model would fail to reproduce data from nucleosynthesis models and galaxy surveys, in other words, structure would not have enough time to form. The critical energy at which this transition occurs marks the deconfinement scale. As mentioned in section 2.1, this is the one parameter not specified by the Lagrangian of $SU(N_c)$ theories. It is also directly related to the mass of the glueballs because it specifies the range of gluons'

interactions. Within our model, this is a free parameter as well.

Among the many checks that must be performed to ascertain the validity of this model as a viable explanation to the Inflationary period, in this work we dedicate ourselves to find the produced number of efoldings and a graceful exit to inflation. The first step in this process is to study the new equation of state for the Early Universe.

3.4 Equation of state

3.4.1 Early Universe

It can be shown [4] that, according to the Standard Model of Particle Physics, in the radiation dominated Early Universe, the energy density is given by:

$$\varepsilon_r = \kappa T^4 \tag{3.4}$$

$$\kappa = \frac{\pi^2}{30}\left(g_b + \frac{7}{8}g_f\right) \tag{3.5}$$

where g_b represents the bosonic degrees of freedom and g_f, the fermionic degrees of freedom of the relativistic particles. In addition, pressure p and energy density ε are related by:

$$p_r = \frac{\varepsilon_r}{3} \tag{3.6}$$

Note that we can only account for the degrees of freedom of the relativistic particles in equilibrium. This means that g_b and g_f are functions of temperature, because, as the universe cools, more particles decouple from the plasma. This phenomenon is illustrated in figure 8.

In this context, the addiction of extra particles would increase the number of degrees of freedom of the primordial plasma if, at some point, they were in thermal equilibrium. This is only possible if they interacted. In our model this is not the case, so we must account separately for the contributions from the plasma and dark matter particles, forcing us to write new equations of state:

$$\begin{aligned} p_{T\geqslant T_c} &= p_{SU(N_c)} - 3\zeta\frac{\dot{a}}{a} + \kappa T^4 \\ \varepsilon_{T\geqslant T_c} &= \varepsilon_{SU(N_c)} + 3\kappa T^4 \end{aligned} \tag{3.7}$$

The terms $p_{SU(N_c)}$ and $\varepsilon_{SU(N_c)}$ in the expressions above represent, respectively, the pressure and energy density of the $SU(N_c)$ fluid before and during the deconfinement transition. In addiction, as already discussed in section 1.2, the presence of the bulk viscosity ζ modifies

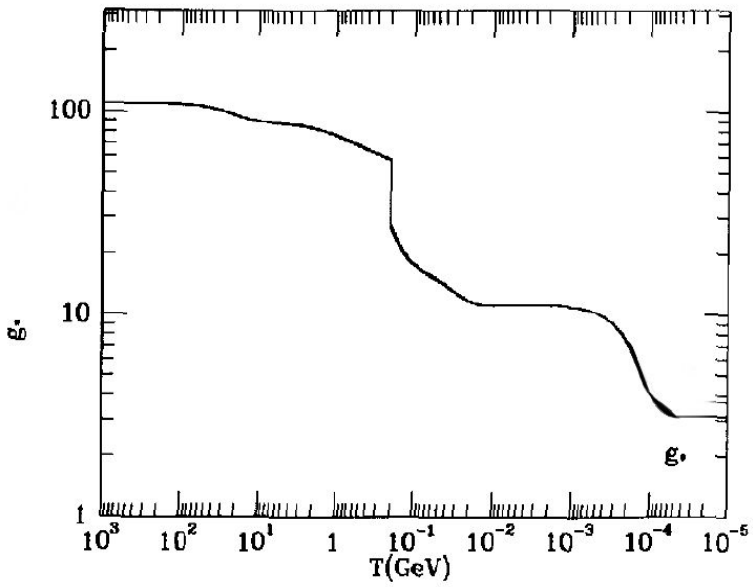

Figure 8 – Degrees of freedom in terms of temperature in GeV. Adapted figure from [31].

the energy-momentum tensor of the perfect fluid by adding an extra term. It can be rewritten as a perfect fluid tensor (1.22) if the pressure p is replaced by an effective pressure p^*. In the equation above, $p^* = -3\zeta\frac{\dot{a}}{a} + \kappa T^4$.

For completeness, we also write the equation of state for the primordial plasma of the Early Universe after the deconfinement transition takes place. Because the $SU(N_c)$ glueballs are stable and they do not interact with standard matter, their total number of particles is conserved. This information is translated in the differential equation below.

$$\begin{aligned} p_{T<T_c} &= n\frac{T}{m} + \kappa T^4 \\ \varepsilon_{T<T_c} &= 3\frac{nT}{2} + 3\kappa T^4 \\ n_0 &= m^2 T_c K_2\left(\frac{m}{T_c}\right) \\ \frac{dn}{dt} + & \quad n\frac{\dot{a}}{a} = 0 \end{aligned} \tag{3.8}$$

Note that K_2 stands for the modified Bessel function of the second kind.

3.4.2 $SU(N_c)$ plasma

To solve the adapted Friedmann equations for an imperfect energy-momentum tensor (1.22), we must first find analytical or numerical expressions for the equation of state of the Early universe with the $SU(N_c)$ plasma (3.7). In particular, we must find the quantities $p_{SU(N_c)}$ and

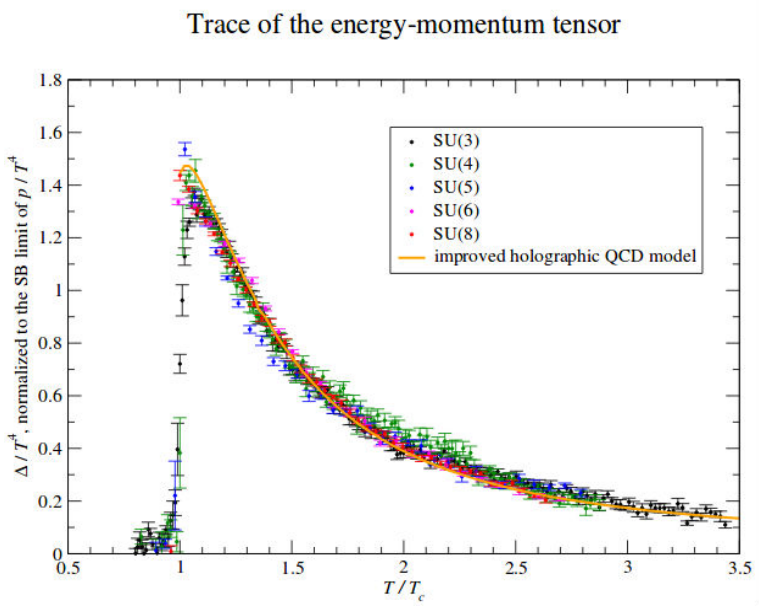

Figure 9 – Trace of the energy-momentum tensor normalized by the Steffan-Boltzmann limit of p/T^4 over temperature T^4 in terms of temperature over critical temperature for different colour configurations. A comparison with an holografic model is performed. Results and figure from [21].

$\varepsilon_{SU(N_c)}$. They are related to s, the entropy density, and Δ, the trace of the energy-momentum tensor of this fluid, by [5]:

$$\Delta = \varepsilon - 3p \tag{3.9}$$

$$s = \frac{dp}{dT} = \frac{\varepsilon + p}{T} \tag{3.10}$$

We begin by taking the data of the trace of the energy-momentum tensor from the lattice. These specific simulations were performed on a four-dimensional Euclidean hypercubic, isotropic lattice with periodic boundary conditions in all directions, for number of colours $N_c = 3, 4, 5, 6, 8$ [21]. The results were normalized so that they could be represented on a same graph and compared.

We repeat here figure 5b for a more detailed explanation of its features. Note that the y axis represents $\Delta/[(\pi^2) * R_I * (N_c^2 - 1)T^4/45]$ and the x axis, T/T_c. R_I is a dimensionless numeric factor equal to 1.2129 that corrects the deviation from the continuum limit introduced by lattice cut-off effects.

We analyzed the data from each colour separately and fitted a function for each trace of the energy-momentum tensor, focusing on the peak around the critical temperature T_c. Results are illustrated in figure 10. All numerical calculations in this research were performed with the software Mathematica©, version 10.4 and the codes are available at the appendices.

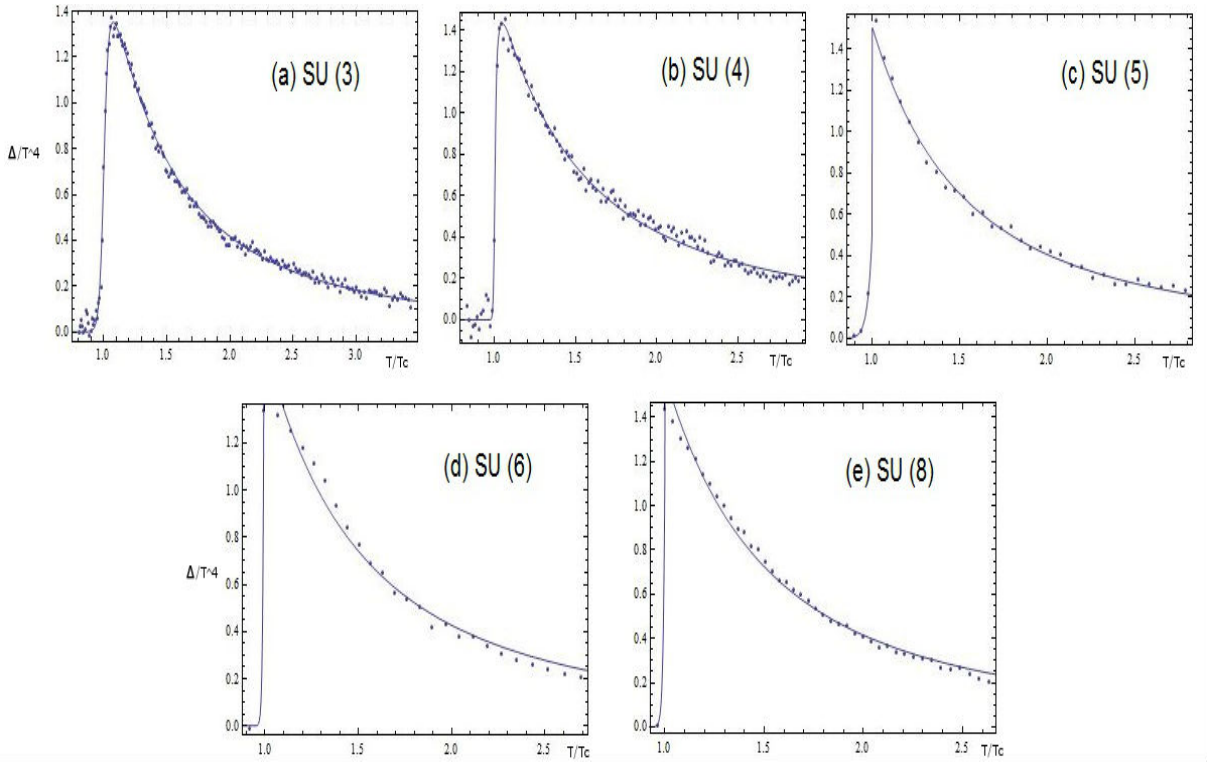

Figure 10 – Normalized trace of the energy-momentum tensor over T^4 in terms of temperature over critical temperature for the number of colours: a) $N_c = 3$, b) $N_c = 4$, c) $N_c = 5$, d) $N_c = 6$ and e) $N_c = 8$.

The normalization performed by [21] renders equivalent to work with any of the fits produced, so we chose to work with the results from $SU(3)$ simulations, due to the bigger amount of data available, which results in a more accurate fit to the trace of the energy-momentum tensor and, consequently, to all other thermodynamic quantities of interest.

The expression found for the fit of the normalized trace of the energy-momentum tensor was:

$$\begin{aligned} f\left(\frac{T}{T_c}\right) = & -0.14460\left(\frac{T}{T_c}\right)^{43.29179}\left[1+\tanh\left(27.91175\left(1-\frac{T}{T_c}\right)\right)\right]+ \\ & + \frac{0.85284}{(T/T_c)^{2.0323}}\left[1+\tanh\left(27.91175\left(-1+\frac{T}{T_c}\right)\right)\right] \end{aligned} \tag{3.11}$$

Considering that:

$$T\frac{d}{dT}\left(\frac{p}{T^4}\right) = \frac{1}{T^3}\frac{dp}{dT} - 4\frac{p}{T^4} \tag{3.12}$$

and using relation 3.10, the expression 3.12 can be rewritten as:

$$T\frac{d}{dT}\left(\frac{p}{T^4}\right) = \frac{\varepsilon - 3p}{T^4} = \frac{\Delta}{T^4} \tag{3.13}$$

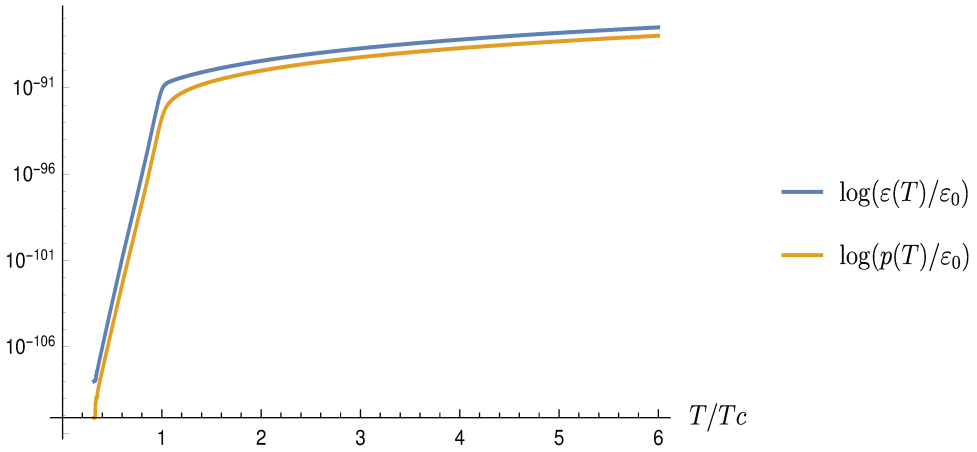

Figure 11 – Logarithm of pressure (p) and energy density (ε) over $\varepsilon_0 = 10^{91} eV^4$ of the $SU(N_c)$ fluid in terms of temperature over critical temperature.

Thus, to find the quantities ε and p, it suffices to calculate:

$$\begin{aligned} p &= T^4 \int_0^T \frac{\Delta}{T'^5} dT' \\ \varepsilon &= \frac{dp}{dT} T - p \end{aligned} \tag{3.14}$$

These operations were performed numerically, resulting in the non-analytical temperature dependent expressions illustrated in figure 11. This is the expected behaviour of these quantities, as we can see in figure 12, where we repeated two figures from section 2.3. As discussed in that section, the jump in the energy density around T_c is proportional to the number of colours N_c. However, our data was normalized to compare results from several numbers of colours, so this information is not evident in our expression for $\varepsilon(T)$.

Because our goal is to solve the Friedmann equations - which are time dependent - it becomes useful to rewrite the equations of state to make their temperature dependence implicit. To simplify the numerical resolution of this system of differential equations, we chose to write pressure in terms of energy density. Thus, we inverted the function $p(T)$ to obtain $T(p)$, temperature in terms of pressure. Afterwards, we composed this function with the expression $\varepsilon(T)$ to find $\varepsilon(p)$. These numerical expressions are illustrated in figure 13 and 3.13. A disadvantage of rewriting the equations of state like this is that we lost any chance of easily recovering the number of colours from their features, like the energy density jump.

The last step in the calculation of this equation of state is to find an analytic expression for the function $\varepsilon(p)$. This is another attempt to simplify the solving of the Friedmann equations, to be performed next. We took special care to reproduce the non-trivial behaviour of this function around the critical temperature T_c, as it represents the deconfinement transition. The fitting is illustrated in figure 15 and the expression found is explicited in equation 3.15.

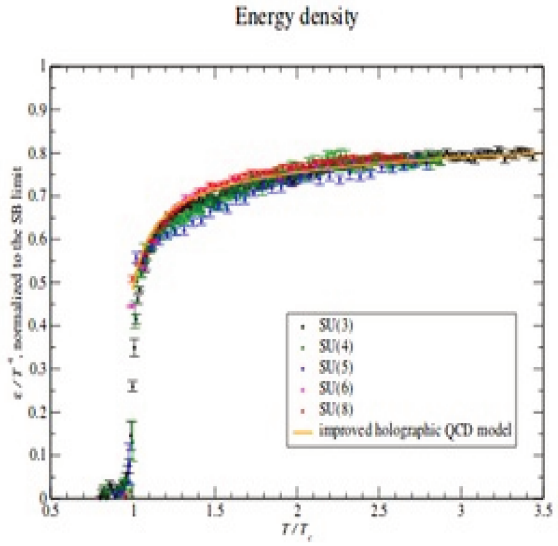

(a) Energy density over temperature T^4 normalized by its Steffan-Boltzmann limit in terms of temperature over critical temperature for different colour configurations.

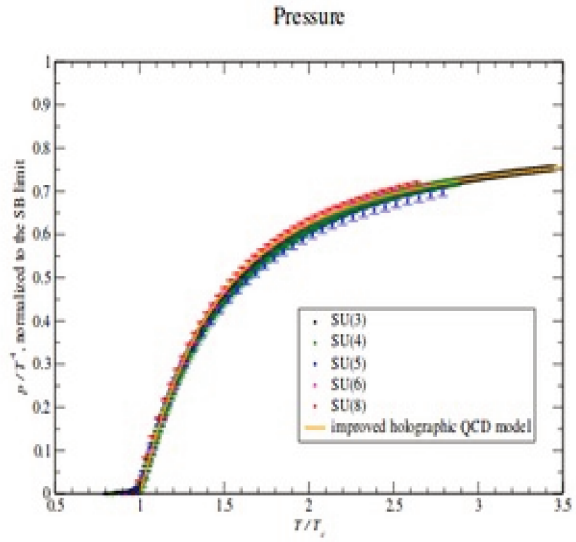

(b) Pressure over temperature T^4 normalized by its Steffan-Boltzmann limit in terms of temperature over critical temperature for different colour configurations.

Figure 12 – Energy density (Figure 12a) and pressure (Figure 12b) in terms of temperature for different colour configurations. A comparison with an holografic model is performed. Results and figures from [21].

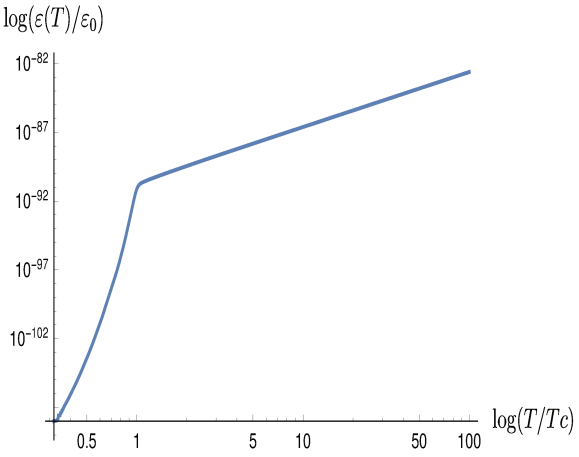

(a) Log-log plot of energy density ε over $\varepsilon_0 = 10^{91} eV^4$ in terms of temperature over critical temperature.

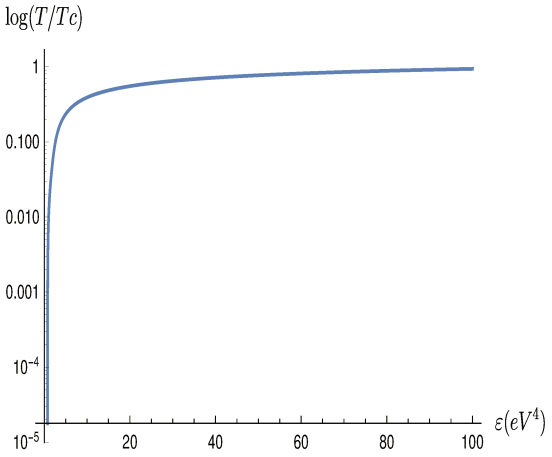

(b) Logarithm of temperature over critical temperature in terms of energy density ε.

Figure 13 – Energy density in terms of temperature (Figure 13a) and its inverse function (Figure 13b).

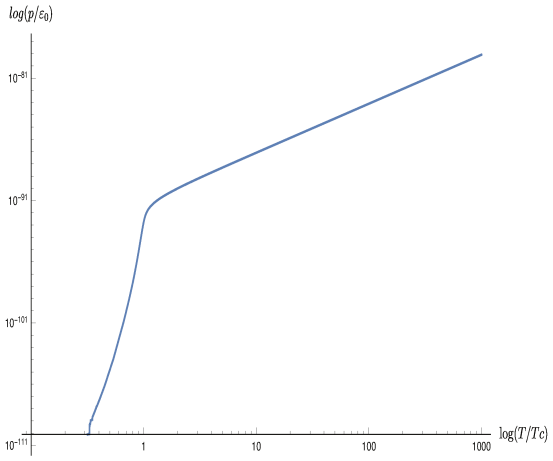

(a) Log-log plot of pressure over $\varepsilon_0 = 10^{91} eV^4$ in terms of temperature over critical temperature.

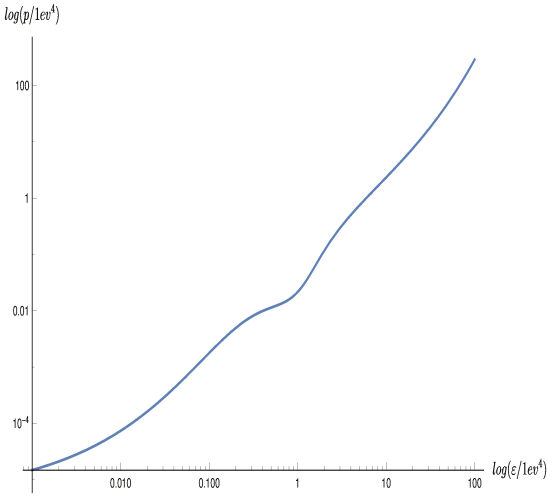

(b) Log-log plot of pressure in terms of energy density.

Figure 14 – Pressure in terms of temperature (Figure 14a) and in terms of energy density (Figure 14b).

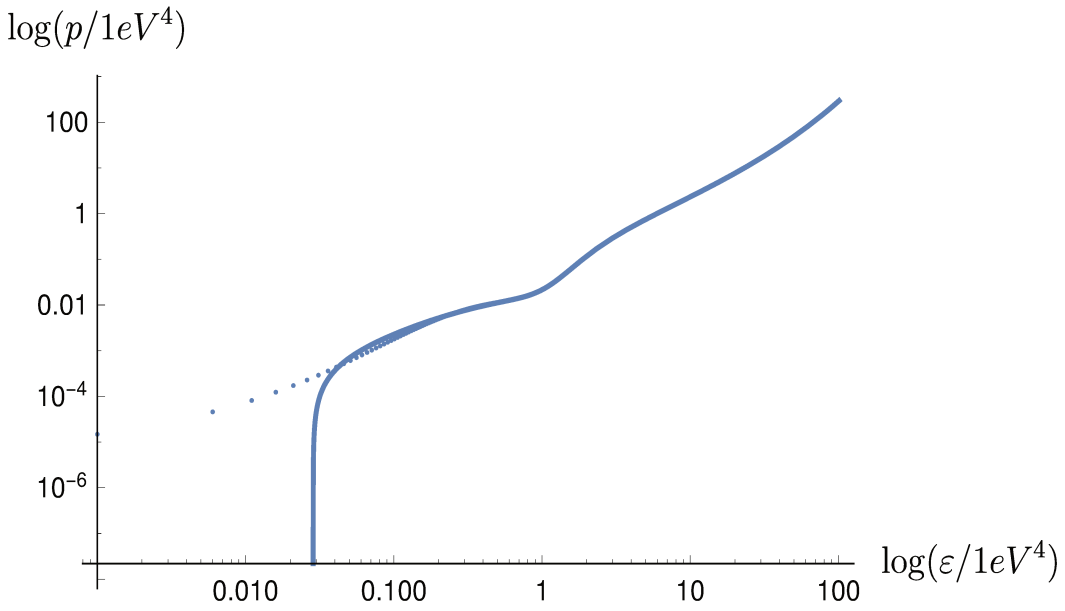

Figure 15 – Data points from the function pressure in terms of energy density and its respective log-log fit.

$$
\begin{aligned}
p' \quad & SU(N_c)\left(\frac{e}{e_c}\right) = -0.070 + 0.012\left(\frac{e}{e_c}\right)^{2.105} + \\
+ \quad & \left[0.001\left(\frac{e}{e_c}\right)^{2.2} - 1.187 * 10^{-6}\left(\frac{e}{e_c}\right)^{4} + 0.018\left(\frac{e}{e_c}\right)\right]\tanh\left(0.058 - 0.128\frac{e}{e_c}\right) - \\
- \quad & 0.108\tanh\left(-0.766 + 1.08\frac{e}{e_c}\right) + \left(1.655 + 0.386\frac{e}{e_c}^{0.3}\right)\tanh\left(-0.001 + 0.056\frac{e}{e_c}\right)
\end{aligned}
\tag{3.15}
$$

It is evident that this fit only reproduces the behaviour of the function for the region $e/e_c \geqslant 3,7.10^{-2}$. However, this accuracy is sufficient because its asymptotic behaviour for $e < e_c$ must be added by hand, regardless of the quality of the fit, since the data points do not get much of that region. The fit we found previously describes well $e/e_c \geqslant 10^{-1}$, while the asymptotic behaviour $p(e) = e/3$ dominates for $e/e_c < 10^{-1}$. Therefore, the final expression for $p_{SU(N_c)}$ is:

$$p_{SU(N_c)}\left(\frac{e}{e_c}\right) = p'_{SU(N_c)}\left(\frac{e}{e_c}\right)\left[\frac{1+\tanh\left(650-\frac{e}{ec}\right)}{2}\right]+\frac{e}{3}\left[\frac{1+\tanh\left(-650+\frac{e}{ec}\right)}{2}\right] \tag{3.16}$$

3.5 Results

3.5.1 Rewriting the Friedmann equations

Despite the simplifications performed in the equation of state of the $SU(N_c)$ plasma in the previous section, it is still computationally demanding to solve the Friedmann equations. The system has to deal with intricate, although analytic, expressions and derivatives of first and second order in coupled equations. To mitigate this situation, we rewrite Friedmann equations (1.15) in terms of the conformal time $d\tau = \dfrac{dt}{a(t)}$. Noting that:

$$\begin{aligned} \dot{a}(t) &= \frac{da}{d\tau}\frac{d\tau}{dt} = \frac{1}{a}\frac{da}{d\tau} = \frac{a'}{a} \\ \ddot{a}(t) &= \frac{d}{dt}(\dot{a}) = \left(\frac{1}{a}\right)^2\frac{d^2a}{d\tau^2} - \frac{1}{a^3}\left(\frac{da}{d\tau}\right)^2 \end{aligned} \tag{3.17}$$

and defining $\dfrac{da}{d\tau} = a'$ [28], we find:

$$\begin{aligned} \left(\frac{a'}{a}\right)^2 &= 2\alpha\varepsilon a^2 - k \\ \frac{a''}{a} &= \alpha(\varepsilon - 3p)a^2 - k \\ \varepsilon' + & \ 3\frac{a'}{a}(\varepsilon + p) = 0 \end{aligned} \tag{3.18}$$

where α stands for the constant $\dfrac{4\pi G}{3}$. The third relation in 3.18 comes from the equation of conservation of energy 1.17. This system can be further simplified:

$$\begin{aligned} f &= \frac{a'}{a} \\ f' + f^2 &= \frac{1}{2}\left(\frac{\varepsilon - 3p}{\varepsilon}\right)(f^2 + k) - k \end{aligned} \tag{3.19}$$

It is now necessary to replace pressure p for the effective pressure p^* to account for the bulk viscosity peak. In conformal time coordinates this is:

$$p^* = p_{SU(N_c)} - 3g(\varepsilon)\varepsilon^{3/4}\frac{f}{a} + \frac{\varepsilon}{3} \tag{3.20}$$

Now, the adapted Friedmann equations for an universe with bulk viscosity in conformal time are given by equation 3.21. This is the system of equations one has to solve to find the evolution of the scale factor a with time and calculate the number of efoldings for a specific equation of state.

$$\begin{aligned} f &= \frac{a'}{a} \\ f' + f^2 &= -3\alpha a^2\left(p_{SU(N_c)} - \frac{6g(\varepsilon)f^2\alpha\varepsilon^{7/4}}{f^2+k}\right) - k \end{aligned} \tag{3.21}$$

Here, $g(\varepsilon)$ represents the bulk viscosity peak. As mentioned in section 2.3, we do not have enough experimental data to parametrize this quantity, therefore, we will use a Gaussian function as a first approximation (3.22). We know it peaks at the critical temperature T_c, represented here by the critical energy ε_c. A and B are free parameters, corresponding, respectively, to the Gaussian's height and width.

$$g(\varepsilon) = A\exp\left[-B\left(\frac{\varepsilon}{\varepsilon_c} - 1\right)^2\right] \tag{3.22}$$

3.5.2 Solving the Friedmann equations

It can be shown that the expression for the number of efoldings does not change in conformal time, remaining equation 1.29. Therefore, we solve Friedmann equations 3.21 to find $a(\tau_f)$ and $a(\tau_i)$, τ_f representing the conformal time Inflation ended and τ_i, the conformal time Inflation began. We are also interested in the evolution of the effective pressure with conformal time, because we want to investigate whether there is a graceful exit for Inflation.

Graphically, the Inflationary and the decelerating Friedmann expansions can be identified by the behaviour of the effective pressure. When this quantity gets negative, it means that the bulk viscosity peak is bigger than the $SU(N_c)$ pressure, producing Inflation. As the bulk viscosity peak diminishes, the effective pressure should return to positive values, indicating that Inflation is over. However, this reasoning can not be reversed to find the desirable parameters for the bulk viscosity peak because, as seen in equation 3.20, the bulk viscosity term in the effective pressure is multiplied by the scale factor and its derivative. We also highlight that, although the quantities A and B in equation 3.22 are somehow related to the number of colours N_c of the equations of state considered, this dependence is not obvious and it was not investigated in this study.

Initial conditions

The last information we need to provide the software for the resolution of the Friedmann equations are the initial conditions of the system. As mentioned in section 1.4, the initial time for Inflation is usually set to Planck time. Following this indication, we consider $\tau_i = -10^{-20}\text{MeV}^{-1} \approx t_P$. Note that conformal times before and during Inflation are negative due to the choice of the origin of the coordinate system [28].

To find the initial conditions for the scale factor a and the auxiliary function $f = \frac{da}{d\tau}\frac{1}{a}$, we must solve Friedmann equations for $\tau_i = -10^{-20}$, this is, in the asymptotic limit of the equation of state. Note that in this limit the bulk viscosity Gaussian tends to zero. This system can be further simplified if we choose the curvature of the manifold $k = 0$, in agreement with experimental data from CMB radiation [1]. Thus, the system of equations 3.21 becomes:

$$\begin{aligned} f &= \frac{da}{d\tau}\frac{1}{a} \\ f' &= -\frac{3f^2}{2} \end{aligned} \tag{3.23}$$

It can be solved analytically resulting in:

$$\begin{aligned} f &= \frac{2}{3\tau} \\ a &= \left(\frac{\tau}{10^{38}}\right)^{2/3} \end{aligned} \tag{3.24}$$

The constants were chosen such that $a(\tau_0 = 10^{38}) = 1$, where τ_0 represents nowadays conformal time. Therefore, $f_i = -2/3 * 10^{20}\text{MeV}$ and $a_i = (-10^{-58})^{2/3}$, a dimensionless quantity. Finally, we set the initial energy density to be the Planck energy divided by the Planck volume:

$$\varepsilon_i = \frac{E_p}{l_p^3} = \frac{10^{22}\text{MeV}}{10^{-69}\text{MeV}^{-3}} = 10^{91}\text{MeV}^4 \tag{3.25}$$

Our free parameters N_c and T_c translate themselves in this set of equations as, respectively, the Gaussian parameters A and B and the critical energy density ε_c. We set ε_c to ε_i, $\varepsilon_i * 10^{-1}$, $\varepsilon_i * 10^{-2}$, $\varepsilon_i * 10^{-3}$ and $\varepsilon_i * 10^{-4}$, varying each time the height of the Gaussian, from 10^5 to 10^{-5} in intervals of the power of 10 and holding fixed the width of the Gaussian $B = 100$. This parameter was chosen not to be varied at this moment because it was found that the number of efoldings N_c does not depend much on it. The final time τ_f was set individually to each configuration of A, B and ε_c because different combinations of these values allowed for different regions where the equations were solvable.

The calculation of the number of efoldings, from initial time τ_i to final time τ_f, in this conditions is illustrated in figure 16. Note that there is a region, around $A \geqslant 10^{-1}$, for which

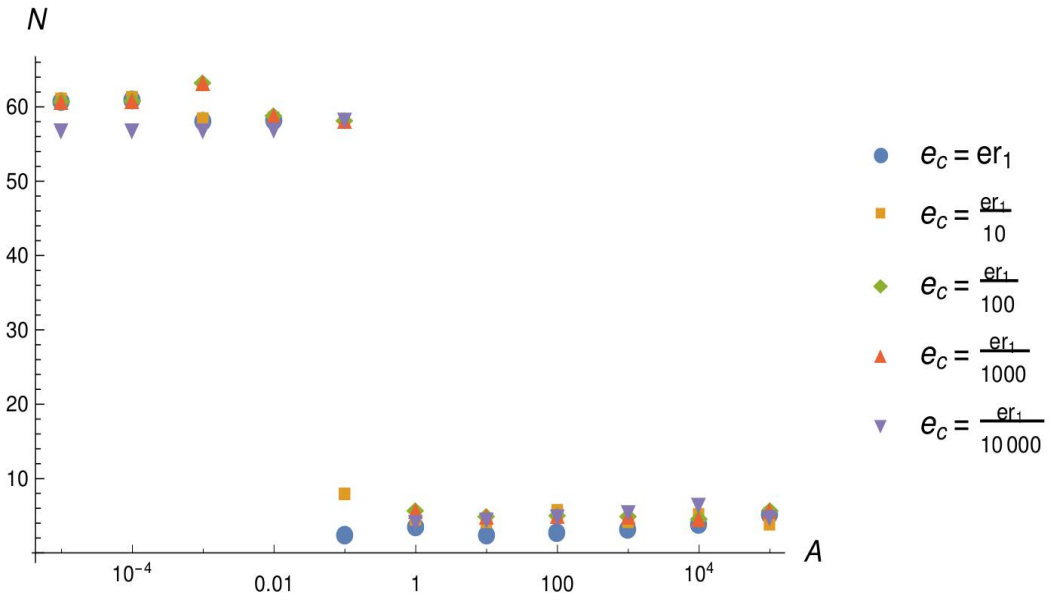

Figure 16 – Number of efoldings in terms of A, the height of the Gaussian representing the bulk viscosity peak, for its width $B = 100$ and critical energy density e_c varying from ε_i to $\varepsilon_i * 10^{-4}$.

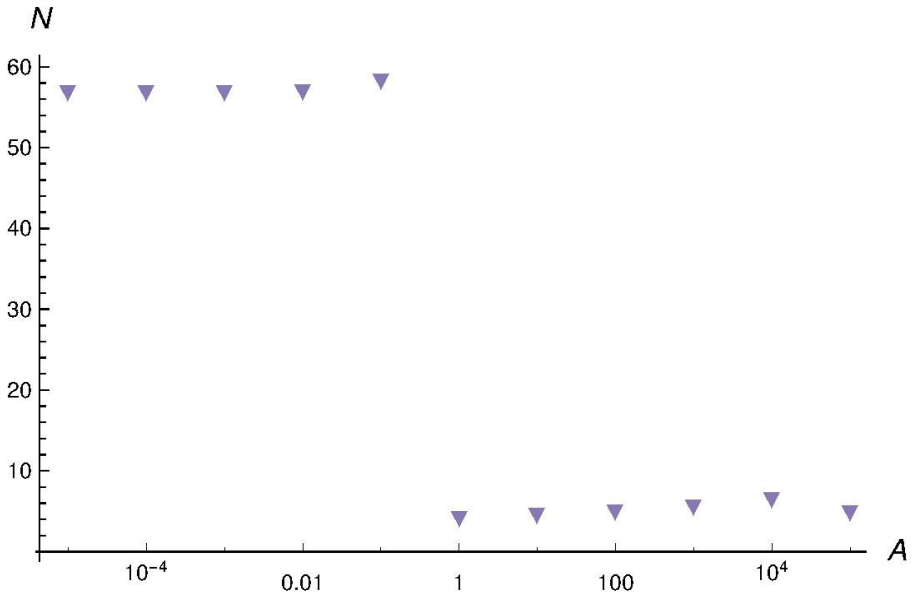

Figure 17 – Number of efoldings in terms of A, the height of the bulk viscosity peak, for its width $B = 100$ and critical energy density $\varepsilon_c = \varepsilon_i * 10^{-4}$.

the number of efoldings is approximately 60. To further investigate this phenomenon, we fixed the critical energy to $\varepsilon_c = \varepsilon_i * 10^{-4}$ and recorded the effective pressure and their respective number of efolds for the same values of the amplitude A investigated previously. The result is shown in figures 17 and 18.

For values of $A \geqslant 1$, the effective pressure gets negative but it never returns to be positive, even after the importance of the bulk viscosity peak is reduced with time. These scenarios fail to reproduce a Friedmann expansion, thus they can not represent our universe. In

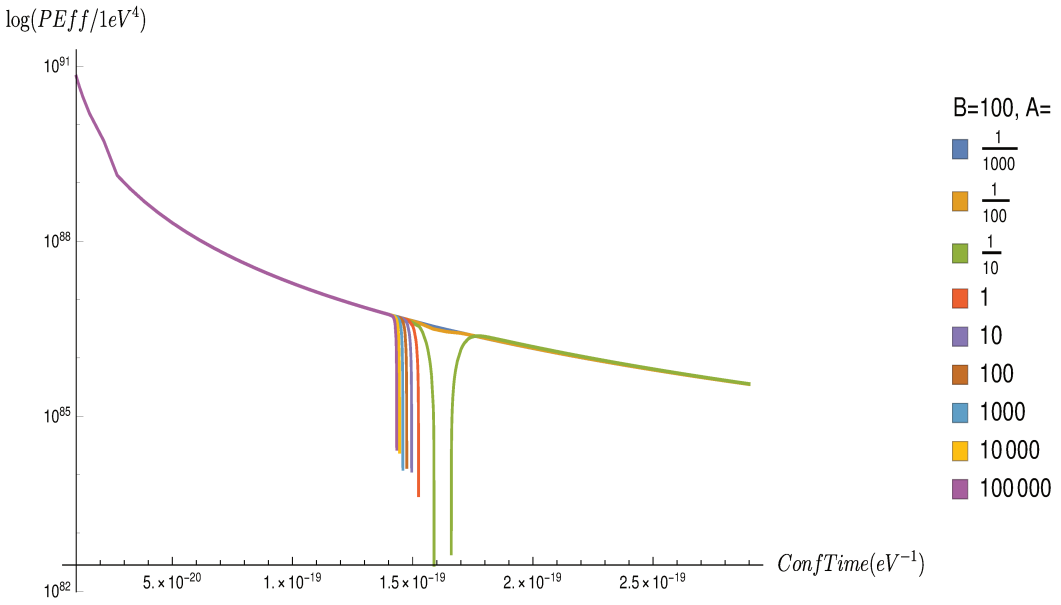

Figure 18 – Logarithm of effective pressure (PEff) in terms of conformal time (ConfTime). Parameter A varying from 10^{-3} to 10^{5}, $B = 100$ and $\varepsilon_c = \varepsilon_i * 10^{-4}$.

addition, they generate a very low number of efoldings, around $N = 6$. For values of $A \leqslant 10^{-1}$, the obtained number of efoldings is around the expected, but the effective pressure never gets negative. This indicates that the height of the bulk viscosity peak is too small compared to the asymptotic limit. Therefore, this expansion is generated by the radiation, which can not expand the universe fast enough to explain its homogeneity and isotropy.

Finally, there is a configuration that produces a reasonable number of efolds ($N = 58$) and where the effective pressure gets negative, eventually returning smoothly to be positive. This happens for $A = 10^{-1}$, $B = 100$ and $\varepsilon_c = \varepsilon_i * 10^{-4}$. However, as the effective pressure is negative for a period of time much smaller than $\tau_f - \tau_i$ - the interval in which we calculated the number of efolds - it is important to re-perform the calculation of the number of efolds, now only accounting for the period where this peak is negative. These results are shown in figure 19.

We can see that for $A \approx 0.33$ it is possible to achieve values of $N \sim \mathcal{O}(10)$, which is reasonable to describe our universe. The existence of those scenarios proves that our inflationary model is capable of generating Inflation with the same characteristics of a scalar-field Inflation regarding the number of efoldings produced and the presence of a smooth transition to a Friedmann expansion.

Further scenarios have been investigated, varying the critical energy density ε_c (figure 20) and the width of the gaussian B (figure 21). Note that, as we vary those parameters, the amplitude at which a minimum value of $N = 10$ is achieved, A_c, also varies. This is particularly evident in figure 22.

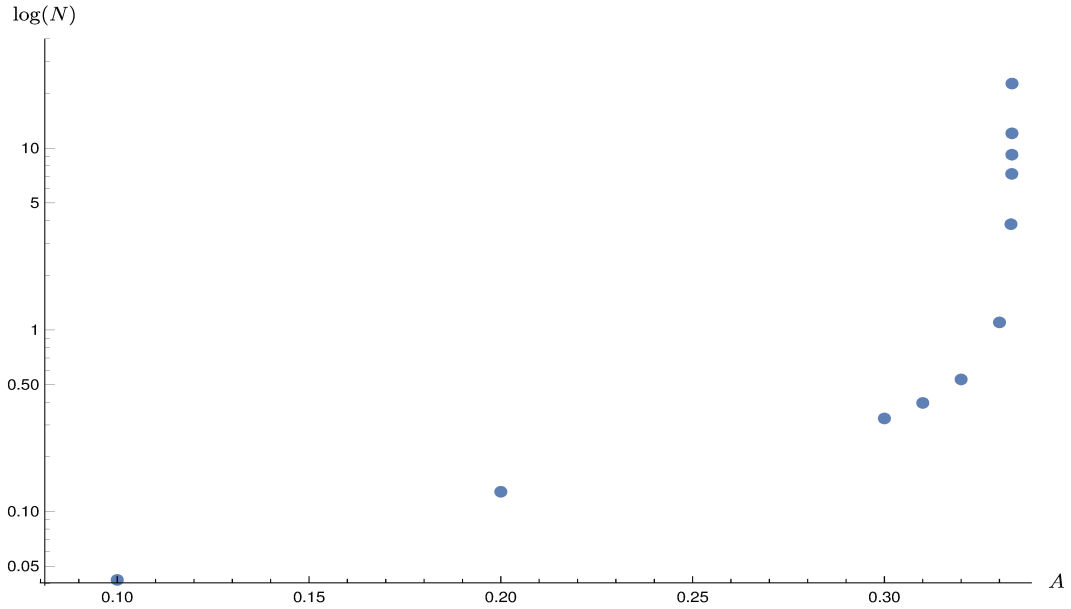

Figure 19 – Number of efoldings in terms of A, the height of the bulk viscosity peak, for its width $B = 100$ and critical energy density $\varepsilon_c = \varepsilon_i * 10^{-4}$, calculated only where the effective pressure is negative.

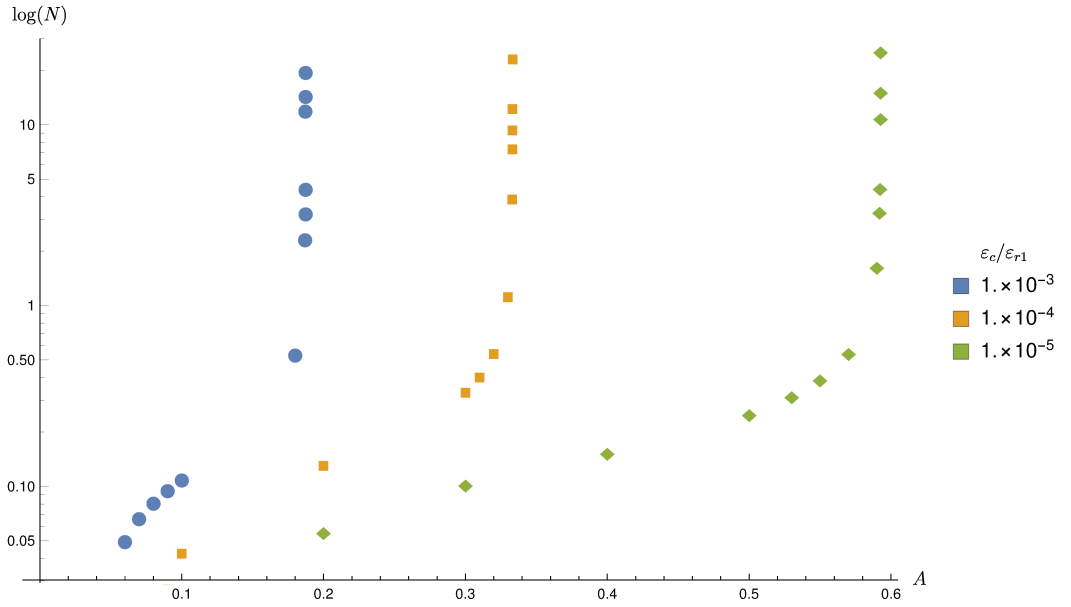

Figure 20 – Number of efoldings in terms of A, the height of the bulk viscosity peak, for width $B = 10$ and critical energy densities $\varepsilon_c = \varepsilon_i * 10^{-3}, \varepsilon_i * 10^{-4}, \varepsilon_i * 10^{-5}$, calculated only where the effective pressure is negative.

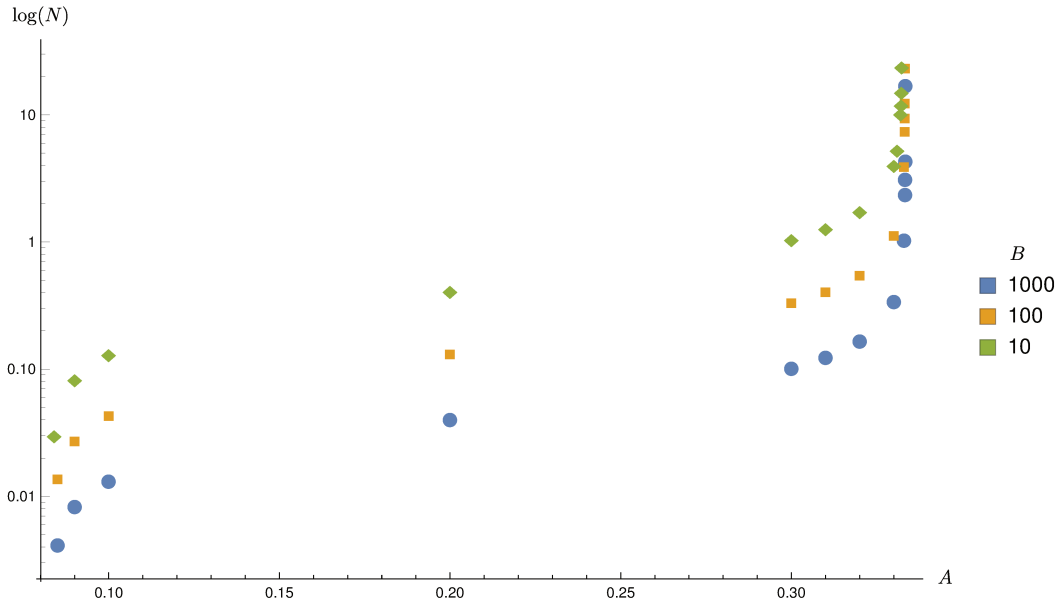

Figure 21 – Number of efoldings in terms of A, the height of the bulk viscosity peak, for widths $B = 10, 100, 1000$ and critical energy density $\varepsilon_c = \varepsilon_i * 10^{-4}$, calculated only where the effective pressure is negative.

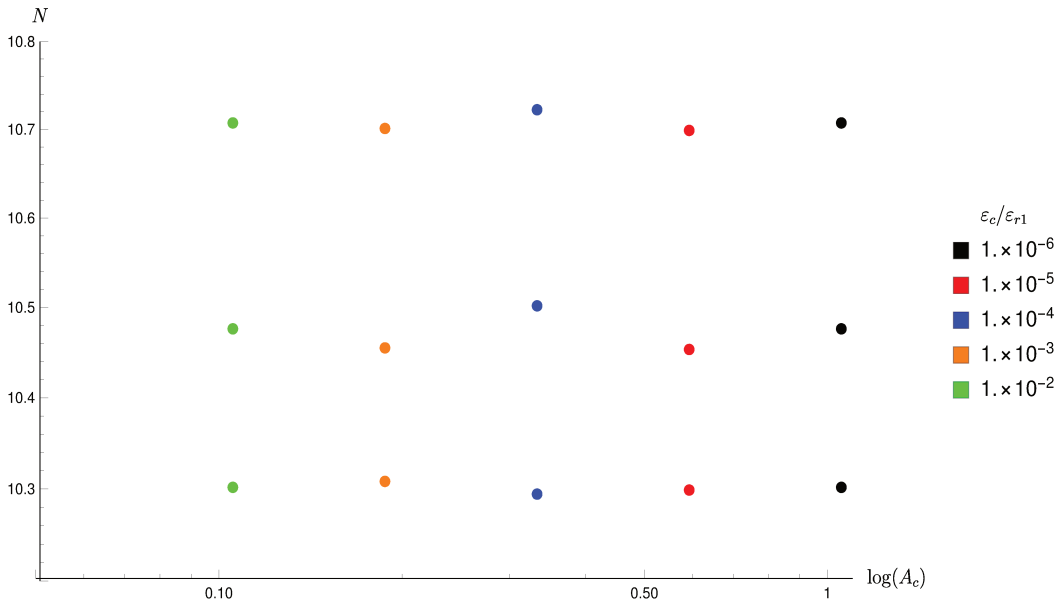

Figure 22 – Number of efoldings in terms of A_c, defined on the text, for width $B = 100$ and various critical energy density ε_c.

4 Conclusions and perspectives

The inflationary model proposed by this work was proven to generate a negative effective pressure, which produced a period of exponential expansion. In addition, in some scenarios, the number of efoldings calculated was compatible with the number produced by the scalar-field Inflation model and a smooth transition from this expansionary regime to a decelerated Friedmann expansion was found. This proves that the model proposed here is equivalent to the Standard Inflationary model, regarding the number of efoldings produced, the presence of two regimes of expansion and a smooth transition between them.

As expected, the number of efoldings and the effective pressure for the different configurations tested were more sensitive to the amplitude A of the Gaussian function representing the bulk viscosity peak than to its width B. This is consistent with the localized nature of the deconfinement transition -consequently, of the bulk viscosity peak- at the the critical temperature T_c. It was also noted that not all configurations of A and B produce negative effective pressure, which indicates that the bulk viscosity peak must overcome the equation of state of the Standard Model $p_r = \varepsilon/3$ to change the effective pressure. Finally, we point out that, within the range $10^{87} \leqslant \varepsilon_c \leqslant 10^{91}$, it was observed little sensibility in the number of efolds to the critical energy density.

We also highlight that the tests performed by this research are preliminary and there are many open questions to be investigated within this proposal. First of all, it is possible that the successful cases described above represent only some points in regions of viable scenarios, found by varying slightly the relevant parameters. It is crucial to specify those regions and their dependence with the gaussian parameters. From this information, one can try to identify the sensibility of the number of efoldings and the smooth transition to the variable parameters.

Another relevant path of investigation is to specify the relation between the free parameters of the model, N_c and T_c, to the variables ε_c and the ones related to the Gaussian, A and B. If this is accomplished, one can use the results found in this work to discover the parameters of the generic Yang-Mills theory proposed here. This allows for a more complete description of the model, in specific regarding the properties of the glueballs, the dark matter candidates.

So far, the extension to the Standard Model proposed by this work has only reproduced indirect consequences of Inflation, therefore, no results in this thesis provide direct evidence of this model correctness. However, even at this initial stage of research, it is possible to falsify this proposal. One of our strongest hypothesis, that this extension is not coupled to the Standard Model, guarantees that no indirect detection of dark matter will ever occur. Any experimental evidence contrary to this claim will force us to revisit one of our central assumptions. In

this same direction, in the future, it is necessary to study the equation of state of the Yang-Mills fluid after the deconfinement transition to calculate the expected density of dark matter particles nowadays. This is an experimentally accessible quantity, determined by CMB observations, thus, reproducing its values would be a test for this model.

Bibliography

1 AL, P. A. R. A. et. Planck 2013 results. xvi. cosmological parameters. *Astronomy and Astrophysics*, v. 571, n. A16, November 2014. Disponível em: <https://arxiv.org/pdf/1303.5076.pdf>.

2 WEINBERG, S. *Gravitation and cosmology: principles and applications of the general theory of relativity*. Cambridge: John Wiley & Sons, 1972. ISBN 0-471-92567-5.

3 CARROLL, S. *Spacetime and Geometry: An Introduction to General Relativity*. San Francisco: Addison Wesley, 2004. ISBN 0-8053-8732-3.

4 MUKHANOV, V. *Physical Foundations of Cosmology*. Cambridge: Cambridge University Press, 2005.

5 LIDDLE, A.; LYTH, D. *Cosmological Inflation and Large-Scale Structure*. Cambridge: Cambridge University Press, 2000. (Cosmological Inflation and Large-scale Structure). ISBN 9780521575980.

6 JI, X. Introduction to qcd and the standard model. Disponível em: <http://www.physics.umd.edu/courses/Phys741/xji/chapter1.pdf>.

7 GROSS, D. J. Gauge theory-past, present, and future? *Chinese Journal of Physics*, v. 30, n. 7, p. 955–972, Dec 1992. ISSN 0577-9073. Disponível em: <http://psroc.org/cjp/issues.php?vol=30&num=7>.

8 GATTRINGER, C. B. L. a. C. *Quantum Chromodynamics on the Lattice: An Introductory Presentation*. 1. ed. Heidelberg: Springer-Verlag Berlin Heidelberg, 2010. (Lecture Notes in Physics 788). ISBN 3642018491,9783642018497.

9 SATZ, H. The thermodynamics of quarks and gluons. In: ____. Heidelberg: Springer Berlin Heidelberg, 2009. (Lecture Notes in Physics, The Physics of the Quark-Gluon Plasma: Introductory Lectures), cap. 1, p. 1–21. ISBN 978-3-642-02286-9.

10 KARSCH, F.; LAERMANN, E.; PEIKERT, A. The pressure in 2, 2+1 and 3 flavour qcd. *Physics Letters B*, v. 478, n. 4, p. 447 – 455, 2000. ISSN 0370-2693. Disponível em: <http://www.sciencedirect.com/science/article/pii/S0370269300002926>.

11 PAQUET, J.-F.; SHEN, C.; DENICOL, G. S.; LUZUM, M.; SCHENKE, B.; JEON, S.; GALE, C. Production of photons in relativistic heavy-ion collisions. *Physical Review C*, American Physical Society (APS), v. 93, n. 4, Apr 2016. ISSN 2469-9993. Disponível em: <http://dx.doi.org/10.1103/PhysRevC.93.044906>.

12 PAQUET, J.-F. *Characterizing the non-equilibrium quark-gluon plasma with photons and hadrons*. Tese (Doutorado) — McGill University, Montreal, September 2015. Disponível em: <http://digitool.library.mcgill.ca/R/8CXERVXY2MYIK9CVQG394628MSFHQKUHME67N2V83QE5KTVLYH-09382?func=results-jump-full&set_entry=000001&set_number=001612&base=GEN01>.

13 KAJANTIE, K.; KAPUSTA, J.; MCLERRAN, L.; MEKJIAN, A. Dilepton emission and the qcd phase-transition in ultrarelativistic nuclear collisions. *Physical Review D*, v. 34, n. 9, p. 2746–2754, nov. 1986.

14 AL, K. et. The review of particle physics. *Chin. Phys. C*, v. 38, n. 090001, 2014. Disponível em: <http://pdg.lbl.gov/2015/>.

15 LUCINI, B.; PANERO, M. Introductory lectures to large-n qcd phenomenology and lattice results. *Progress in Particle and Nuclear Physics*, v. 75, n. Supplement C, p. 1 – 40, 2014. ISSN 0146-6410. Disponível em: <http://www.sciencedirect.com/science/article/pii/S0146641014000027>.

16 VERA, M. F. G. *Investigating the large N limit of SU(N) Yang-Mills gauge theories on the lattice*. Tese (Doutorado) — Humboldt-Universitat zu Berlin, Mathematisch-Naturwissenschaftliche Fakultat, Berlin, June 2017. Disponível em: <https://edoc.hu-berlin.de/handle/18452/18793>.

17 LUCINI, B.; TEPER, M. Su(n) gauge theories in four-dimensions: Exploring the approach to n = infinity. *JHEP*, v. 06, p. 050, 2001. Disponível em: <https://arxiv.org/pdf/hep-lat/0103027.pdf>.

18 LUCINI, B.; TEPER, M.; WENGER, U. Properties of the deconfining phase transition in su(n) gauge theories. *JHEP*, v. 02, p. 033, 2005. Disponível em: <https://arxiv.org/pdf/hep-lat/0502003.pdf>.

19 LUCINI, B.; RAGO, A.; RINALDI, E. Su(n_c) gauge theories at deconfinement. *Phys. Lett.*, B712, p. 279–283, 2012. Disponível em: <https://arxiv.org/pdf/1202.6684.pdf>.

20 DATTA, S.; GUPTA, S. Continuum thermodynamics of the $gluon_c$ plasma. *Phys. Rev.*, D82, p. 114505, 2010. Disponível em: <https://arxiv.org/pdf/1006.0938.pdf>.

21 PANERO, M. Thermodynamics of the qcd plasma and the large-n limit. *Phys. Rev. Lett.*, v. 103, p. 232001, 2009. Disponível em: <https://arxiv.org/pdf/0907.3719.pdf>.

22 KARSCH, F.; KHARZEEV, D.; TUCHIN, K. Universal properties of bulk viscosity near the qcd phase transition. *Phys. Lett.*, B663, p. 217–221, 2008. Disponível em: <https://arxiv.org/pdf/0711.0914.pdf>.

23 MEYER, H. B. A calculation of the bulk viscosity in su(3) gluodynamics. *Phys. Rev. Lett.*, v. 100, p. 162001, 2008. Disponível em: <https://arxiv.org/pdf/0710.3717.pdf>.

24 KHARZEEV, D.; TUCHIN, K. Bulk viscosity of qcd matter near the critical temperature. *Journal of High Energy Physics*, v. 2008, n. 09, p. 093, 2008. Disponível em: <http://iopscience.iop.org/article/10.1088/1126-6708/2008/09/093/pdf>.

25 PAECH, K.; PRATT, S. Origins of bulk viscosity in relativistic heavy ion collisions. *Phys. Rev. C*, American Physical Society, v. 74, p. 014901, Jul 2006. Disponível em: <https://arxiv.org/pdf/nucl-th/0604008.pdf>.

26 HARUTYUNYAN, A.; RISCHKE, D. H.; SEDRAKIAN, A. Transport coefficients of two-flavor quark matter from the kubo formalism. *Phys. Rev.*, D95, n. 11, p. 114021, 2017. Disponível em: <https://arxiv.org/pdf/1702.04291.pdf>.

27 MEYER, H. B. A calculation of the shear viscosity in su(3) gluodynamics. *Phys. Rev.*, D76, p. 101701, 2007. Disponível em: <https://arxiv.org/pdf/0704.1801.pdf>.

28 BAUMANN, D. Cosmology, part iii mathematical tripos. Disponível em: <http://www.damtp.cam.ac.uk/user/db275/Cosmology/Lectures.pdf>.

29 GARRETT, K.; DUDA, G. Dark Matter: A Primer. *Adv. Astron.*, v. 2011, p. 968283, 2011.

30 ROTT, C. Status of dark matter searches (rapporteur talk). *PoS ICRC*, n. 1119, 2017. Disponível em: <https://arxiv.org/abs/1712.00666>.

31 KOLB, E.; TURNER, M. *The Early Universe*. [S.l.]: Avalon Publishing, 1994. v. 69. (Frontiers in physics, v. 69). ISBN 9780813346458.

Appendix

APPENDIX A – Codes for the numerical calculations

```
SU3data = {{0.801742, 0.001074}, {0.811087, 0.025189}, {0.820493, 0.051497},
   {0.829959, 0.025627}, {0.839485, 0.000632}, {0.849072, 0.013656},
   {0.858719, 0.091965}, {0.868426, 0.076393}, {0.878192, 0.036275},
   {0.888019, -0.01272}, {0.897904, 0.002379}, {0.90785, 0.059816},
   {0.917854, 0.034798}, {0.927917, 0.05017}, {0.938039, 0.089943},
   {0.94822, 0.060019}, {0.95846, 0.125736}, {0.968758, 0.146868},
   {0.979114, 0.193744}, {0.989528, 0.396226}, {1., 0.721148},
   {1.01053, 0.962336}, {1.021117, 1.128489}, {1.031762, 1.230001},
   {1.042464, 1.258942}, {1.053223, 1.331593}, {1.064039, 1.374322},
   {1.074912, 1.287931}, {1.085841, 1.328149}, {1.096827, 1.345659},
   {1.107869, 1.289628}, {1.118968, 1.289898}, {1.130122, 1.296408},
   {1.141332, 1.272211}, {1.152597, 1.251725}, {1.163918, 1.257515},
   {1.175294, 1.237645}, {1.186726, 1.213716}, {1.198212, 1.17597},
   {1.209754, 1.145387}, {1.22135, 1.169127}, {1.233, 1.123933}, {1.244705, 1.072},
   {1.256465, 1.088117}, {1.268278, 1.052175}, {1.280146, 1.062387},
   {1.292067, 1.019255}, {1.304043, 1.006715}, {1.316071, 0.989344},
   {1.328154, 0.976319}, {1.34029, 0.956389}, {1.352479, 0.902937},
   {1.364721, 0.900721}, {1.377017, 0.907807}, {1.389365, 0.847448},
   {1.401767, 0.868257}, {1.414221, 0.801243}, {1.426728, 0.812699},
   {1.439288, 0.787744}, {1.4519, 0.807947}, {1.464565, 0.782323},
   {1.477283, 0.765474}, {1.490053, 0.705317}, {1.502875, 0.698136},
   {1.515749, 0.680372}, {1.528676, 0.694201}, {1.541656, 0.703567},
   {1.554687, 0.691247}, {1.567771, 0.65708}, {1.580907, 0.656823},
   {1.594096, 0.651981}, {1.607336, 0.63649}, {1.620629, 0.611744},
   {1.633974, 0.614611}, {1.647372, 0.610956}, {1.660822, 0.623653},
   {1.674324, 0.582151}, {1.687879, 0.550757}, {1.701487, 0.573398},
   {1.715147, 0.545812}, {1.72886, 0.563714}, {1.742626, 0.54762},
   {1.756444, 0.513408}, {1.770316, 0.504704}, {1.784241, 0.504296},
   {1.798219, 0.497836}, {1.81225, 0.483539}, {1.826336, 0.462899},
   {1.840474, 0.479329}, {1.854667, 0.457971}, {1.868914, 0.48051},
   {1.883215, 0.467682}, {1.897571, 0.451446}, {1.911981, 0.440689},
   {1.926447, 0.442527}, {1.940967, 0.414185}, {1.955543, 0.406184},
   {1.970175, 0.37693}, {1.984863, 0.381541}, {1.999606, 0.382047},
   {2.014407, 0.406013}, {2.029264, 0.408479}, {2.044179, 0.410644},
   {2.059151, 0.374339}, {2.074181, 0.394612}, {2.089269, 0.364649},
   {2.104415, 0.380211}, {2.119621, 0.339312}, {2.134886, 0.368773},
   {2.150211, 0.360224}, {2.165597, 0.373108}, {2.181043, 0.391337},
   {2.19655, 0.350445}, {2.212118, 0.357035}, {2.227749, 0.35291},
   {2.243443, 0.339672}, {2.2592, 0.320994}, {2.27502, 0.34895},
   {2.290905, 0.316548}, {2.306854, 0.311759}, {2.322869, 0.32495},
   {2.33895, 0.312037}, {2.355097, 0.302527}, {2.371312, 0.312755},
   {2.387594, 0.29494}, {2.403945, 0.279982}, {2.420366, 0.31139},
   {2.436856, 0.289751}, {2.453417, 0.284341}, {2.470049, 0.289815},
   {2.486754, 0.266598}, {2.503531, 0.294358}, {2.520382, 0.2736},
   {2.537308, 0.265359}, {2.554309, 0.267216}, {2.571386, 0.250913},
   {2.58854, 0.259511}, {2.605773, 0.259524}, {2.623084, 0.246865},
   {2.640474, 0.235416}, {2.657946, 0.262268}, {2.675499, 0.218737},
   {2.693135, 0.236759}, {2.710855, 0.218018}, {2.728659, 0.247995},
```

```
    {2.746549, 0.238522}, {2.764526, 0.217894}, {2.782591, 0.198552},
    {2.800744, 0.236603}, {2.818988, 0.221255}, {2.837324, 0.202357},
    {2.855752, 0.226609}, {2.874273, 0.175664}, {2.89289, 0.209898},
    {2.911603, 0.226011}, {2.930414, 0.198542}, {2.949323, 0.187839},
    {2.968332, 0.18637}, {2.987443, 0.173721}, {3.006657, 0.196118},
    {3.025975, 0.178129}, {3.045399, 0.154842}, {3.06493, 0.173641},
    {3.08457, 0.150514}, {3.10432, 0.183898}, {3.124182, 0.173504},
    {3.144157, 0.173424}, {3.164247, 0.173324}, {3.184453, 0.160808},
    {3.204778, 0.161083}, {3.225223, 0.189858}, {3.245789, 0.175179},
    {3.266479, 0.116076}, {3.287293, 0.141001}, {3.308235, 0.156441},
    {3.329306, 0.138471}, {3.350507, 0.170139}, {3.371841, 0.157327},
    {3.393309, 0.149694}, {3.414914, 0.141905}, {3.436657, 0.110058}};

SU3error = {0.018787, 0.033356, 0.031306, 0.026917, 0.034604, 0.027728, 0.027815,
    0.019878, 0.020881, 0.030212, 0.024332, 0.021534, 0.022975, 0.02678, 0.016324,
    0.032323, 0.031724, 0.053071, 0.048587, 0.099183, 0.035906, 0.059078, 0.032809,
    0.032754, 0.015116, 0.020192, 0.013569, 0.029283, 0.02245, 0.012014, 0.012332,
    0.01524, 0.02166, 0.012161, 0.016245, 0.015226, 0.015885, 0.017655, 0.012538,
    0.020704, 0.017557, 0.014745, 0.015301, 0.017371, 0.018573, 0.023682, 0.007466,
    0.018229, 0.010446, 0.020911, 0.018078, 0.031046, 0.021827, 0.022625, 0.021786,
    0.025026, 0.030749, 0.018882, 0.018723, 0.026785, 0.015677, 0.02412, 0.026118,
    0.017227, 0.023937, 0.026415, 0.023033, 0.015797, 0.014072, 0.012144, 0.014988,
    0.021954, 0.01685, 0.020172, 0.023724, 0.010682, 0.017848, 0.0186, 0.023984,
    0.01622, 0.015919, 0.018467, 0.023742, 0.014241, 0.020862, 0.026435, 0.01966,
    0.018321, 0.012384, 0.020431, 0.01993, 0.007451, 0.015144, 0.016943, 0.017901,
    0.023223, 0.01456, 0.019299, 0.018255, 0.017668, 0.018569, 0.021977, 0.017858,
    0.014817, 0.010884, 0.013159, 0.005978, 0.015366, 0.012744, 0.019274, 0.012446,
    0.008912, 0.016025, 0.013166, 0.019093, 0.010801, 0.009405, 0.013794,
    0.011625, 0.014733, 0.012078, 0.016136, 0.015554, 0.01458, 0.016562, 0.021586,
    0.010583, 0.011091, 0.017093, 0.017061, 0.00866, 0.019435, 0.012149, 0.016967,
    0.015269, 0.021453, 0.008995, 0.021126, 0.021491, 0.01656, 0.015382, 0.016379,
    0.01068, 0.015295, 0.014404, 0.013583, 0.010035, 0.01165, 0.013251, 0.013763,
    0.014495, 0.013899, 0.012627, 0.014292, 0.01315, 0.014578, 0.016968, 0.019408,
    0.008625, 0.015302, 0.020574, 0.014381, 0.015943, 0.018389, 0.017381, 0.016045,
    0.017144, 0.016685, 0.016202, 0.01413, 0.020431, 0.015291, 0.008146, 0.014739,
    0.014784, 0.014499, 0.015389, 0.015421, 0.011557, 0.019841, 0.012443};

Clear[f, g, h, x, a, b, c, d, e, fit]

f[x_] := (Tanh[(x - 1) / a] + 1) / 2;
g[x_] := (Tanh[(1 - x) / a] + 1) / 2;
h[x_] := b (x^c) g[x] + d (x^-e) f[x];

SU3error2 = 1 / (SU3error^2);

fit = NonlinearModelFit[SU3data, h[x], {a, b, c, d, e},
  x, VarianceEstimatorFunction → (1 &), Weights → SU3error2]
```

$$\text{FittedModel}\left[-0.144608\, x^{43.2918}\,(1+\text{Tanh}[27.9118\,(1-x)])+\frac{0.852846\,(1+\text{Tanh}[27.9118\,(-1+x)])}{x^{2.03235}}\right]$$

```
Show[ListPlot[SU3data], Plot[fit[x], {x, -2, 4}], Frame → True]
```

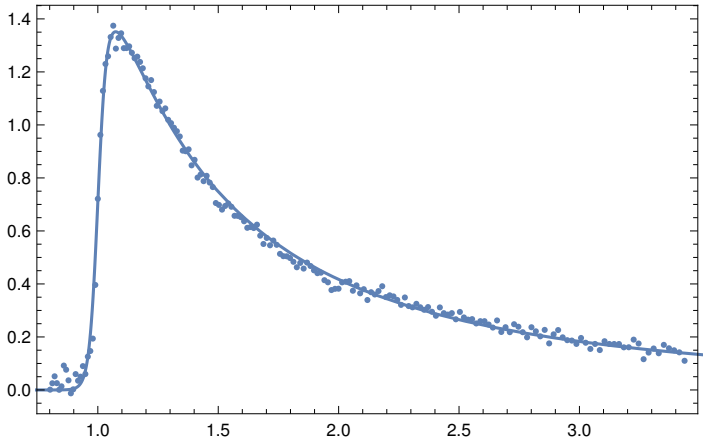


```
fit["AdjustedRSquared"]
```

```
0.998708
```

```
(*finding an inverse function for e(T), using the unfitted expressions*)

Clear[f, g, h, h2, energy, press, pressure, inv, u, data, data2, merged, fit, fit2]

f[x_] := -0.14460764377951374 x^43.29179403782954 (1 + Tanh[27.911759831465123 (1 - x)]) +
   (0.8528461795749493 (1 + Tanh[27.911759831465123 (-1 + x)])) / x^2.032352696537285
(* trace of energy-momentum tensor from SU(3) data *)
g[x_] := f[x] / x
press[y_?NumberQ] := NIntegrate[g[x], {x, 0, y}, Method -> "LocalAdaptive"]
pressure[T_] := (T^4) press[T] (*pressure from numerical integration*)

energy[T_] := f[T] (T^4) + 3 pressure[T] (*energy, from numerical integration*)

LogPlot[{energy[T], pressure[T], pressure[T] / energy[T]},
 {T, 0, 6}, PlotLegends → "Expressions", PlotRange → All]
```

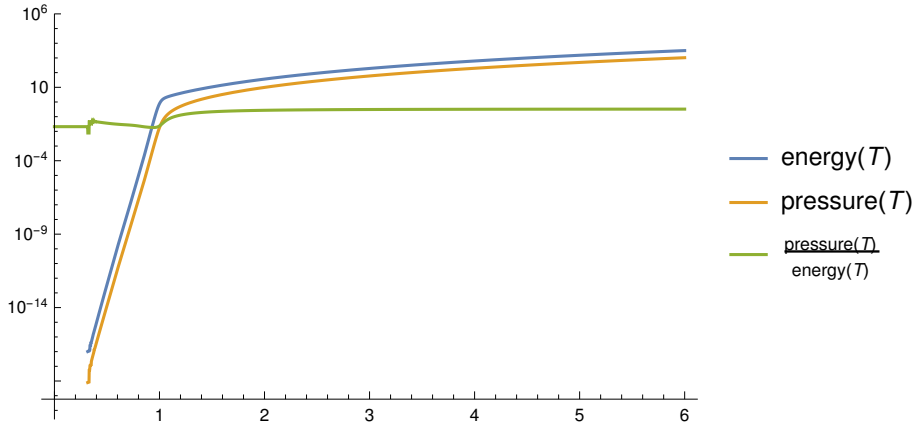


```
LogLogPlot[energy[T], {T, 10^(-6), 10^2}, PlotRange → All,
 PlotLabel → "Energia x temperatura", AxesLabel → {T, e}]
```

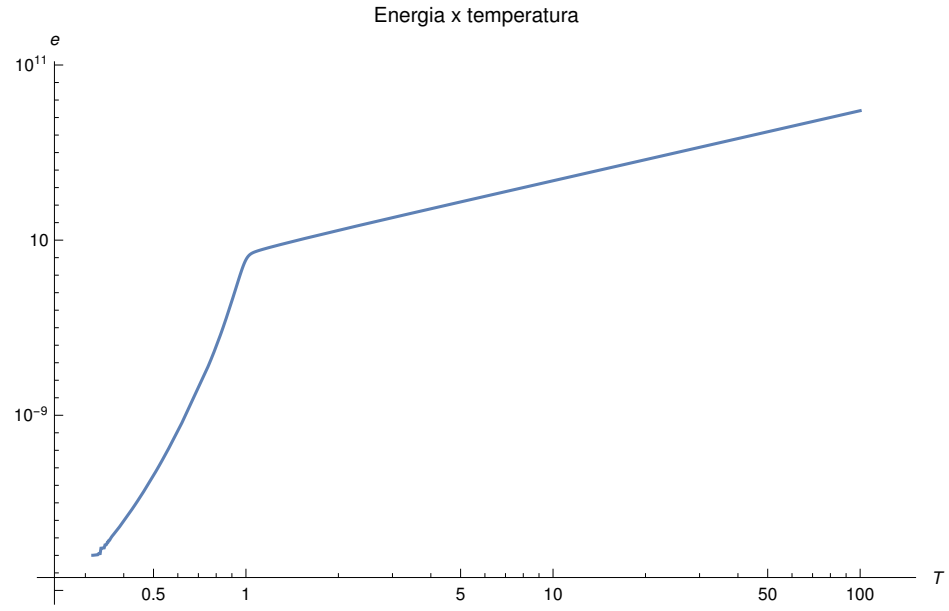


```
(*as f(x) was fitted with Exp(x), we must continue to use that here*)
```

```
LogPlot[{energy[Exp[T]], pressure[Exp[T]], pressure[Exp[T]] / energy[Exp[T]]},
 {T, 0, 6}, PlotLegends → "Expressions", PlotRange → All]
```

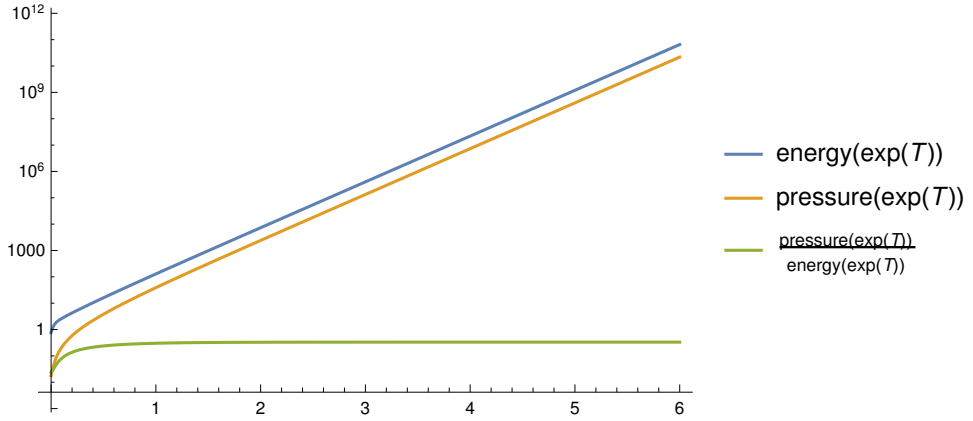


```
inv[f_, s_] := Function[{t}, s /. FindRoot[f - t, {s, 1}]]
(*code from Mathematica to invert the functions*)
u = inv[energy[Exp[T]], T] (*T[energy]*)
```

```
Function[{t$},
 T /. FindRoot[(3 ℯ^(4 T) press[ℯ^T] + ℯ^(4 T) (-0.144608 (ℯ^T)^43.2918 (1 + Tanh[27.9118 (1 - ℯ^T)]) +
       0.852846 (1 + Tanh[27.9118 (-1 + ℯ^T)]))/(ℯ^T)^2.03235) - t$, {T, 1}]]
```

```
u[energy[Exp[0.1]]] (*it seems good*)
```

```
0.1
```

```
LogPlot[u[x], {x, 10^(-8), 10^2}, PlotRange → All,
 PlotLabel → "Temperatura x energia", AxesLabel → {e, T}]
```

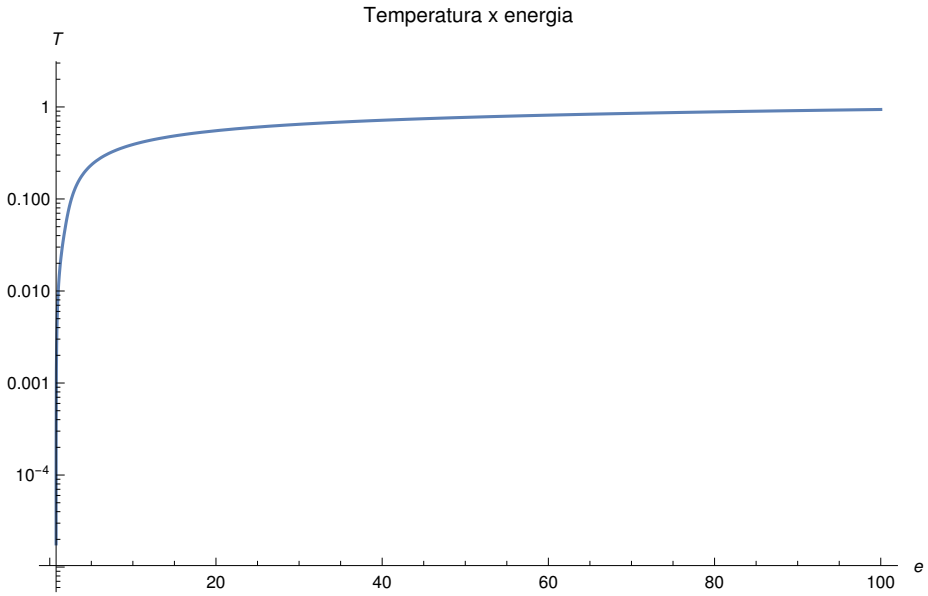

```
(*u[x] is the inverse function and it looks very much like a tanh[x]*)

LogPlot[Tanh[0.5 * x] / 3, {x, 0, 10}, PlotRange → All]
```

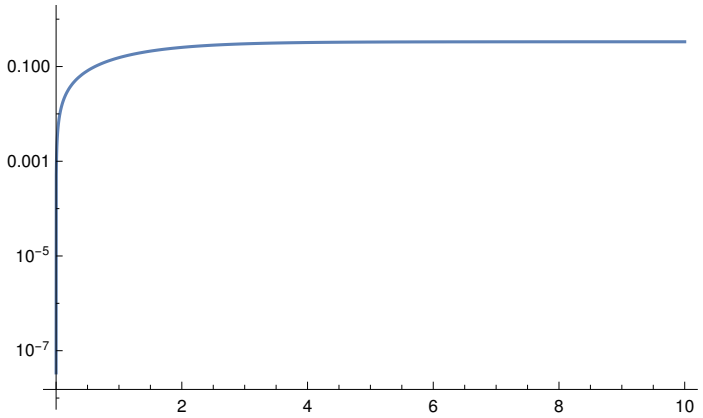


```
(*let's try to fit it*)

data = Table[u[x], {x, 10^(-3), 10, 0.05}];
data2 = Table[x, {x, 10^(-3), 10, 0.05}];

Do[
    Sow[
     Flatten[ReplacePart[{a, b}, {1 → Take[data2, {u}], 2 → Take[data, {u}]
       }]

     ]],
    {u, 1, 161, 1}
   ] // Reap // Last;
```

merged = %[[1]]

```
{{0.001, -0.127971}, {0.051, -0.0567367}, {0.101, -0.044241}, {0.151, -0.0366665},
 {0.201, -0.0311066}, {0.251, -0.0266442}, {0.301, -0.0228694},
 {0.351, -0.0195628}, {0.401, -0.0165928}, {0.451, -0.0138741}, {0.501, -0.011348},
 {0.551, -0.00897201}, {0.601, -0.00671437}, {0.651, -0.00455043},
 {0.701, -0.00246055}, {0.751, -0.000428583}, {0.801, 0.001559},
 {0.851, 0.00351387}, {0.901, 0.0054463}, {0.951, 0.00736551}, {1.001, 0.00928002},
 {1.051, 0.0111978}, {1.101, 0.0131264}, {1.151, 0.0150734}, {1.201, 0.0170458},
 {1.251, 0.0190511}, {1.301, 0.0210964}, {1.351, 0.0231891}, {1.401, 0.0253367},
 {1.451, 0.0275466}, {1.501, 0.0298263}, {1.551, 0.032183}, {1.601, 0.0346238},
 {1.651, 0.0371551}, {1.701, 0.0397824}, {1.751, 0.0425101}, {1.801, 0.0453409},
 {1.851, 0.0482756}, {1.901, 0.0513128}, {1.951, 0.0544484}, {2.001, 0.0576762},
 {2.051, 0.0609877}, {2.101, 0.0643727}, {2.151, 0.0678195}, {2.201, 0.0713163},
 {2.251, 0.074851}, {2.301, 0.0784121}, {2.351, 0.081989}, {2.401, 0.0855722},
 {2.451, 0.0891536}, {2.501, 0.0927262}, {2.551, 0.0962841}, {2.601, 0.0998226},
 {2.651, 0.103338}, {2.701, 0.106827}, {2.751, 0.110287}, {2.801, 0.113718},
 {2.851, 0.117116}, {2.901, 0.120482}, {2.951, 0.123814}, {3.001, 0.127113},
 {3.051, 0.130378}, {3.101, 0.133608}, {3.151, 0.136805}, {3.201, 0.139968},
 {3.251, 0.143097}, {3.301, 0.146192}, {3.351, 0.149255}, {3.401, 0.152284},
 {3.451, 0.155281}, {3.501, 0.158247}, {3.551, 0.16118}, {3.601, 0.164083},
 {3.651, 0.166955}, {3.701, 0.169796}, {3.751, 0.172608}, {3.801, 0.17539},
 {3.851, 0.178143}, {3.901, 0.180868}, {3.951, 0.183565}, {4.001, 0.186234},
 {4.051, 0.188877}, {4.101, 0.191492}, {4.151, 0.194081}, {4.201, 0.196644},
 {4.251, 0.199182}, {4.301, 0.201695}, {4.351, 0.204183}, {4.401, 0.206647},
 {4.451, 0.209087}, {4.501, 0.211504}, {4.551, 0.213897}, {4.601, 0.216268},
 {4.651, 0.218617}, {4.701, 0.220944}, {4.751, 0.223249}, {4.801, 0.225533},
 {4.851, 0.227796}, {4.901, 0.230039}, {4.951, 0.232261}, {5.001, 0.234464},
 {5.051, 0.236647}, {5.101, 0.238811}, {5.151, 0.240956}, {5.201, 0.243082},
 {5.251, 0.24519}, {5.301, 0.24728}, {5.351, 0.249352}, {5.401, 0.251407},
 {5.451, 0.253444}, {5.501, 0.255465}, {5.551, 0.257469}, {5.601, 0.259456},
 {5.651, 0.261428}, {5.701, 0.263383}, {5.751, 0.265323}, {5.801, 0.267247},
 {5.851, 0.269157}, {5.901, 0.271051}, {5.951, 0.272931}, {6.001, 0.274796},
 {6.051, 0.276646}, {6.101, 0.278483}, {6.151, 0.280306}, {6.201, 0.282115},
 {6.251, 0.28391}, {6.301, 0.285693}, {6.351, 0.287462}, {6.401, 0.289218},
 {6.451, 0.290962}, {6.501, 0.292693}, {6.551, 0.294412}, {6.601, 0.296118},
 {6.651, 0.297813}, {6.701, 0.299495}, {6.751, 0.301166}, {6.801, 0.302825},
 {6.851, 0.304473}, {6.901, 0.30611}, {6.951, 0.307736}, {7.001, 0.309351},
 {7.051, 0.310955}, {7.101, 0.312548}, {7.151, 0.314131}, {7.201, 0.315703},
 {7.251, 0.317265}, {7.301, 0.318817}, {7.351, 0.320359}, {7.401, 0.321892},
 {7.451, 0.323414}, {7.501, 0.324927}, {7.551, 0.326431}, {7.601, 0.327925},
 {7.651, 0.329409}, {7.701, 0.330885}, {7.751, 0.332352}, {7.801, 0.33381},
 {7.851, 0.335259}, {7.901, 0.336699}, {7.951, 0.33813}, {8.001, 0.339554}}
```

```
Show[LogPlot[{u[x]}, {x, 10^(-3), 10},
  PlotLegends → "Expressions", PlotRange → All] , ListLogPlot[merged]]
```

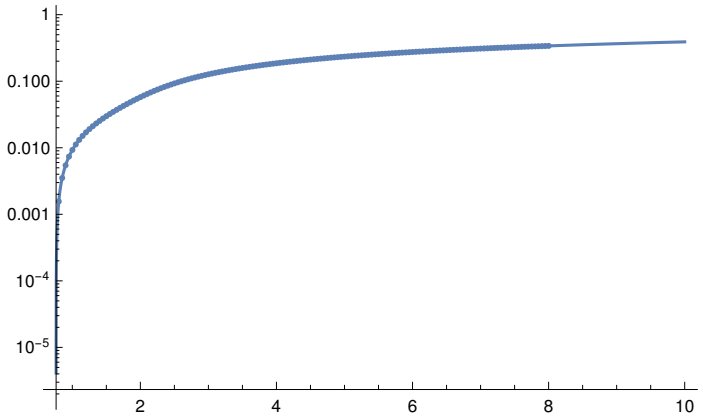


```
Show[LogPlot[{u[x]}, {x, 10^(-3), 0.8},
  PlotLegends → "Expressions", PlotRange → All] , ListLogPlot[merged]]
```

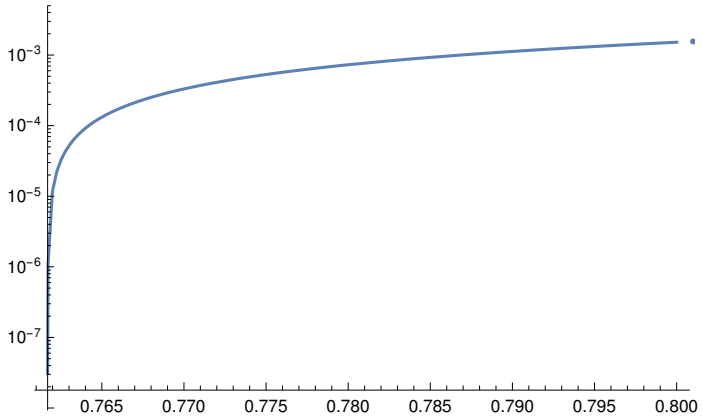


```
(*try to fit with hiperbolic tangent*)

h[x_] := c1 * Tanh[c2 * (x^c3)] + c4 * x^c5 + c6

fit = NonlinearModelFit[merged, h[x], {c1, c2, c3, c4, c5, c6}, x]
```

FittedModel[$-0.156213+0.319384\,x^{0.379692}-0.201485\,\text{Tanh}[1.06554\,x^{0.984876}]$]

```
fit["AdjustedRSquared"] (*seems good, the drop is not perfect, but it shall do*)
```

0.999712

```
Show[LogPlot[{fit[x]}, {x, 10^(-3), 10},
  PlotLegends → "Expressions", PlotRange → All] , ListLogPlot[merged]]
```

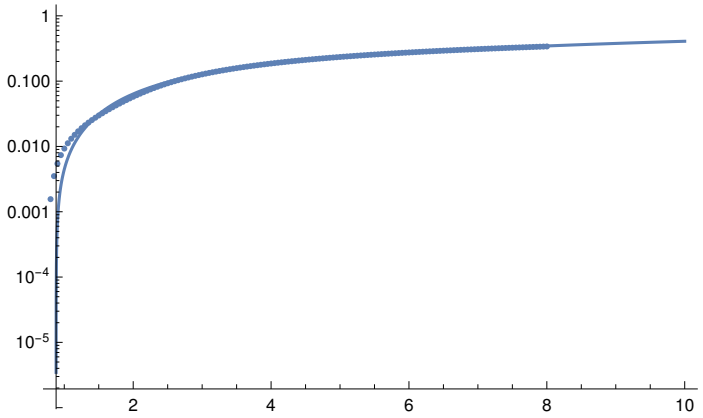


```
Show[LogPlot[{fit[x]}, {x, 10^(-3), 2},
  PlotLegends → "Expressions", PlotRange → All] , ListLogPlot[merged]]
```

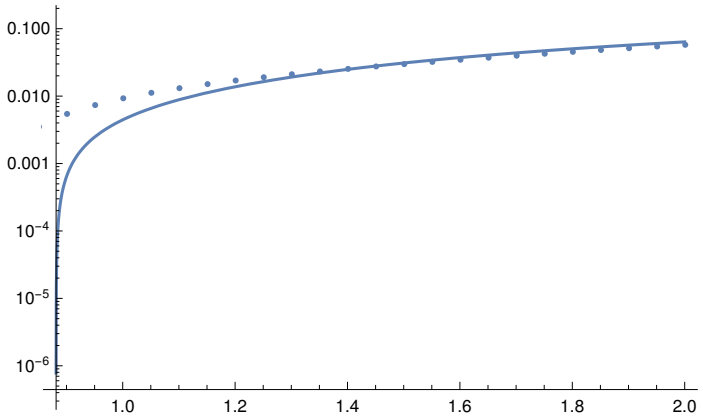


```
h2[x_] := c1 * Tanh[c2 * (x^c3) + c4] + c5
```

```
fit2 = NonlinearModelFit[merged, h2[x], {c1, c2, c3, c4, c5}, x]
```

General::ovfl : Overflow occurred in computation. ≫

General::ovfl : Overflow occurred in computation. ≫

General::ovfl : Overflow occurred in computation. ≫

General::stop : Further output of General::ovfl will be suppressed during this calculation. ≫

NonlinearModelFit::sszero :
The step size in the search has become less than the tolerance prescribed by the PrecisionGoal option, but the gradient is larger than the tolerance specified by the AccuracyGoal option. There is a possibility that the method has stalled at a point that is not a local minimum. ≫

$$\text{FittedModel}\left[\,249.422-249.254\,\text{Tanh}\left[57.9242+\frac{377.982}{x^{10\,308.4}}\right]\,\right]$$

```
fit2["AdjustedRSquared"]
```

General::ovfl : Overflow occurred in computation. >>

General::ovfl : Overflow occurred in computation. >>

General::ovfl : Overflow occurred in computation. >>

General::stop : Further output of General::ovfl will be suppressed during this calculation. >>

```
0.656751
```

```
(*it's probably fitting around the drop and forgetting the other points*)
(*we could weight them, but do we need to?*)
```

```
(*still trying to fit p(e)*)

Clear[f, g, T, press, pressure, p, data, data2, data3,
 data4, data5, data6, dataT1, dataT2, merged, h, fit, h2, fit2,
 h3, fit3, h4, fit4, h5, fit5, h6, fit6, h7, h8, fit8, ss, e, ssfit]

f[x_] := -0.14460764377951374 x^43.29179403782954 (1 + Tanh[27.911759831465123 (1 - x)]) +
   0.8528461795749493 (1 + Tanh[27.911759831465123 (-1 + x)])
                      x^2.032352696537285
(* trace of energy-momentum tensor from SU(3) data *)

g[x_] := f[x] / x
press[y_?NumberQ] := NIntegrate[g[x], {x, 0, y}, Method -> "LocalAdaptive"]
pressure[T_] := (T^4) press[T] (*pressure from numerical integration*)

T[e_] :=
 -0.15621341243069656` + 0.319384339937831` e^0.379692013638506` - 0.20148504091364955`
   Tanh[1.065539056023176` e^0.9848761711059851`] (*temperature in terms of energy*)

p[e_] := pressure[Exp[T[e]]] (*pressure in terms of energy*)

data = Table[p[e], {e, 10^(-3), 3*10^(-1), 5*10^(-3)}];

data2 = Table[p[e], {e, 3*10^(-1), 3*10^0, 5*10^(-3)}];

data3 = Table[p[e], {e, 3*10^0, 10^(2), 5*10^(0)}];

dataT1 = Join[data, data2, data3];

data4 = Table[e, {e, 10^(-3), 3*10^(-1), 5*10^(-3)}];

data5 = Table[e, {e, 3*10^(-1), 3*10^0, 5*10^(-3)}];

data6 = Table[e, {e, 3*10^0, 10^(2), 5*10^(0)}];

dataT2 = Join[data4, data5, data6];

Do[
    Sow[
     Flatten[ReplacePart[{a, b}, {1 → Take[dataT2, {u}], 2 → Take[dataT1, {u}]
       }]

     ]],
    {u, 1, 621, 1}
   ] // Reap // Last;

merged = %[[1]];

h[e_] := (c1*(e^c2)) + (c3*(e^4)) + (c4*Tanh[c5*e]) + (c6*e)

fit = NonlinearModelFit[merged, h[e],
  {c1, c2, c3, c4, c5, c6}, e, MaxIterations → 10 000]

FittedModel[ 0.173122 e + 0.00517911 e^2.24207 + 1.12672 × 10^-6 e^4 - 0.312762 Tanh[0.5535 e] ]
```

```
Show[LogLogPlot[fit[e], {e, 10^(-3), 1.009 * 10^(2)}, PlotLegends → "Expressions"],
 ListLogLogPlot[merged], PlotRange → All]
```

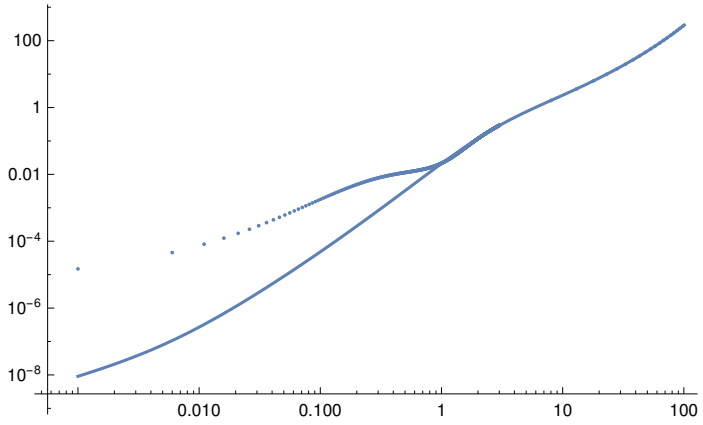


```
(*this is the best fit to the moment*)
```

```
h2[e_] := ((c1 * (e^c2)) + (c3 * (e^4)) + (c4 * Tanh[c5 * e]) + (c6 * e)) Tanh[10^4 * (e - 1)]
```

```
fit2 = NonlinearModelFit[merged, h2[e],
  {c1, c2, c3, c4, c5, c6}, e, MaxIterations → 10 000]
```

$$\text{FittedModel}\left[\text{Tanh}[10\,000\,(-1+e)]\,(0.165723\,e+0.00551846\,e^{2.22794}+1.13634\times10^{-6}\,e^{4}-0.271251\,\text{Tanh}[0.70853\,e])\right]$$

```
Show[LogLogPlot[fit2[e], {e, 10^(-3), 1.009 * 10^(2)}, PlotLegends → "Expressions"],
 ListLogLogPlot[merged], PlotRange → All]
```

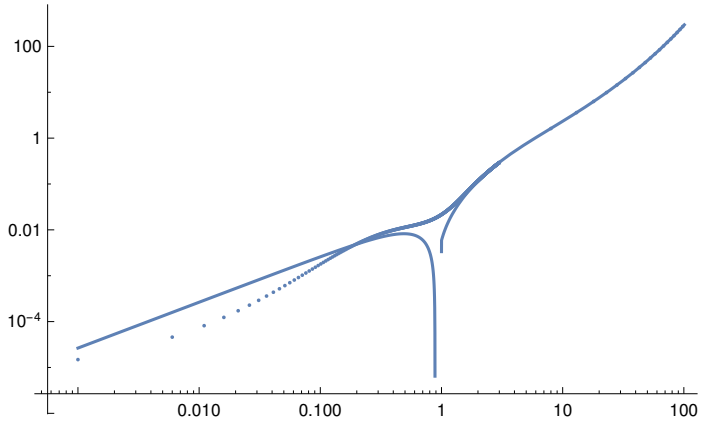


```
h3[e_] :=
 ((c1 * (e^c2)) + (c3 * (e^4)) + (c4 * Tanh[c5 * e]) + (c6 * e)) Tanh[10^4 * (e - 1)] + (c7 * e)
```

```
fit3 = NonlinearModelFit[merged, h3[e],
  {c1, c2, c3, c4, c5, c6, c7}, e, MaxIterations → 10 000]
```

$$\text{FittedModel}\left[0.0184423\,e+\text{Tanh}[10\,000\,(-1+e)]\,(-0.448888\,e+0.0504871\,e^{1.79379}+1.29546\times10^{-6}\,e^{4}+5.87678\,\text{Tanh}[0.069227\,e])\right]$$

```
Show[LogLogPlot[fit3[e], {e, 10^(-3), 1.009 * 10^(2)}, PlotLegends → "Expressions"],
 ListLogLogPlot[merged], PlotRange → All]
```

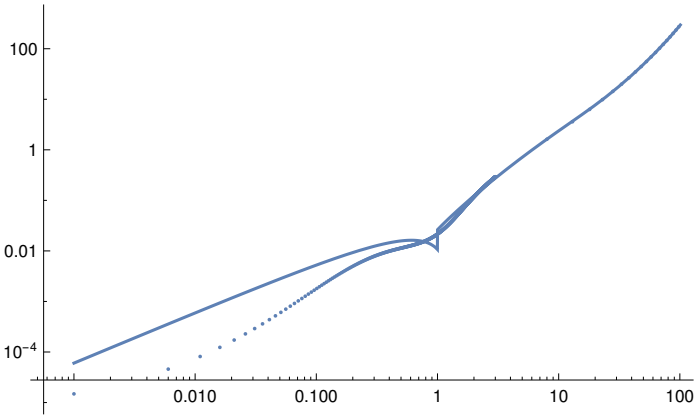


```
h4[e_] := ((c1 * (e^c2)) + (c3 * (e^4)) + (c4 * Tanh[c5 * e]) + (c6 * e)) Tanh[10^4 * (e - 1)] +
  (c7 * e + c8 * e^(-3))
```

```
fit4 = NonlinearModelFit[merged, h4[e],
  {c1, c2, c3, c4, c5, c6, c7, c8}, e, MaxIterations → 10 000]
```

FittedModel[

$$-\frac{2.27022\times10^{-14}}{e^3}+\text{<<21>>}\,e+\text{Tanh}[10\,000\,(-1+e)]\,(0.156454\,e+0.00526725\,e^{2.23833}+\text{<<23>>}\,e^4-0.299621\,\text{Tanh}[0.594053\,e])$$

]

```
Show[LogLogPlot[fit4[e], {e, 10^(-3), 1.009 * 10^(2)}, PlotLegends → "Expressions"],
 ListLogLogPlot[merged], PlotRange → All]
```

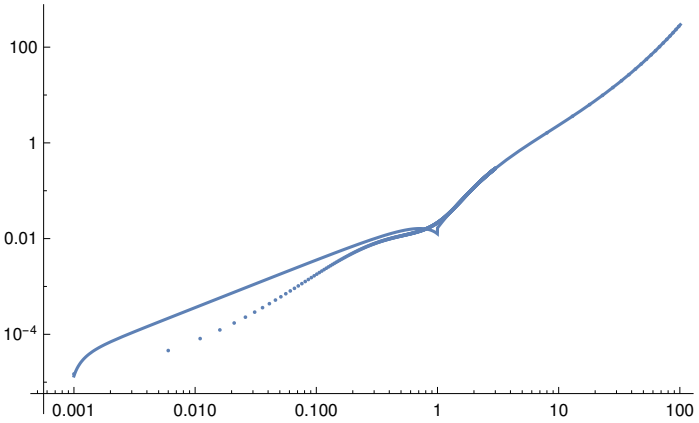


```
h5[e_] := ((c1 * (e^c2)) + (c3 * (e^4)) + (c4 * e)) Tanh[10^4 * (e - 1)] + (c5 * e + c6 * e^(-1))
```

```
fit5 = NonlinearModelFit[merged, h5[e],
  {c1, c2, c3, c4, c5, c6}, e, MaxIterations → 10 000]
```

FittedModel[

$$-\frac{5.13097\times10^{-6}}{e}+0.0354037\,e+(0.00202089\,e+0.0165757\,e^{1.98421}+1.30073\times10^{-6}\,e^4)\,\text{Tanh}[10\,000\,(-1+e)]$$

]

```
Show[LogLogPlot[fit5[e], {e, 10^(-3), 1.009 * 10^(2)}, PlotLegends → "Expressions"],
 ListLogLogPlot[merged], PlotRange → All]
```

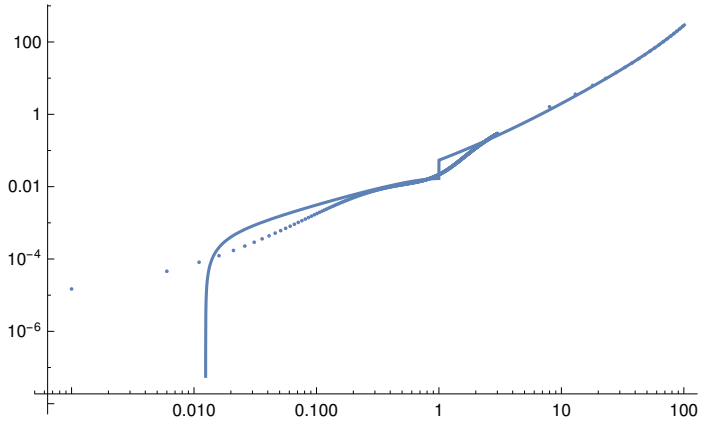


```
h6[e_] := ((c1 * (e^c2)) + (c3 * (e^4)) + (c4 * e)) Tanh[10^4 * (e - 1)] +
  (c5 * e + c6 * (e^(-2))) + (c7 * e) Tanh[10^4 * (e - 0.07)]
```

```
fit6 = NonlinearModelFit[merged, h6[e],
  {c1, c2, c3, c4, c5, c6, c7}, e, MaxIterations → 10 000]
```

FittedModel[$-\frac{6.78315\times10^{-12}}{e^2}+0.0251497\,e+(0.00202447\,e+0.0165759\,e^{\ll19\gg}+1.30073\times10^{-6}\,e^4)\,\text{Tanh}[\ll1\gg]+0.0102489\,e\,\text{Tanh}[10\,000\,(-0.07+e)]$]

```
fit6[x]
```

$$-\frac{6.78315\times10^{-12}}{x^2}+0.0251497\,x+\left(0.00202447\,x+0.0165759\,x^{1.9842}+1.30073\times10^{-6}\,x^4\right)\text{Tanh}[10\,000\,(-1+x)]+0.0102489\,x\,\text{Tanh}[10\,000\,(-0.07+x)]$$

```
Show[LogLogPlot[fit6[e], {e, 10^(-3), 1.009 * 10^(2)}, PlotLegends → "Expressions"],
 ListLogLogPlot[merged], PlotRange → All]
```

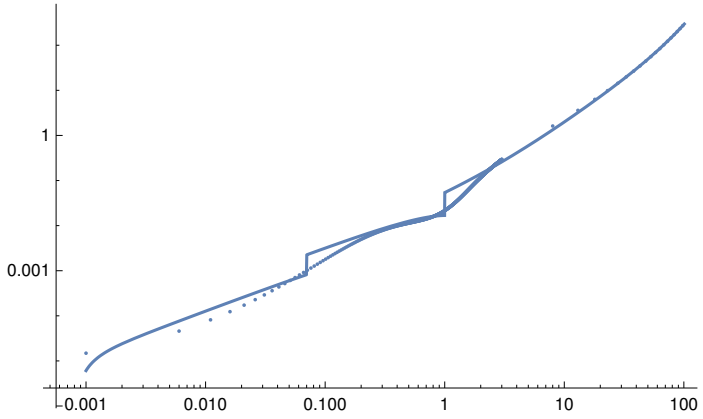


```
h9[e_] := ((c1 * (e^c2)) + (c3 * (e^4)) + (c4 * e)) Tanh[10^4 * (e - 1)] +
  ((c7 * e) + (c8 * e^(0.5)) Tanh[10^4 * (e - 0.07)])
```

```
fit9 = NonlinearModelFit[merged, h9[e],
  {c1, c2, c3, c4, c7, c8}, e, MaxIterations → 10 000]
```

```
FittedModel[ 0.213529 e+(-0.0338544 e+0.00645463 e^2.18902+1.17414×10^-6 e^4) Tanh[10 000 (-1+e)]-0.185036 e^0.5 Tanh[10
```

```
Show[LogLogPlot[fit9[e], {e, 10^(-3), 1.009 * 10^(2)}, PlotLegends → "Expressions"],
 ListLogLogPlot[merged], PlotRange → All]
```

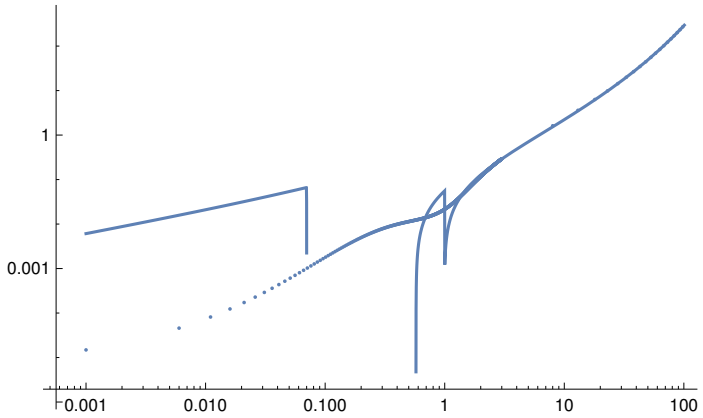


```
(*this seems a good one, let's try to smooth the transitions*)
h7[e_] := (2 / (1 + Exp[-1 (e - 20)])) - 1
```

```
h7[x]
```

$$-1+\frac{2}{1+e^{20-x}}$$

```
Plot[{h7[e], Tanh[10^4 * (e - 10)], Tanh[0.8 * (e - 10)]},
 {e, 10^(-3), 1 * 10^2}, PlotRange → All]
```

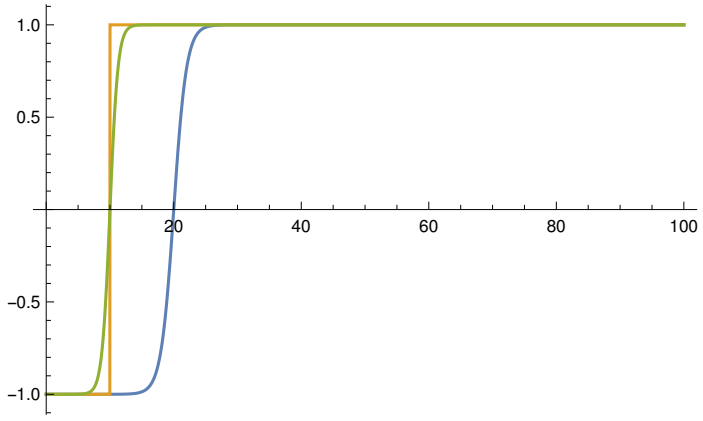


```
h8[e_] := (((c1 * (e^c2)) + (c3 * (e^4)) + (c4 * e)) * (2 / (1 + Exp[-1 * (e - 1)]) - 1)) +
  (c6 * e + c7 * (e^(-2))) + (c8 * e) Tanh[10^4 * (e - 0.07)]
```

```
fit8 = NonlinearModelFit[merged, h8[e],
  {c1, c2, c3, c4, c5, c6, c7, c8}, e, MaxIterations → 10 000]
```

NonlinearModelFit::sszero :
The step size in the search has become less than the tolerance prescribed by the PrecisionGoal option, but the gradient is larger than the tolerance specified by the AccuracyGoal option. There is a possibility that the method has stalled at a point that is not a local minimum. >>

```
FittedModel[
```

$$-\frac{1.10317\times10^{-9}}{e^2}-0.252736\,e+\left(-370\,980.\,e^{0.999999}+370\,979.\,e+1.93956\times10^{-6}\,e^4\right)(\ll1\gg)+0.532744\,e\,\text{Tanh}[10\,000\,(-0.07+e)]$$

```
]
```

```
Show[LogLogPlot[fit8[e], {e, 10^(-3), 1.009 * 10^(2)}, PlotLegends → "Expressions"],
 ListLogLogPlot[merged], PlotRange → All]
```

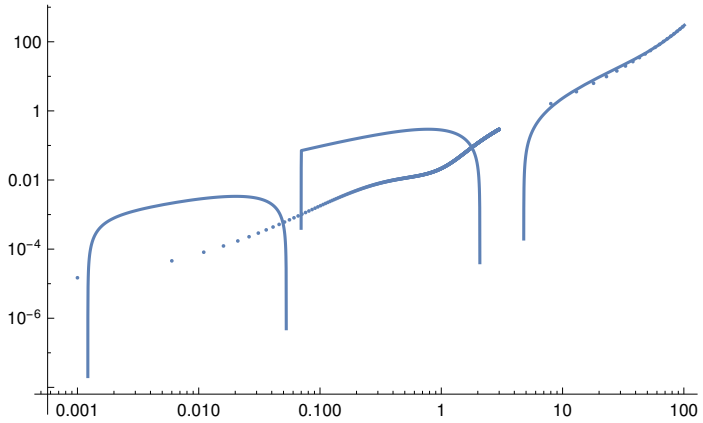


```
test[e_] := -6.783153306196406`*^-12/e^2 + 0.02514966036755684` e +
  (0.002024471323836417` e + 0.016575874026457587` (e^(1.9842)) +
     1.3007294150974632`*^-6 e^4) * ((2 / (1 + Exp[-1 (e - 1)])) - 1) +
  0.010248900088404221` e * ((2 / (1 + Exp[-1 (e - 0.07)])) - 1)
```

```
Show[LogLogPlot[test[e], {e, 10^(-3), 1.009 * 10^(2)}, PlotLegends → "Expressions"],
 ListLogLogPlot[merged], PlotRange → All]
```

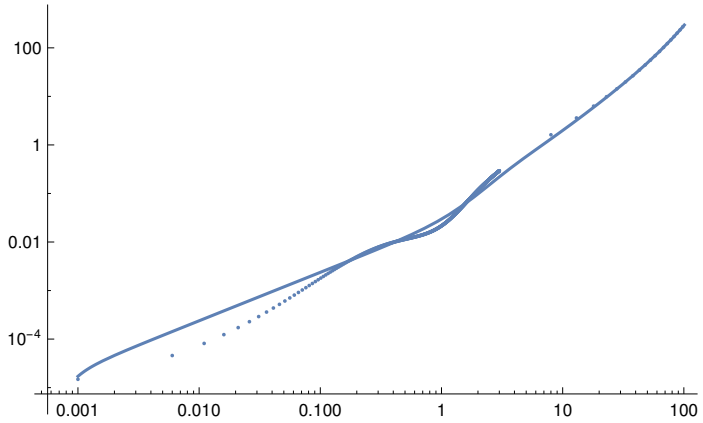


```
(*let's try one more time to fit this*)
```

```
ClearAll[a, conf1, confmax, a01, f01, g, pym, elarge, steplarge, peff, diff, diffe, cn,
 er1, ec, k, Nym, C1, C2, confmax2,  a, e, f2, g2, C12, peff2, diff2, diffe2, g3, C13,
 peff3, diff3, diffe3, g4, C14, peff4, diff4, diffe4, g5, C15, peff5, diff5, diffe5,
 g6, C16, peff6, diff6, diffe6, g7, C17, peff7, diff7, diffe7, g8, C18, peff8,
 diff8, diffe8, g9, C19, peff9, diff9, diffe9, s, s2, s3, s4, s5, s6, s7, s8, s9, N1,
 N2, N3, N4, N5, N6, N7, N8, N9, Amp, LAmp, merged, ColorList, bList, aux6, aux7]

k = 0; (*dimensionless*)
conf1 = 10^(-20);(*MeV^(-1)*)
a01 = (10^(-58))^(2 / 3); (*dimensionless*)
f01 = (2 / 3) * 10^(20); (*MeV*)

g[e_] := C1 * Exp[-C2 * (e / ec - 1)^2 / 2]
elarge = 650 * ec;
steplarge[e1_] := (1 + Tanh[e1 / ec]) / 2

pym[e_] := (-0.0701780768934142` + 0.012829768279227724` (e/ec)^2.10542207822587` +
      (0.0016223939423977366` (e/ec)^2.2` - 1.1874523382499435`*^-6 e^4/ec^4 +
         0.018853186484192017` e/ec) Tanh[0.12809510086441414` (0.45` - e/ec)] -
      0.10893510953199945` Tanh[1.0802023944400028` (-0.71` + e/ec)] +
      (1.6557877362105378` + 0.3864140819569308` (e/ec)^0.3`)
       Tanh[0.05613355687245168` (-0.01` + e/ec)]) *
   steplarge[elarge - e] + (e / 3) * steplarge[e - elarge]

peff[e_, f_] := pym[e] - 3 * g[e] * f * Sqrt[2 * cn * e / (f^2 + k)] * (e^(3 / 4)) + e / 3
diff[e_, f_] := (e - 3 * peff[e, f]) * ((f^2 + k) / (2 * e)) - k - f^2
diffe[e_, f_] := -3 * (e + peff[e, f]) * f

cn = ((4 N[Pi] * (0.000670861 * 10^(-41))) / 3); (*MeV^(-2)*)
er1 = 10^(91);
confmax = 10^15;

(*set of parameters we change*)

ec = er1 * 10^(-4);

C2 = 100;

C1 = 10^(5);

confmax2 = 2.9 * 10^(-19);
```

```
s = NDSolve[
   {f2'[conf2] == diff[e[conf2], f2[conf2]], e'[conf2] == diffe[e[conf2], f2[conf2]],
    f2[conf2] == a'[conf2] / a[conf2], a[conf1] == a01, f2[conf1] == f01, e[conf1] == er1},
   {f2[conf2], e[conf2], a[conf2]}, {conf2, conf1, confmax}, Method → {Shooting}]
```

NDSolve::ndsz :
At conf2 == 2.992044298291134`*^-19, step size is effectively zero; singularity or stiff system suspected. >>

```
{{f2[conf2] → InterpolatingFunction[ 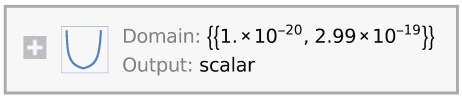 ][conf2],
  e[conf2] → InterpolatingFunction[ 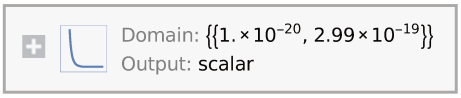 ][conf2],
  a[conf2] → InterpolatingFunction[ 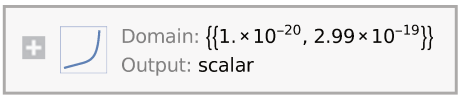 ][conf2]}}
```



```
a[conf2_] = a[conf2] /. s[[1]]
```

```
InterpolatingFunction[ 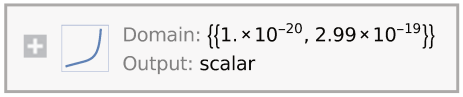 ][conf2]
```



```
e[conf2_] = e[conf2] /. s[[1]]
```

```
InterpolatingFunction[ 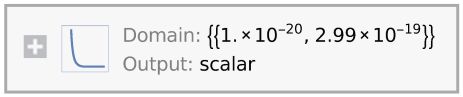 ][conf2]
```



```
f2[conf2_] = f2[conf2] /. s[[1]]
```

```
InterpolatingFunction[ 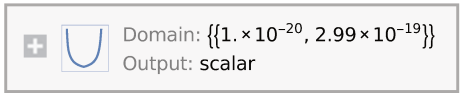 ][conf2]
```



```
N1 = Log[a[2.99 * 10^(-19)] / a[conf1]]
```

```
8.6966
```

```
g2[e_] := C12 * Exp[-C2 * (e / ec - 1)^2 / 2]

peff2[e2_, f22_] :=
 pym[e2] - 3 * g2[e2] * f22 * Sqrt[2 * cn * e2 / (f22^2 + k)] * (e2^(3 / 4)) + e2 / 3
diff2[e2_, f22_] := (e2 - 3 * peff2[e2, f22]) * ((f22^2 + k) / (2 * e2)) - k - f22^2
diffe2[e2_, f22_] := -3 * (e2 + peff2[e2, f22]) * f22

C12 = 10^4;

ClearAll[a2, e2, f22, s2]
```

```
s2 = NDSolve[{f22'[conf2] == diff2[e2[conf2], f22[conf2]],
    e2'[conf2] == diffe2[e2[conf2], f22[conf2]], f22[conf2] == a2'[conf2] / a2[conf2],
    a2[conf1] == a01, f22[conf1] == f01, e2[conf1] == er1},
   {f22[conf2], e2[conf2], a2[conf2]}, {conf2, conf1, confmax}, Method → {Shooting}]
```

NDSolve::ndsz :
At conf2 == 3.017375529160673`*^-19, step size is effectively zero; singularity or stiff system suspected. >>

```
{{f22[conf2] → InterpolatingFunction[ ⟨Domain: {{1.×10^-20, 3.02×10^-19}}, Output: scalar⟩ ][conf2],
  e2[conf2] → InterpolatingFunction[ ⟨Domain: {{1.×10^-20, 3.02×10^-19}}, Output: scalar⟩ ][conf2],
  a2[conf2] → InterpolatingFunction[ ⟨Domain: {{1.×10^-20, 3.02×10^-19}}, Output: scalar⟩ ][conf2]}}
```

```
a2[conf2_] = a2[conf2] /. s2[[1]]
```

```
InterpolatingFunction[ ⟨Domain: {{1.×10^-20, 3.02×10^-19}}, Output: scalar⟩ ][conf2]
```

```
e2[conf2_] = e2[conf2] /. s2[[1]]
```

```
InterpolatingFunction[ ⟨Domain: {{1.×10^-20, 3.02×10^-19}}, Output: scalar⟩ ][conf2]
```

```
f22[conf2_] = f22[conf2] /. s2[[1]]
```

```
InterpolatingFunction[ ⟨Domain: {{1.×10^-20, 3.02×10^-19}}, Output: scalar⟩ ][conf2]
```

```
N2 = Log[a2[3.01 * 10^(-19)] / a2[conf1]]
```

```
7.42975
```

```
peff3[e3_, f23_] :=
 pym[e3] - 3 * g3[e3] * f23 * Sqrt[2 * cn * e3 / (f23^2 + k)] * (e3^(3 / 4)) + e3 / 3
diff3[e3_, f23_] := (e3 - 3 * peff3[e3, f23]) * ((f23^2 + k) / (2 * e3)) - k - f23^2
diffe3[e3_, f23_] := -3 * (e3 + peff3[e3, f23]) * f23
```

```
g3[e_] := C13 * Exp[-C2 * (e / ec - 1)^2 / 2]
```

```
C13 = 10^3;
```

```
ClearAll[a3, e3, f23, s3]
```

```
s3 = NDSolve[{f23'[conf2] == diff3[e3[conf2], f23[conf2]],
    e3'[conf2] == diffe3[e3[conf2], f23[conf2]], f23[conf2] == a3'[conf2] / a3[conf2],
    a3[conf1] == a01, f23[conf1] == f01, e3[conf1] == er1},
   {f23[conf2], e3[conf2], a3[conf2]}, {conf2, conf1, confmax}, Method → {Shooting}]
```

NDSolve::ndsz :
At conf2 == 3.0469975829703546`*^-19, step size is effectively zero; singularity or stiff system suspected. »

```
{{f23[conf2] → InterpolatingFunction[ ⟨Domain: {{1.×10^-20, 3.05×10^-19}}, Output: scalar⟩ ][conf2],
  e3[conf2] → InterpolatingFunction[ ⟨Domain: {{1.×10^-20, 3.05×10^-19}}, Output: scalar⟩ ][conf2],
  a3[conf2] → InterpolatingFunction[ ⟨Domain: {{1.×10^-20, 3.05×10^-19}}, Output: scalar⟩ ][conf2]}}
```

```
a3[conf2_] = a3[conf2] /. s3[[1]]
```

```
InterpolatingFunction[ ⟨Domain: {{1.×10^-20, 3.05×10^-19}}, Output: scalar⟩ ][conf2]
```

```
e3[conf2_] = e3[conf2] /. s3[[1]]
```

```
InterpolatingFunction[ ⟨Domain: {{1.×10^-20, 3.05×10^-19}}, Output: scalar⟩ ][conf2]
```

```
f23[conf2_] = f23[conf2] /. s3[[1]]
```

```
InterpolatingFunction[ ⟨Domain: {{1.×10^-20, 3.05×10^-19}}, Output: scalar⟩ ][conf2]
```

```
N3 = Log[a3[3.04 * 10^(-19)] / a3[conf1]]
```

```
7.5012
```

```
peff4[e4_, f24_] :=
 pym[e4] - 3 * g4[e4] * f24 * Sqrt[2 * cn * e4 / (f24^2 + k)] * (e4^(3 / 4)) + e4 / 3
diff4[e4_, f24_] := (e4 - 3 * peff4[e4, f24]) * ((f24^2 + k) / (2 * e4)) - k - f24^2
diffe4[e4_, f24_] := -3 * (e4 + peff4[e4, f24]) * f24
```

```
g4[e_] := C14 * Exp[-C2 * (e / ec - 1)^2 / 2]
```

```
C14 = 10^2;
```

```
ClearAll[a4, e4, f24, s4]
```

```
s4 = NDSolve[{f24'[conf2] == diff4[e4[conf2], f24[conf2]],
    e4'[conf2] == diffe4[e4[conf2], f24[conf2]], f24[conf2] == a4'[conf2] / a4[conf2],
    a4[conf1] == a01, f24[conf1] == f01, e4[conf1] == er1},
   {f24[conf2], e4[conf2], a4[conf2]}, {conf2, conf1, confmax}, Method → {Shooting}]
```

NDSolve::ndsz :
At conf2 == 3.083101487109392`*^-19, step size is effectively zero; singularity or stiff system suspected. >>

```
{{f24[conf2] → InterpolatingFunction[ 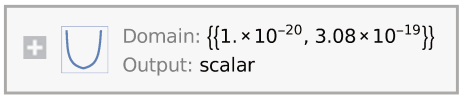 ][conf2],
  e4[conf2] → InterpolatingFunction[ 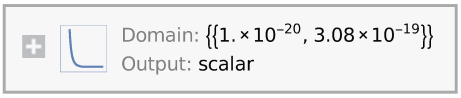 ][conf2],
  a4[conf2] → InterpolatingFunction[ 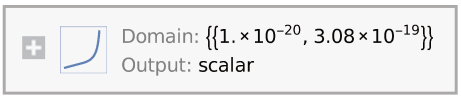 ][conf2]}}
```



```
a4[conf2_] = a4[conf2] /. s4[[1]]
```

```
InterpolatingFunction[ 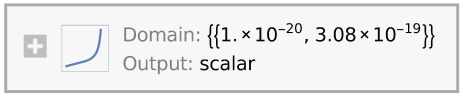 ][conf2]
```



```
e4[conf2_] = e4[conf2] /. s4[[1]]
```

```
InterpolatingFunction[ 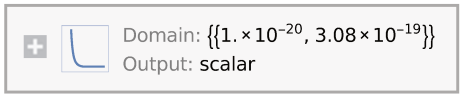 ][conf2]
```



```
f24[conf2_] = f24[conf2] /. s4[[1]]
```

```
InterpolatingFunction[ 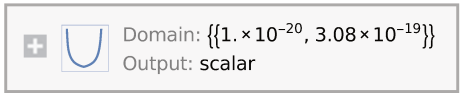 ][conf2]
```



```
N4 = Log[a4[3.08 * 10^(-19)] / a4[conf1]]
```

```
8.33762
```

```
peff5[e5_, f25_] :=
 pym[e5] - 3 * g5[e5] * f25 * Sqrt[2 * cn * e5 / (f25^2 + k)] * (e5^(3 / 4)) + e5 / 3
diff5[e5_, f25_] := (e5 - 3 * peff5[e5, f25]) * ((f25^2 + k) / (2 * e5)) - k - f25^2
diffe5[e5_, f25_] := -3 * (e5 + peff5[e5, f25]) * f25

g5[e_] := C15 * Exp[-C2 * (e / ec - 1)^2 / 2]

C15 = 10^1;

ClearAll[a5, e5, f25, s5]
```

```
s5 = NDSolve[{f25'[conf2] == diff5[e5[conf2], f25[conf2]],
    e5'[conf2] == diffe5[e5[conf2], f25[conf2]], f25[conf2] == a5'[conf2] / a5[conf2],
    a5[conf1] == a01, f25[conf1] == f01, e5[conf1] == er1},
   {f25[conf2], e5[conf2], a5[conf2]}, {conf2, conf1, confmax}, Method → {Shooting}]
```

NDSolve::ndsz :
At conf2 == 3.130569370187667`*^-19, step size is effectively zero; singularity or stiff system suspected. >>

```
{{f25[conf2] → InterpolatingFunction[ ⟨Domain: {{1.×10^-20, 3.13×10^-19}}, Output: scalar⟩ ][conf2],
  e5[conf2] → InterpolatingFunction[ ⟨Domain: {{1.×10^-20, 3.13×10^-19}}, Output: scalar⟩ ][conf2],
  a5[conf2] → InterpolatingFunction[ ⟨Domain: {{1.×10^-20, 3.13×10^-19}}, Output: scalar⟩ ][conf2]}}
```

```
a5[conf2_] = a5[conf2] /. s5[[1]]
```

```
InterpolatingFunction[ ⟨Domain: {{1.×10^-20, 3.13×10^-19}}, Output: scalar⟩ ][conf2]
```

```
e5[conf2_] = e5[conf2] /. s5[[1]]
```

```
InterpolatingFunction[ ⟨Domain: {{1.×10^-20, 3.13×10^-19}}, Output: scalar⟩ ][conf2]
```

```
f25[conf2_] = f25[conf2] /. s5[[1]]
```

```
InterpolatingFunction[ ⟨Domain: {{1.×10^-20, 3.13×10^-19}}, Output: scalar⟩ ][conf2]
```

```
N5 = Log[a5[3.13 * 10^(-19)] / a5[conf1]]
```

```
10.0623
```

```
peff6[e6_, f26_] :=
 pym[e6] - 3 * g6[e6] * f26 * Sqrt[2 * cn * e6 / (f26^2 + k)] * (e6^(3 / 4)) + e6 / 3
diff6[e6_, f26_] := (e6 - 3 * peff6[e6, f26]) * ((f26^2 + k) / (2 * e6)) - k - f26^2
diffe6[e6_, f26_] := -3 * (e6 + peff6[e6, f26]) * f26
```

```
g6[e_] := C16 * Exp[-C2 * (e / ec - 1)^2 / 2]
```

```
C16 = 10^0;
```

```
ClearAll[a6, e6, f26, s6]
```

```
s6 = NDSolve[{f26'[conf2] == diff6[e6[conf2], f26[conf2]],
    e6'[conf2] == diffe6[e6[conf2], f26[conf2]], f26[conf2] == a6'[conf2] / a6[conf2],
    a6[conf1] == a01, f26[conf1] == f01, e6[conf1] == er1},
   {f26[conf2], e6[conf2], a6[conf2]}, {conf2, conf1, confmax}, Method → {Shooting}]
```

NDSolve::ndsz :
At conf2 == 3.206684058172536`*^-19, step size is effectively zero; singularity or stiff system suspected. >>

```
{{f26[conf2] → InterpolatingFunction[ 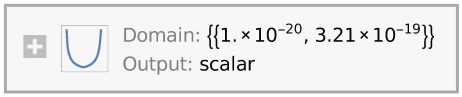 ][conf2],
  e6[conf2] → InterpolatingFunction[ 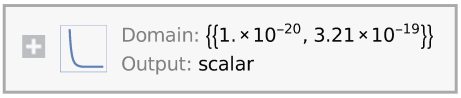 ][conf2],
  a6[conf2] → InterpolatingFunction[ 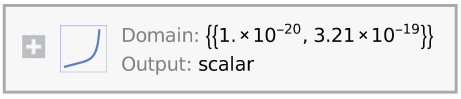 ][conf2]}}
```



```
a6[conf2_] = a6[conf2] /. s6[[1]]
```

```
InterpolatingFunction[ 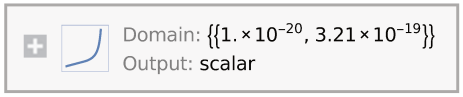 ][conf2]
```



```
e6[conf2_] = e6[conf2] /. s6[[1]]
```

```
InterpolatingFunction[ 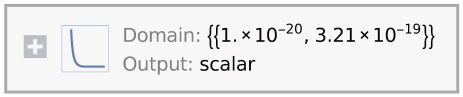 ][conf2]
```



```
f26[conf2_] = f26[conf2] /. s6[[1]]
```

```
InterpolatingFunction[ 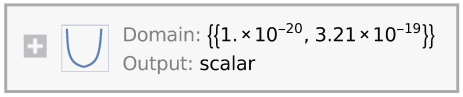 ][conf2]
```



```
aux6[e6_, f26_] := -3 * g6[e6] * f26 * Sqrt[2 * cn * e6 / (f26^2 + k)] * (e6^(3 / 4));
```

```
Plot[{pym[e6[conf2]], peff6[e6[conf2], f26[conf2]],
  e6[conf2] / 3, aux6[e6[conf2], f26[conf2]]},
 {conf2, conf1, confmax2}, PlotLegends → "Expressions",
 AxesLabel → {ConfTime, pym}, AxesStyle → Black, ImageSize → Large]
```

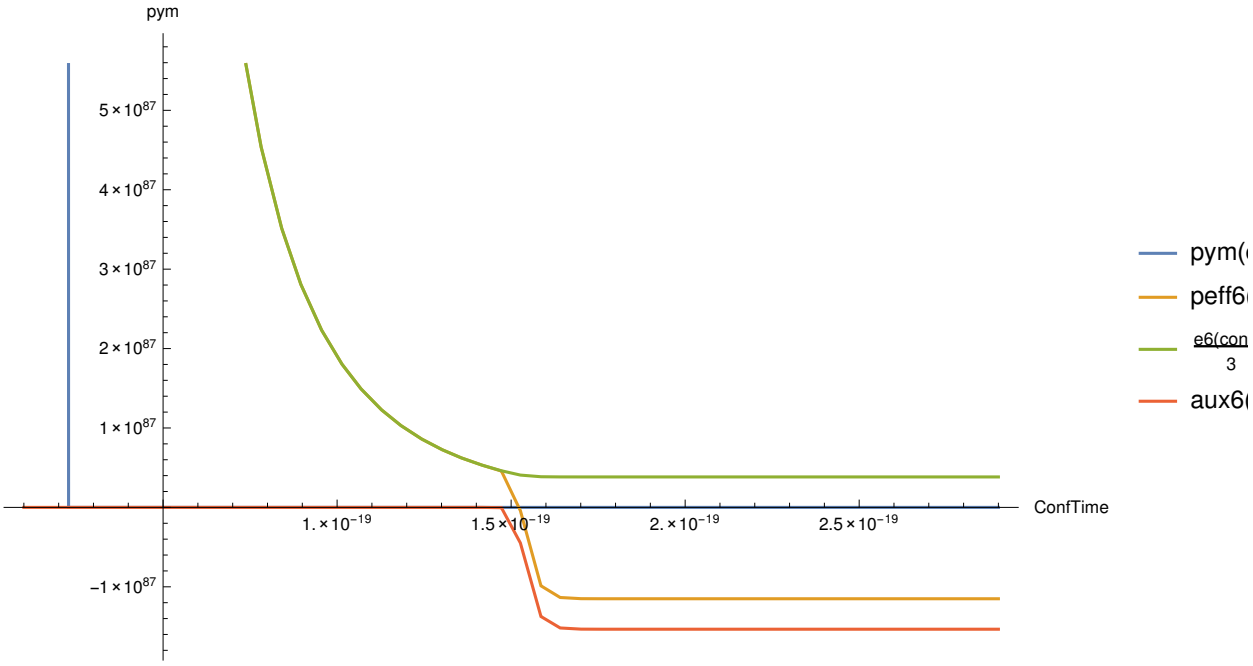


```
LogPlot[{peff6[e6[conf2], f26[conf2]], -aux6[e6[conf2], f26[conf2]]},
 {conf2, conf1, confmax2}, PlotLegends → "Expressions",
 AxesLabel → {ConfTime, pym}, AxesStyle → Black, ImageSize → Large]
```

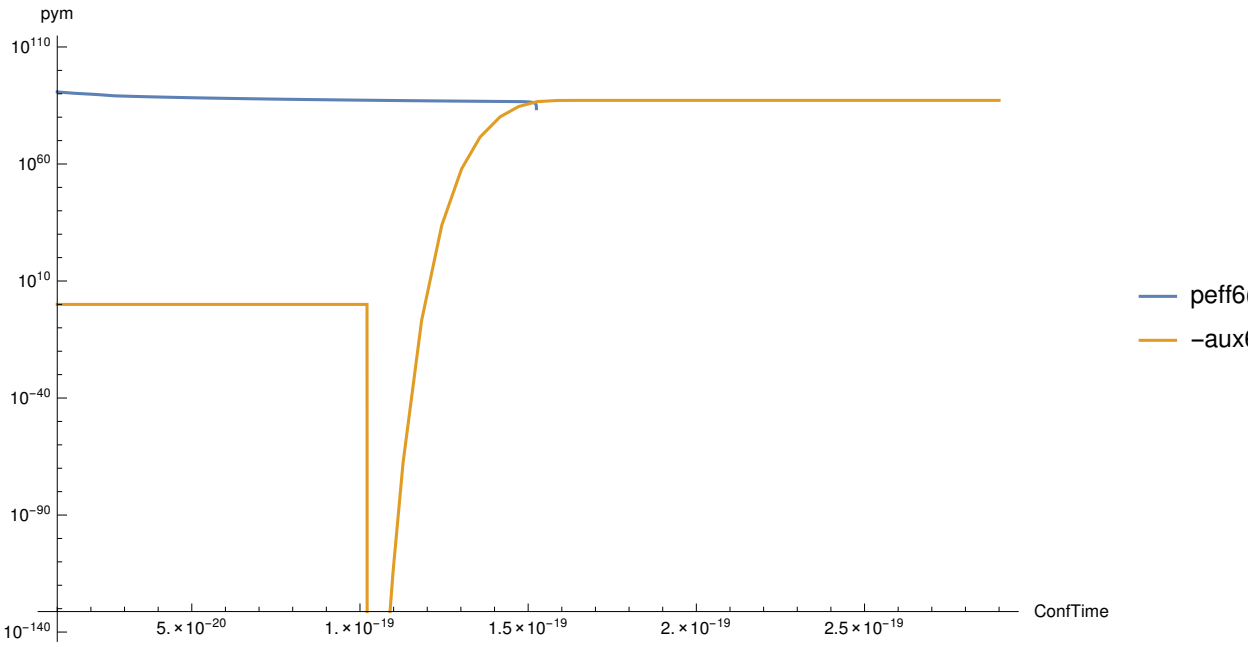

```
N6 = Log[a6[3.20 * 10^(-19)] / a6[conf1]]
```

```
7.64595
```

```
peff7[e7_, f27_] :=
 pym[e7] - 3 * g7[e7] * f27 * Sqrt[2 * cn * e7 / (f27^2 + k)] * (e7^(3 / 4)) + e7 / 3
diff7[e7_, f27_] := (e7 - 3 * peff7[e7, f27]) * ((f27^2 + k) / (2 * e7)) - k - f27^2
diffe7[e7_, f27_] := -3 * (e7 + peff7[e7, f27]) * f27
```

```
g7[e_] := C17 * Exp[-C2 * (e / ec - 1)^2 / 2]
```

```
C17 = 10^(-1);
```

```
ClearAll[a7, e7, f27, s7]
```

```
s7 = NDSolve[{f27'[conf2] == diff7[e7[conf2], f27[conf2]],
    e7'[conf2] == diffe7[e7[conf2], f27[conf2]], f27[conf2] == a7'[conf2] / a7[conf2],
    a7[conf1] == a01, f27[conf1] == f01, e7[conf1] == er1},
  {f27[conf2], e7[conf2], a7[conf2]}, {conf2, conf1, confmax}, Method → {Shooting}]
```

```
NDSolve::ndsz :
  At conf2 == 11085.070537421268`, step size is effectively zero; singularity or stiff system suspected. >>
```

```
{{f27[conf2] → InterpolatingFunction[ ⟨Domain: {{1.×10^-20, 11100.}}  Output: scalar⟩ ][conf2],
  e7[conf2] → InterpolatingFunction[ ⟨Domain: {{1.×10^-20, 11100.}}  Output: scalar⟩ ][conf2],
  a7[conf2] → InterpolatingFunction[ ⟨Domain: {{1.×10^-20, 11100.}}  Output: scalar⟩ ][conf2]}}
```

```
a7[conf2_] = a7[conf2] /. s7[[1]]
```

```
InterpolatingFunction[ ⟨Domain: {{1.×10^-20, 11100.}}  Output: scalar⟩ ][conf2]
```

```
e7[conf2_] = e7[conf2] /. s7[[1]]
```

```
InterpolatingFunction[ ⟨Domain: {{1.×10^-20, 11100.}}  Output: scalar⟩ ][conf2]
```

```
f27[conf2_] = f27[conf2] /. s7[[1]]
```

```
InterpolatingFunction[ ⟨Domain: {{1.×10^-20, 11100.}}  Output: scalar⟩ ][conf2]
```

```
peff7[e7[1.6 * 10^(-19)], f27[1.6 * 10^(-19)]]
```

```
-3.6887 × 10^85
```

```
LogPlot[{peff7[e7[conf2], f27[conf2]]}, {conf2, conf1, confmax2},
 PlotLegends → "Expressions", AxesLabel → {ConfTime, pym},
 AxesStyle → Black, ImageSize → Large, PlotRange → All]
```

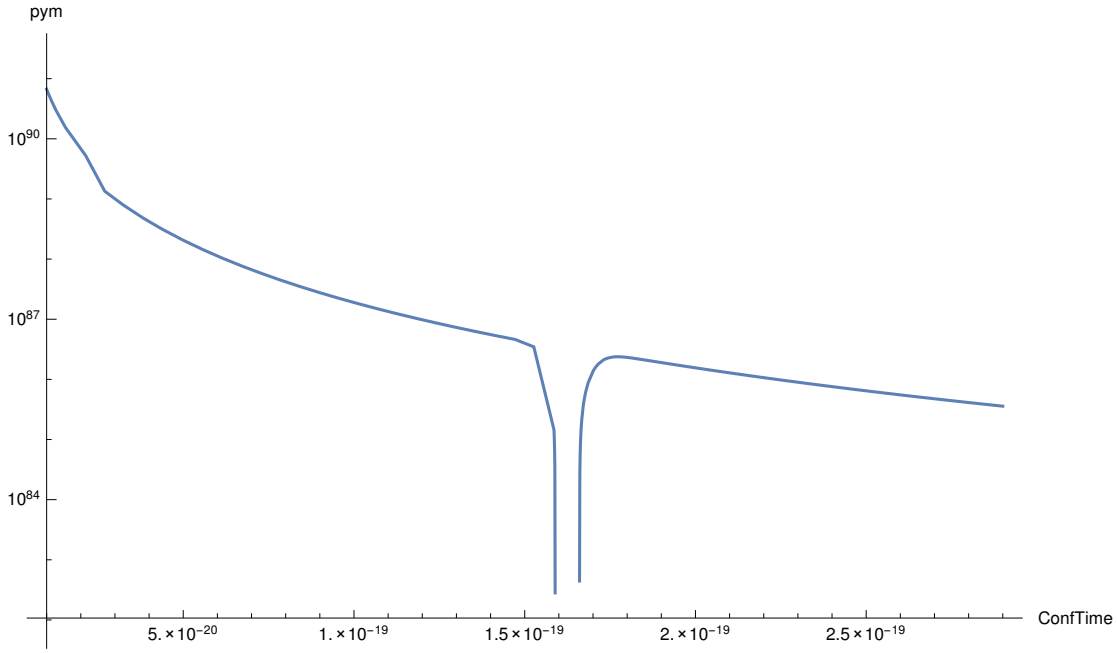


```
N7 = Log[a7[1.1 * 10^(4)] / a7[conf1]]
```

```
58.3699
```

```
Nextra = Log[a7[2 * 10^(-19)] / a7[conf1]]
```

```
2.38074
```

```
(*the peak is not the responsible for inflation*)
```

```
aux7[e7_, f27_] := -3 * g7[e7] * f27 * Sqrt[2 * cn * e7 / (f27^2 + k)] * (e7^(3 / 4));
```

```
LogPlot[{pym[e7[conf2]], peff7[e7[conf2], f27[conf2]], e7[conf2] / 3},
 {conf2, conf1, confmax2}, PlotLegends → "Expressions",
 AxesLabel → {ConfTime, pym}, AxesStyle → Black, ImageSize → Large, PlotRange → All]
```

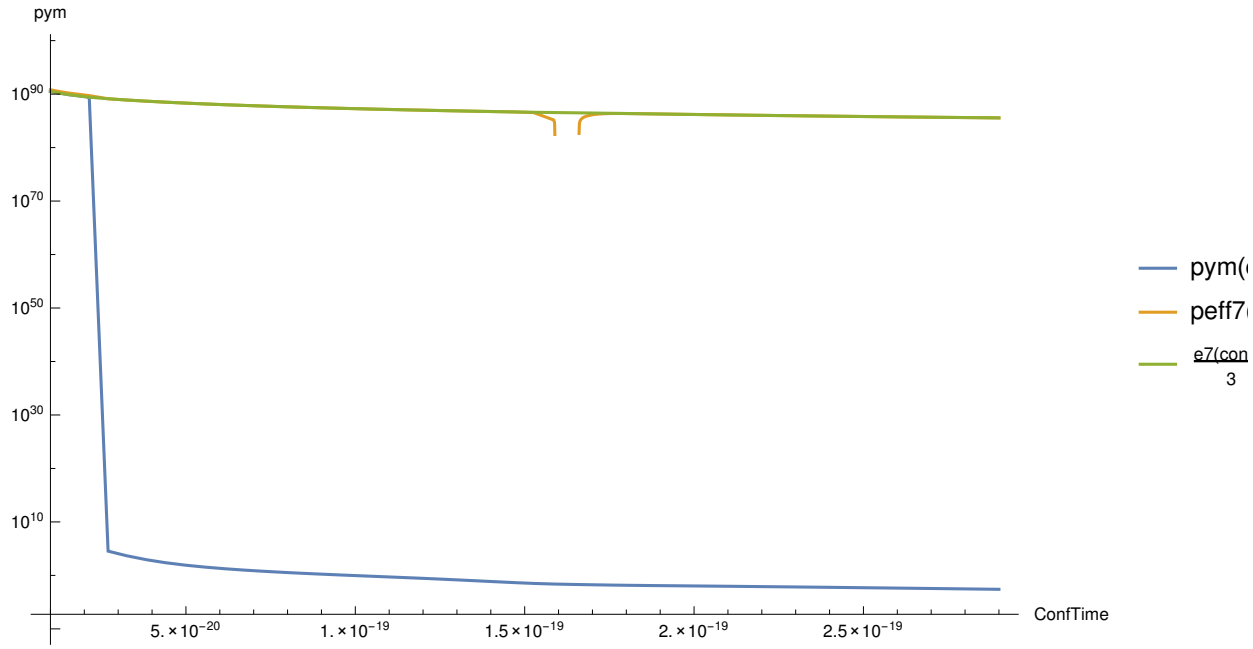


```
LogPlot[{-peff7[e7[conf2], f27[conf2]], -aux7[e7[conf2], f27[conf2]]},
 {conf2, conf1, confmax2}, PlotLegends → "Expressions",
 AxesLabel → {ConfTime, pym}, AxesStyle → Black, ImageSize → Large, PlotRange → All]
```

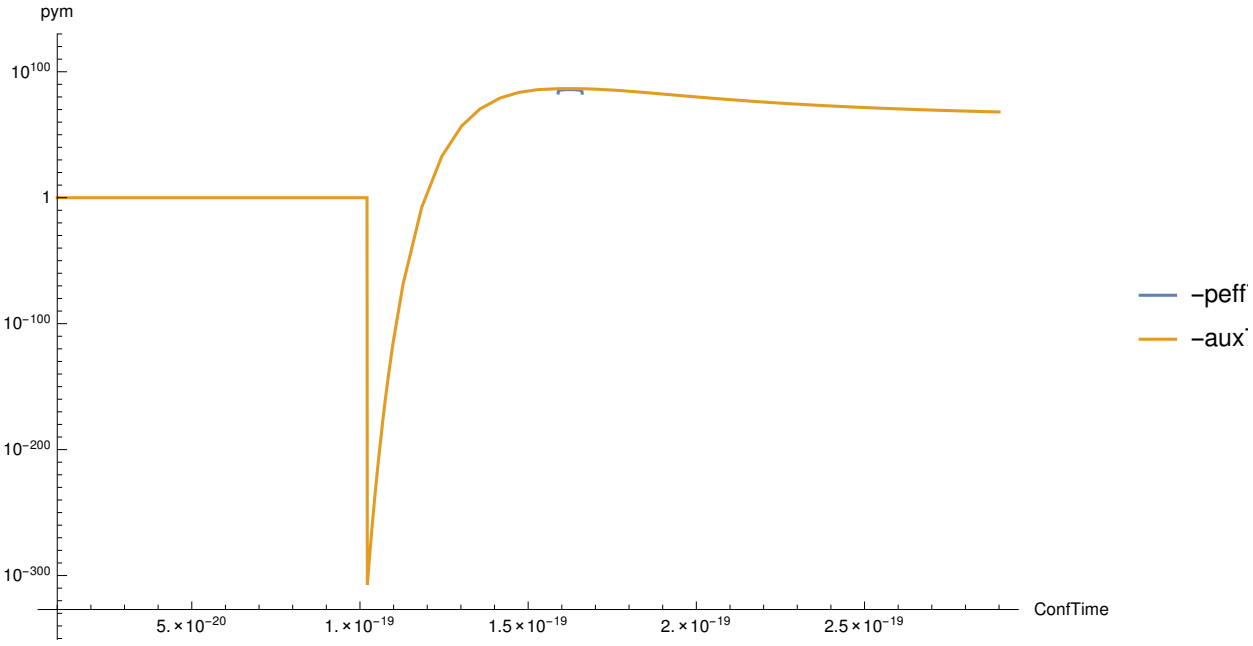

```
LogPlot[{-aux7[e7[conf2], f27[conf2]], -aux6[e6[conf2], f26[conf2]]},
 {conf2, conf1, confmax2}, PlotLegends → "Expressions",
 AxesLabel → {ConfTime, pym}, AxesStyle → Black, ImageSize → Large, PlotRange → All]
```

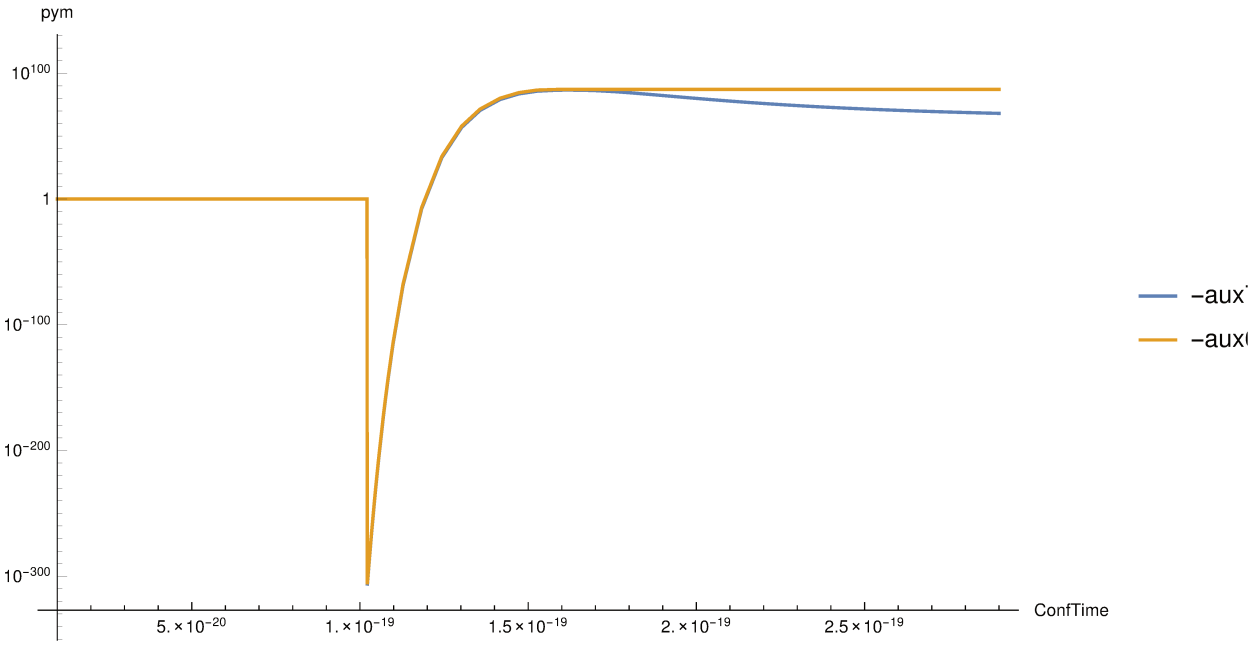


```
ClearAll[a8, e8, f28, s8]

peff8[e8_, f28_] :=
 pym[e8] - 3 * g8[e8] * f28 * Sqrt[2 * cn * e8 / (f28^2 + k)] * (e8^(3 / 4)) + e8 / 3
diff8[e8_, f28_] := (e8 - 3 * peff8[e8, f28]) * ((f28^2 + k) / (2 * e8)) - k - f28^2
diffe8[e8_, f28_] := -3 * (e8 + peff8[e8, f28]) * f28

g8[e_] := C18 * Exp[-C2 * (e / ec - 1)^2 / 2]

C18 = 10^(-2);

s8 = NDSolve[{f28'[conf2] == diff8[e8[conf2], f28[conf2]],
    e8'[conf2] == diffe8[e8[conf2], f28[conf2]], f28[conf2] == a8'[conf2] / a8[conf2],
    a8[conf1] == a01, f28[conf1] == f01, e8[conf1] == er1},
   {f28[conf2], e8[conf2], a8[conf2]}, {conf2, conf1, confmax}, Method → {Shooting}]
```

NDSolve::ndsz :
At conf2 == 11335.16812174941`, step size is effectively zero; singularity or stiff system suspected. ≫

```
{{f28[conf2] → InterpolatingFunction[ ⟨Domain: {{1.×10^-20, 1.13×10^4}}, Output: scalar⟩ ][conf2],
  e8[conf2] → InterpolatingFunction[ ⟨Domain: {{1.×10^-20, 1.13×10^4}}, Output: scalar⟩ ][conf2],
  a8[conf2] → InterpolatingFunction[ ⟨Domain: {{1.×10^-20, 1.13×10^4}}, Output: scalar⟩ ][conf2]}}
```

```
a8[conf2_] = a8[conf2] /. s8[[1]]
```

```
InterpolatingFunction[ Domain: {{1.×10^-20, 1.13×10^4}}
                       Output: scalar ][conf2]
```

```
e8[conf2_] = e8[conf2] /. s8[[1]]
```

```
InterpolatingFunction[ Domain: {{1.×10^-20, 1.13×10^4}}
                       Output: scalar ][conf2]
```

```
f28[conf2_] = f28[conf2] /. s8[[1]]
```

```
InterpolatingFunction[ Domain: {{1.×10^-20, 1.13×10^4}}
                       Output: scalar ][conf2]
```

```
N8 = Log[a8[1.13 * 10^(4)] / a8[conf1]]
```

```
59.2532
```

```
LogPlot[{pym[e8[conf2]], peff8[e8[conf2], f28[conf2]], e8[conf2] / 3},
 {conf2, conf1, 3.2 * 10^(-19)}, PlotLegends → "Expressions",
 AxesLabel → {ConfTime, pym}, AxesStyle → Black, ImageSize → Large, PlotRange → All]
```

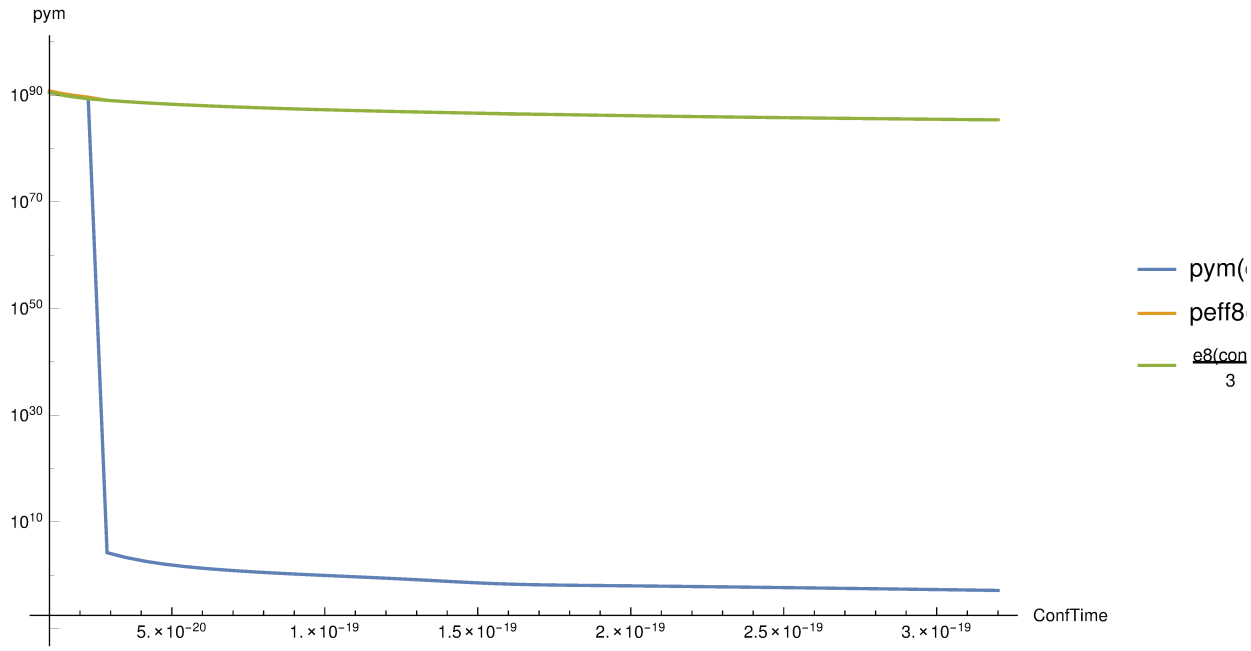


```
ClearAll[a9, e9, f29, s9]
```

```
peff9[e9_, f29_] :=
 pym[e9] - 3 * g9[e9] * f29 * Sqrt[2 * cn * e9 / (f29^2 + k)] * (e9^(3 / 4)) + e9 / 3
diff9[e9_, f29_] := (e9 - 3 * peff9[e9, f29]) * ((f29^2 + k) / (2 * e9)) - k - f29^2
diffe9[e9_, f29_] := -3 * (e9 + peff9[e9, f29]) * f29
```

```
g9[e_] := C19 * Exp[-C2 * (e / ec - 1)^2 / 2]
```

```
C19 = 10^(-3);
```

```
s9 = NDSolve[{f29'[conf2] == diff9[e9[conf2], f29[conf2]],
    e9'[conf2] == diffe9[e9[conf2], f29[conf2]], f29[conf2] == a9'[conf2]/a9[conf2],
    a9[conf1] == a01, f29[conf1] == f01, e9[conf1] == er1},
   {f29[conf2], e9[conf2], a9[conf2]}, {conf2, conf1, confmax}, Method → {Shooting}]
```

NDSolve::ndsz :
At conf2 == 11354.965101854486`, step size is effectively zero; singularity or stiff system suspected. »

```
{{f29[conf2] → InterpolatingFunction[ ⟨Domain: {{1.×10^-20, 11400.}}  Output: scalar⟩ ][conf2],
  e9[conf2] → InterpolatingFunction[ ⟨Domain: {{1.×10^-20, 11400.}}  Output: scalar⟩ ][conf2],
  a9[conf2] → InterpolatingFunction[ ⟨Domain: {{1.×10^-20, 11400.}}  Output: scalar⟩ ][conf2]}}
```

```
a9[conf2_] = a9[conf2] /. s9[[1]]
```

```
InterpolatingFunction[ ⟨Domain: {{1.×10^-20, 11400.}}  Output: scalar⟩ ][conf2]
```

```
e9[conf2_] = e9[conf2] /. s9[[1]]
```

```
InterpolatingFunction[ ⟨Domain: {{1.×10^-20, 11400.}}  Output: scalar⟩ ][conf2]
```

```
f29[conf2_] = f29[conf2] /. s9[[1]]
```

```
InterpolatingFunction[ ⟨Domain: {{1.×10^-20, 11400.}}  Output: scalar⟩ ][conf2]
```

```
N9 = Log[a9[1.13 * 10^(4)]/a9[conf1]]
```

```
58.8067
```

```
LogPlot[{peff9[e9[conf2], f29[conf2]],
  peff8[e8[conf2], f28[conf2]], peff7[e7[conf2], f27[conf2]],
  peff6[e6[conf2], f26[conf2]], peff5[e5[conf2], f25[conf2]],
  peff4[e4[conf2], f24[conf2]], peff3[e3[conf2], f23[conf2]],
  peff2[e2[conf2], f22[conf2]], peff[e[conf2], f2[conf2]]},
 {conf2, conf1, confmax2}, PlotLegends → SwatchLegend[
   {C1, C12, C13, C14, C15, C16, C17, C18, C19}, LegendLabel → "B=100, A="],
 AxesLabel → {ConfTime, Log[PEff]}, AxesStyle → Black, ImageSize → Large]
```

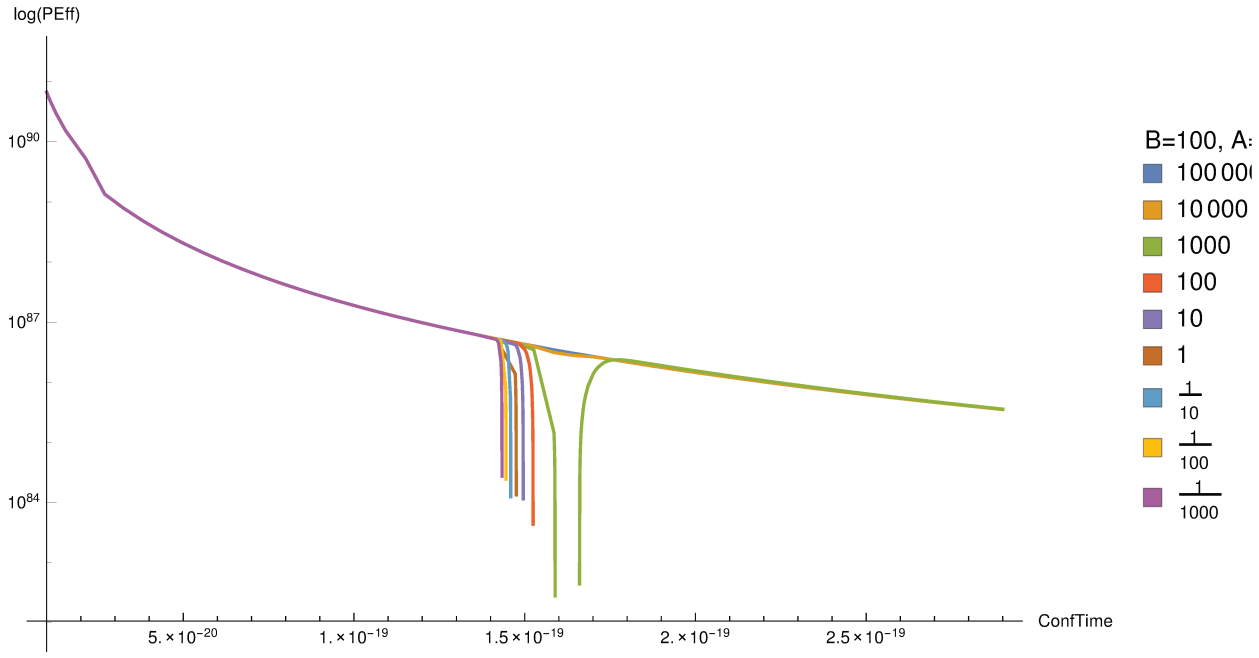


```
(*Export["peff.PDF",%]*)
```

```
(*:O*)
```

```
LogLogPlot[{e9[conf2] / ec, e8[conf2] / ec, e7[conf2] / ec, e6[conf2] / ec,
  e5[conf2] / ec, e4[conf2] / ec, e3[conf2] / ec, e2[conf2] / ec, e[conf2] / ec},
 {conf2, conf1, confmax2}, PlotLegends → SwatchLegend[
   {C1, C12, C13, C14, C15, C16, C17, C18, C19}, LegendLabel → "B=100, A="],
 AxesLabel → {Log[ConfTime], Log[Energy / Ec]}, AxesStyle → Black, ImageSize → Large]
```

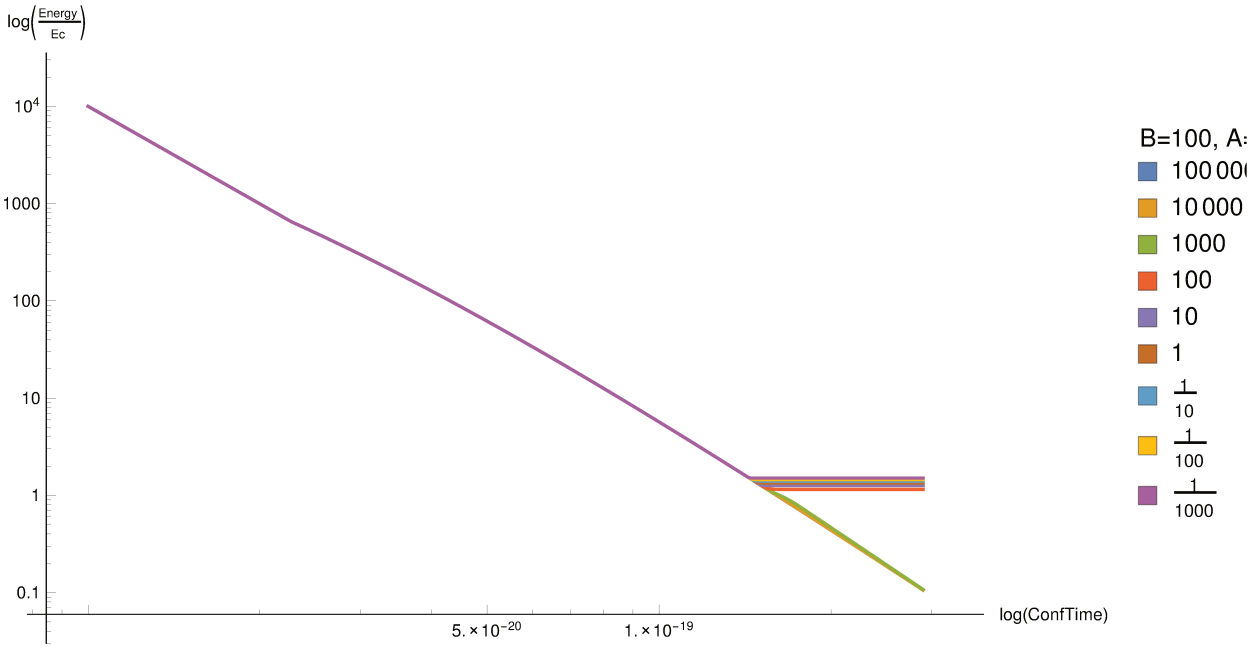


```
(*Export["e.PDF",%]*)
```

```
ParametricPlot[{{Log[peff[e[conf2], f2[conf2]]], Log[e[conf2] / ec]},
   {Log[peff2[e2[conf2], f22[conf2]]], Log[e2[conf2] / ec]},
   {Log[peff3[e3[conf2], f23[conf2]]], Log[e3[conf2] / ec]},
   {Log[peff4[e4[conf2], f24[conf2]]], Log[e4[conf2] / ec]},
   {Log[peff5[e5[conf2], f25[conf2]]], Log[e5[conf2] / ec]},
   {Log[peff6[e6[conf2], f26[conf2]]], Log[e6[conf2] / ec]},
   {Log[peff7[e7[conf2], f27[conf2]]], Log[e7[conf2] / ec]},
   {Log[peff8[e8[conf2], f28[conf2]]], Log[e8[conf2] / ec]},
   {Log[peff9[e9[conf2], f29[conf2]]], Log[e9[conf2] / ec]}},
  {conf2, conf1, confmax2}, PlotRange → All, AxesLabel → {Log[peff], Log[Energy / Ec]},
  PlotLegends → SwatchLegend[{C1, C12, C13, C14, C15, C16, C17, C18, C19},
    LegendLabel → "B=100, A="], AxesStyle → Black, ImageSize → Large]
```

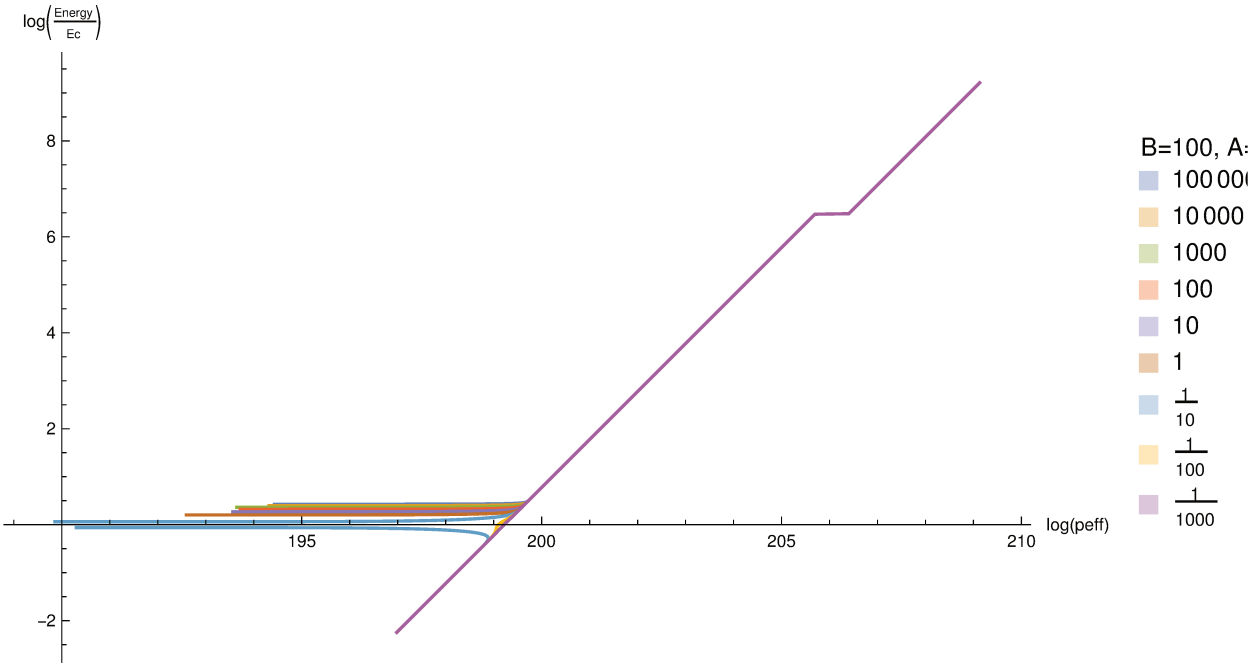


```
(*Export["ExPeff.PDF",%]*)

Nym = {N1, N2, N3, N4, N5, N6, N7, N8, N9};
Amp = {C1, C12, C13, C14, C15, C16, C17, C18, C19};
LAmp = Log10[Amp];
Do[
    Sow[
     Flatten[ReplacePart[{a, b}, {1 → Take[LAmp, {u}], 2 → Take[Nym, {u}]
       }]

     ]],
    {u, 1, Length[Nym], 1}
   ] // Reap // Last;
merged = %[[1]];

ColorList = {Blue, Blue, Blue, Blue, Blue, Blue, Green, Blue, Blue};
```

```
bList = {#} & /@ merged
```

```
{{{5, 8.6966}}, {{4, 7.42975}}, {{3, 7.5012}}, {{2, 8.33762}}, {{1, 10.0623}},
 {{0, 7.64595}}, {{-1, 58.3699}}, {{-2, 59.2532}}, {{-3, 58.8067}}}
```

```
ListPlot[bList, AxesLabel → {Log[Ampl], NEfolds},
 AxesStyle → Black, PlotStyle → ColorList, ImageSize → Large]
```

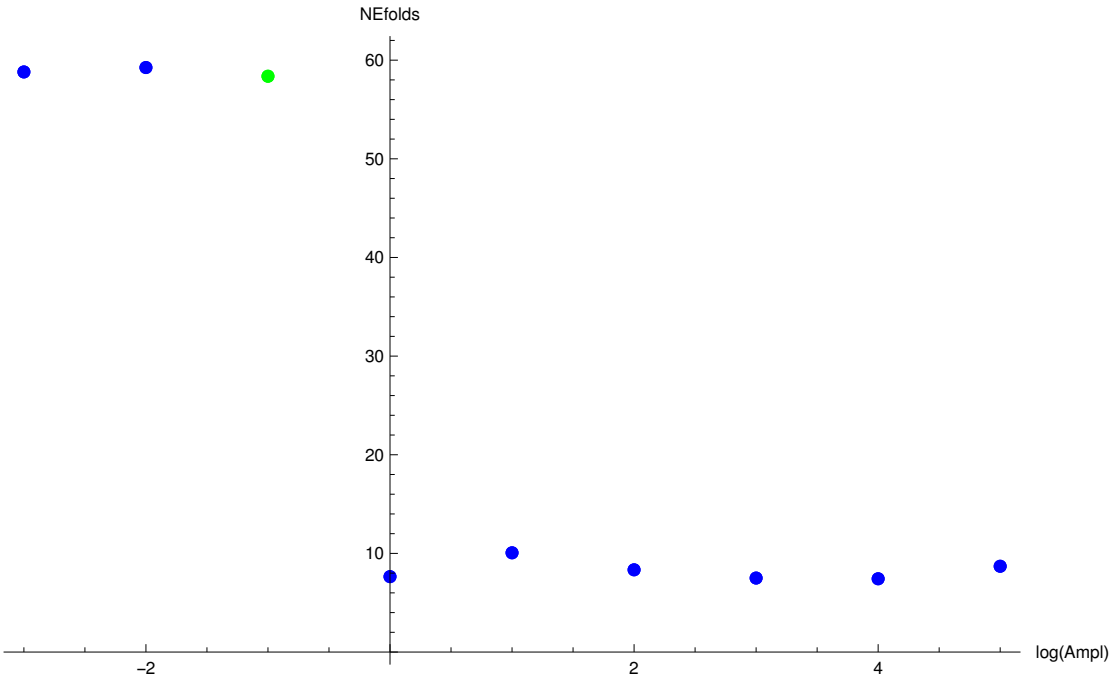


```
Export["N1.pdf", %]
```

```
N1.pdf
```

```
(*contar tempo q fica negativa a pressao e esperar power law=
 linha reta num gráfico loglog*)

(*variar amplitude ao redor do ponto A=10^3*)

(*endireitar casos k=1 e k=-1, dimensões e condições iniciais*)
```

```
(*graph w multiple lines changing B*)

ClearAll[a, conf1, confmax, a01, f01, g, pym, e, elarge, steplarge,
 peff, diff, diffe, cn, er1, ec, k, confmax2, Nym, C1, C2, merged, s,
 N1, f2, g2, peff2, diff2, diffe2, g3, peff3, diff3, diffe3, g4, peff4,
 diff4, diffe4, g5, peff5, diff5, diffe5, g6, peff6, diff6, diffe6, g7,
 peff7, diff7, diffe7, g8, peff8, diff8, diffe8, g9, peff9, diff9, diffe9]

k = 0; (*dimensionless*)
conf1 = 10^(-20);(*MeV^(-1)*)
a01 = (10^(-58))^(2 / 3); (*dimensionless*)
f01 = (2 / 3) * 10^(20); (*MeV*)

g[e_] := C1 * Exp[-C2 * (e / ec - 1)^2 / 2]
elarge = 650 * ec;
steplarge[e1_] := (1 + Tanh[e1 / ec]) / 2

pym[e_] := (-0.0701780768934142` + 0.012829768279227724` (e/ec)^2.10542207822587` +
      (0.0016223939423977366` (e/ec)^2.2` - 1.1874523382499435`*^-6 e^4/ec^4 +
         0.018853186484192017` e/ec) Tanh[0.12809510086441414` (0.45` - e/ec)] -
      0.10893510953199945` Tanh[1.0802023944400028` (-0.71` + e/ec)] +
      (1.6557877362105378` + 0.3864140819569308` (e/ec)^0.3`)
       Tanh[0.05613355687245168` (-0.01` + e/ec)]) *
    steplarge[elarge - e] + (e / 3) * steplarge[e - elarge]

peff[e_, f_] := pym[e] - 3 * g[e] * f * Sqrt[2 * cn * e / (f^2 + k)] * (e^(3 / 4)) + e / 3
diff[e_, f_] := (e - 3 * peff[e, f]) * ((f^2 + k) / (2 * e)) - k - f^2
diffe[e_, f_] := -3 * (e + peff[e, f]) * f

cn = ((4 N[Pi] * (0.000670861 * 10^(-41))) / 3); (*MeV^(-2)*)
er1 = 10^(91);
confmax = 10^15;

(*set of parameters we change*)

ec = er1 * 10^(-4);

C1 = 10^(2);

confmax2 = 2.9 * 10^(-19);

C2 = 10^(5);
```

```
s = NDSolve[
   {f2'[conf2] == diff[e[conf2], f2[conf2]], e'[conf2] == diffe[e[conf2], f2[conf2]],
    f2[conf2] == a'[conf2] / a[conf2], a[conf1] == a01, f2[conf1] == f01, e[conf1] == er1},
   {f2[conf2], e[conf2], a[conf2]}, {conf2, conf1, confmax}, Method → {Shooting}]
```

NDSolve::ndsz :
At conf2 == 11357.123406873614`, step size is effectively zero; singularity or stiff system suspected. >>

```
{{f2[conf2] → InterpolatingFunction[ 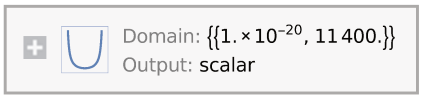 ][conf2],
  e[conf2] → InterpolatingFunction[ 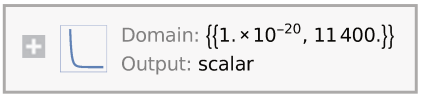 ][conf2],
  a[conf2] → InterpolatingFunction[ 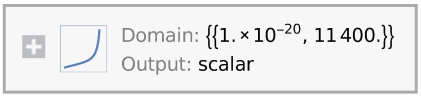 ][conf2]}}
```



```
a[conf2_] = a[conf2] /. s[[1]]
```

```
InterpolatingFunction[ 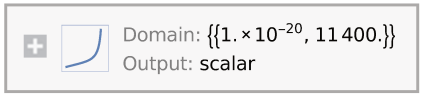 ][conf2]
```



```
e[conf2_] = e[conf2] /. s[[1]]
```

```
InterpolatingFunction[ 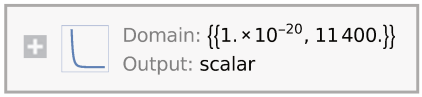 ][conf2]
```



```
f2[conf2_] = f2[conf2] /. s[[1]]
```

```
InterpolatingFunction[ 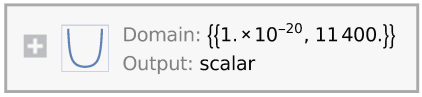 ][conf2]
```

```
Plot[{pym[e[conf2]], Log[peff[e[conf2], f2[conf2]]], Log[e[conf2] / 3]},
 {conf2, conf1, 1.1 * 10^4}, PlotLegends → "Expressions",
 AxesLabel → {ConfTime, pym}, AxesStyle → Black, ImageSize → Large, PlotRange → All]
```

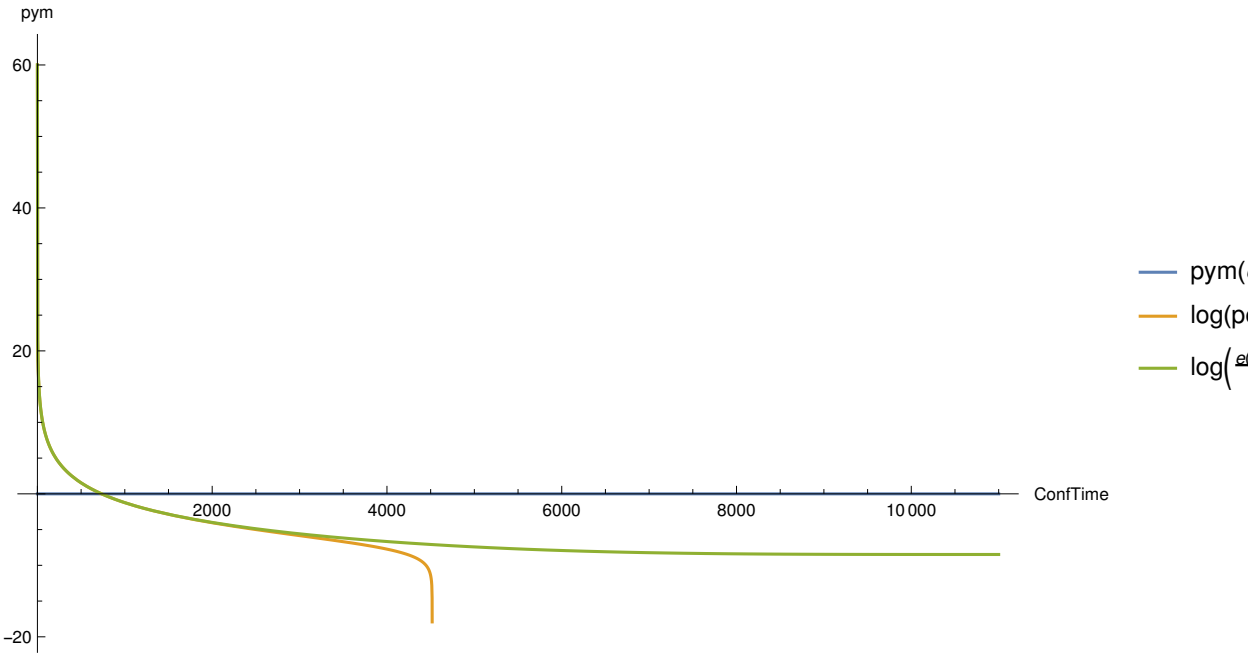


```
g2[e_] := C1 * Exp[-C22 * (e / ec - 1)^2 / 2]

peff2[e2_, f22_] :=
 pym[e2] - 3 * g2[e2] * f22 * Sqrt[2 * cn * e2 / (f22^2 + k)] * (e2^(3 / 4)) + e2 / 3
diff2[e2_, f22_] := (e2 - 3 * peff2[e2, f22]) * ((f22^2 + k) / (2 * e2)) - k - f22^2
diffe2[e2_, f22_] := -3 * (e2 + peff2[e2, f22]) * f22

C22 = 10^4;

ClearAll[a2, e2, f22, s2]
```

```
s2 = NDSolve[{f22'[conf2] == diff2[e2[conf2], f22[conf2]],
    e2'[conf2] == diffe2[e2[conf2], f22[conf2]], f22[conf2] == a2'[conf2] / a2[conf2],
    a2[conf1] == a01, f22[conf1] == f01, e2[conf1] == er1},
   {f22[conf2], e2[conf2], a2[conf2]}, {conf2, conf1, confmax}, Method → {Shooting}]
```

NDSolve::ndsz :
At conf2 == 3.297375020781971`*^-19, step size is effectively zero; singularity or stiff system suspected. >>

```
{{f22[conf2] → InterpolatingFunction[ 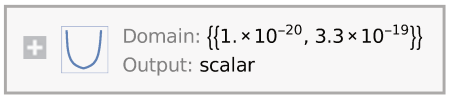 ][conf2],
  e2[conf2] → InterpolatingFunction[ 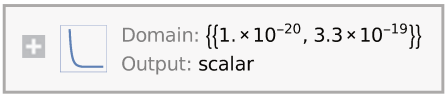 ][conf2],
  a2[conf2] → InterpolatingFunction[ 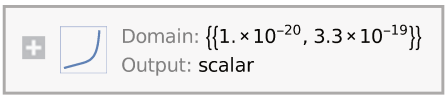 ][conf2]}}
```



```
a2[conf2_] = a2[conf2] /. s2[[1]]
```

```
InterpolatingFunction[ 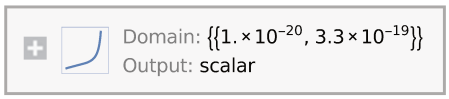 ][conf2]
```



```
e2[conf2_] = e2[conf2] /. s2[[1]]
```

```
InterpolatingFunction[ 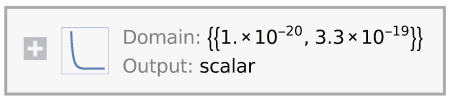 ][conf2]
```



```
f22[conf2_] = f22[conf2] /. s2[[1]]
```

```
InterpolatingFunction[ 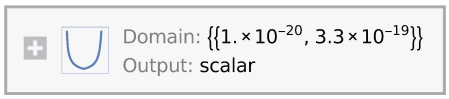 ][conf2]
```

```
Plot[{pym[e2[conf2]], peff2[e2[conf2], f22[conf2]], e2[conf2] / 3},
 {conf2, conf1, 3.2 * 10^(-19)}, PlotLegends → "Expressions",
 AxesLabel → {ConfTime, pym}, AxesStyle → Black, ImageSize → Large]
```

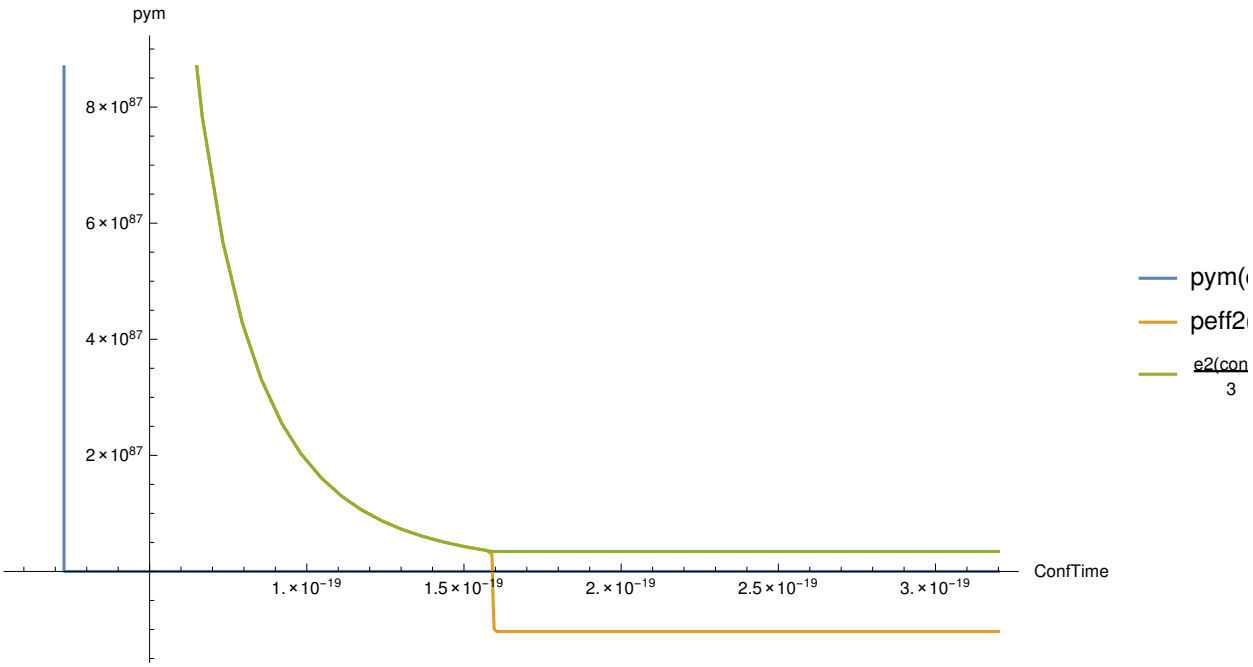


```
peff3[e3_, f23_] :=
 pym[e3] - 3 * g3[e3] * f23 * Sqrt[2 * cn * e3 / (f23^2 + k)] * (e3^(3 / 4)) + e3 / 3
diff3[e3_, f23_] := (e3 - 3 * peff3[e3, f23]) * ((f23^2 + k) / (2 * e3)) - k - f23^2
diffe3[e3_, f23_] := -3 * (e3 + peff3[e3, f23]) * f23
```

```
g3[e_] := C1 * Exp[-C23 * (e / ec - 1)^2 / 2]
```

```
C23 = 10^3;
```

```
ClearAll[a3, e3, f23, s3]
```

```
s3 = NDSolve[{f23'[conf2] == diff3[e3[conf2], f23[conf2]],
    e3'[conf2] == diffe3[e3[conf2], f23[conf2]], f23[conf2] == a3'[conf2] / a3[conf2],
    a3[conf1] == a01, f23[conf1] == f01, e3[conf1] == er1},
   {f23[conf2], e3[conf2], a3[conf2]}, {conf2, conf1, confmax}, Method → {Shooting}]
```

NDSolve::ndsz :
At conf2 == 3.2394828304398226`*^-19, step size is effectively zero; singularity or stiff system suspected. >>

```
{{f23[conf2] → InterpolatingFunction[ ⟨Domain: {{1.×10^-20, 3.24×10^-19}}, Output: scalar⟩ ][conf2],
  e3[conf2] → InterpolatingFunction[ ⟨Domain: {{1.×10^-20, 3.24×10^-19}}, Output: scalar⟩ ][conf2],
  a3[conf2] → InterpolatingFunction[ ⟨Domain: {{1.×10^-20, 3.24×10^-19}}, Output: scalar⟩ ][conf2]}}
```

```
a3[conf2_] = a3[conf2] /. s3[[1]]
```

```
InterpolatingFunction[ ⟨Domain: {{1.×10^-20, 3.24×10^-19}}, Output: scalar⟩ ][conf2]
```

```
e3[conf2_] = e3[conf2] /. s3[[1]]
```

```
InterpolatingFunction[ ⟨Domain: {{1.×10^-20, 3.24×10^-19}}, Output: scalar⟩ ][conf2]
```

```
f23[conf2_] = f23[conf2] /. s3[[1]]
```

```
InterpolatingFunction[ ⟨Domain: {{1.×10^-20, 3.24×10^-19}}, Output: scalar⟩ ][conf2]
```

```
Plot[{pym[e3[conf2]], peff3[e3[conf2], f23[conf2]], e3[conf2] / 3},
 {conf2, conf1, 3.2 * 10^(-19)}, PlotLegends → "Expressions",
 AxesLabel → {ConfTime, pym}, AxesStyle → Black, ImageSize → Large]
```

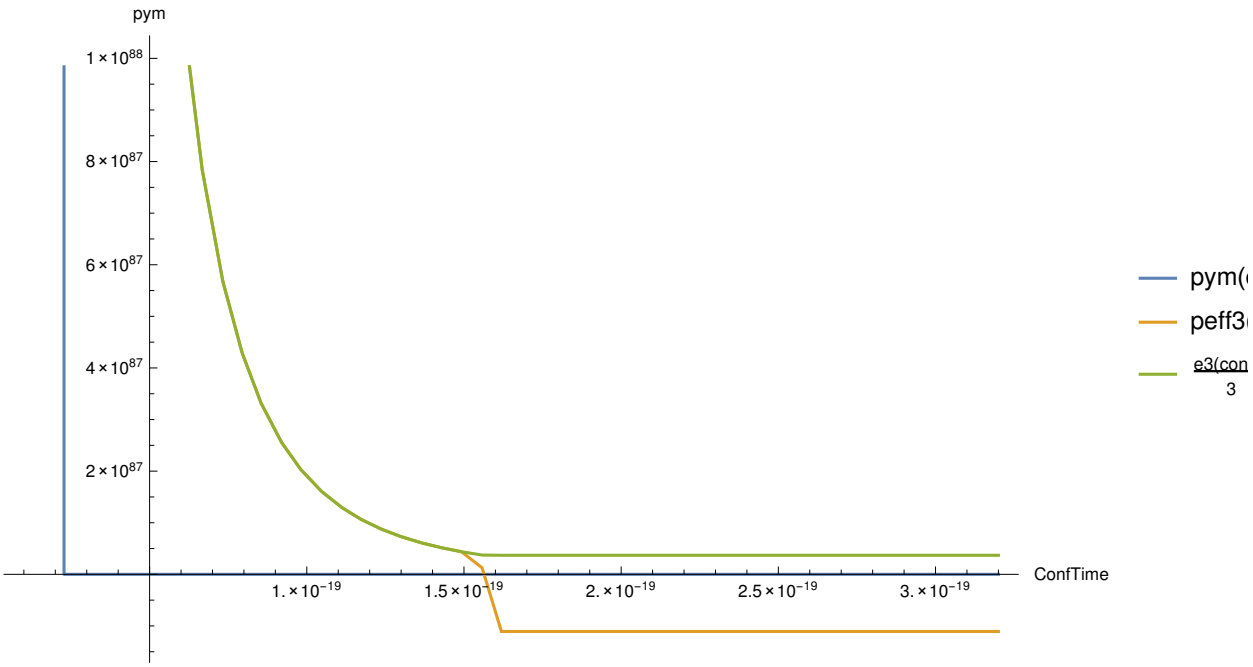


```
peff4[e4_, f24_] :=
 pym[e4] - 3 * g4[e4] * f24 * Sqrt[2 * cn * e4 / (f24^2 + k)] * (e4^(3 / 4)) + e4 / 3
diff4[e4_, f24_] := (e4 - 3 * peff4[e4, f24]) * ((f24^2 + k) / (2 * e4)) - k - f24^2
diffe4[e4_, f24_] := -3 * (e4 + peff4[e4, f24]) * f24
```

```
g4[e_] := C1 * Exp[-C24 * (e / ec - 1)^2 / 2]
```

```
C24 = 10^2;
```

```
ClearAll[a4, e4, f24, s4]
```

```
s4 = NDSolve[{f24'[conf2] == diff4[e4[conf2], f24[conf2]],
    e4'[conf2] == diffe4[e4[conf2], f24[conf2]], f24[conf2] == a4'[conf2] / a4[conf2],
    a4[conf1] == a01, f24[conf1] == f01, e4[conf1] == er1},
   {f24[conf2], e4[conf2], a4[conf2]}, {conf2, conf1, confmax}, Method → {Shooting}]
```

NDSolve::ndsz :
At conf2 == 3.083101487109392`*^-19, step size is effectively zero; singularity or stiff system suspected. >>

```
{{f24[conf2] → InterpolatingFunction[ ⟨Domain: {{1.×10^-20, 3.08×10^-19}}, Output: scalar⟩ ][conf2],
  e4[conf2] → InterpolatingFunction[ ⟨Domain: {{1.×10^-20, 3.08×10^-19}}, Output: scalar⟩ ][conf2],
  a4[conf2] → InterpolatingFunction[ ⟨Domain: {{1.×10^-20, 3.08×10^-19}}, Output: scalar⟩ ][conf2]}}
```

```
a4[conf2_] = a4[conf2] /. s4[[1]]
```

```
InterpolatingFunction[ ⟨Domain: {{1.×10^-20, 3.08×10^-19}}, Output: scalar⟩ ][conf2]
```

```
e4[conf2_] = e4[conf2] /. s4[[1]]
```

```
InterpolatingFunction[ ⟨Domain: {{1.×10^-20, 3.08×10^-19}}, Output: scalar⟩ ][conf2]
```

```
f24[conf2_] = f24[conf2] /. s4[[1]]
```

```
InterpolatingFunction[ ⟨Domain: {{1.×10^-20, 3.08×10^-19}}, Output: scalar⟩ ][conf2]
```

```
peff5[e5_, f25_] :=
 pym[e5] - 3 * g5[e5] * f25 * Sqrt[2 * cn * e5 / (f25^2 + k)] * (e5^(3 / 4)) + e5 / 3
diff5[e5_, f25_] := (e5 - 3 * peff5[e5, f25]) * ((f25^2 + k) / (2 * e5)) - k - f25^2
diffe5[e5_, f25_] := -3 * (e5 + peff5[e5, f25]) * f25

g5[e_] := C1 * Exp[-C25 * (e / ec - 1)^2 / 2]

C25 = 10^1;

ClearAll[a5, e5, f25, s5]
```

```
s5 = NDSolve[{f25'[conf2] == diff5[e5[conf2], f25[conf2]],
    e5'[conf2] == diffe5[e5[conf2], f25[conf2]], f25[conf2] == a5'[conf2] / a5[conf2],
    a5[conf1] == a01, f25[conf1] == f01, e5[conf1] == er1},
   {f25[conf2], e5[conf2], a5[conf2]}, {conf2, conf1, confmax}, Method → {Shooting}]
```

NDSolve::ndsz :
At conf2 == 2.7481865783328945`*^-19, step size is effectively zero; singularity or stiff system suspected. >>

```
{{f25[conf2] → InterpolatingFunction[ 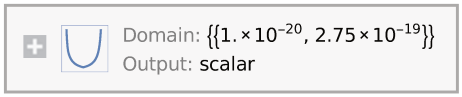

][conf2],

  e5[conf2] → InterpolatingFunction[ 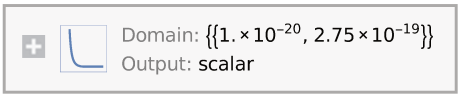

][conf2],

  a5[conf2] → InterpolatingFunction[ 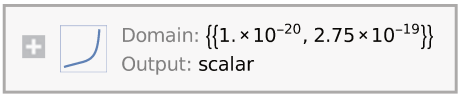

][conf2]}}
```

```
a5[conf2_] = a5[conf2] /. s5[[1]]
```

```
InterpolatingFunction[ 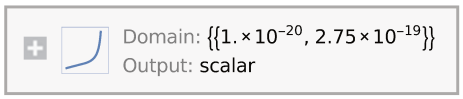

][conf2]
```

```
e5[conf2_] = e5[conf2] /. s5[[1]]
```

```
InterpolatingFunction[ 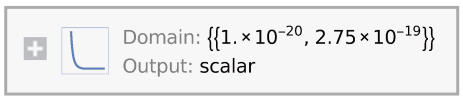

][conf2]
```

```
f25[conf2_] = f25[conf2] /. s5[[1]]
```

```
InterpolatingFunction[ 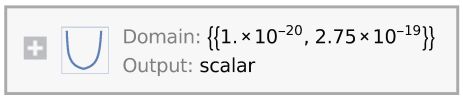

][conf2]
```

```
Plot[{peff5[e5[conf2], f25[conf2]], peff4[e4[conf2], f24[conf2]],
  peff3[e3[conf2], f23[conf2]], peff2[e2[conf2], f22[conf2]],
  peff[e[conf2], f2[conf2]]}, {conf2, conf1, 2.7 * 10^(-19)},
 PlotLegends → SwatchLegend[{C2, C22, C23, C24, C25}, LegendLabel → "A=100, B="],
 AxesLabel → {ConfTime, PEff}, AxesStyle → Black, ImageSize → Large]
```

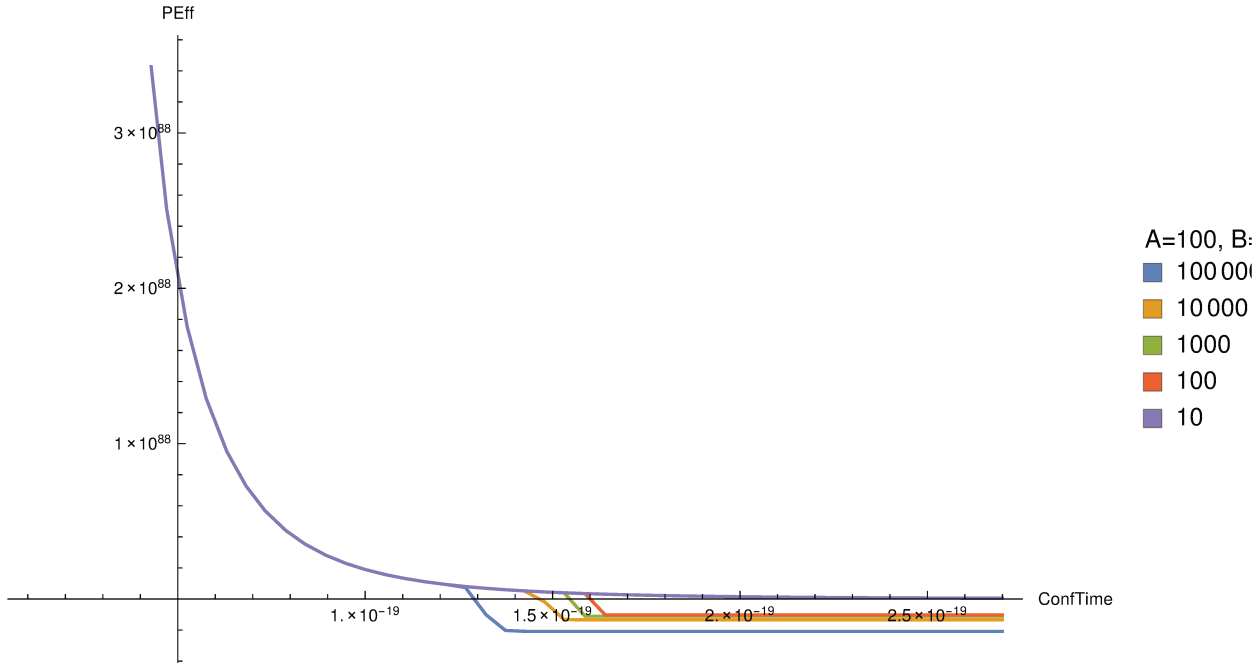


```
Plot[peff[e[conf2], f2[conf2]], {conf2, conf1, 1.1 * 10^4},
 PlotLegends → SwatchLegend[{C2}, LegendLabel → "A=100, B="],
 AxesLabel → {ConfTime, PEff}, AxesStyle → Black, ImageSize → Large]
```

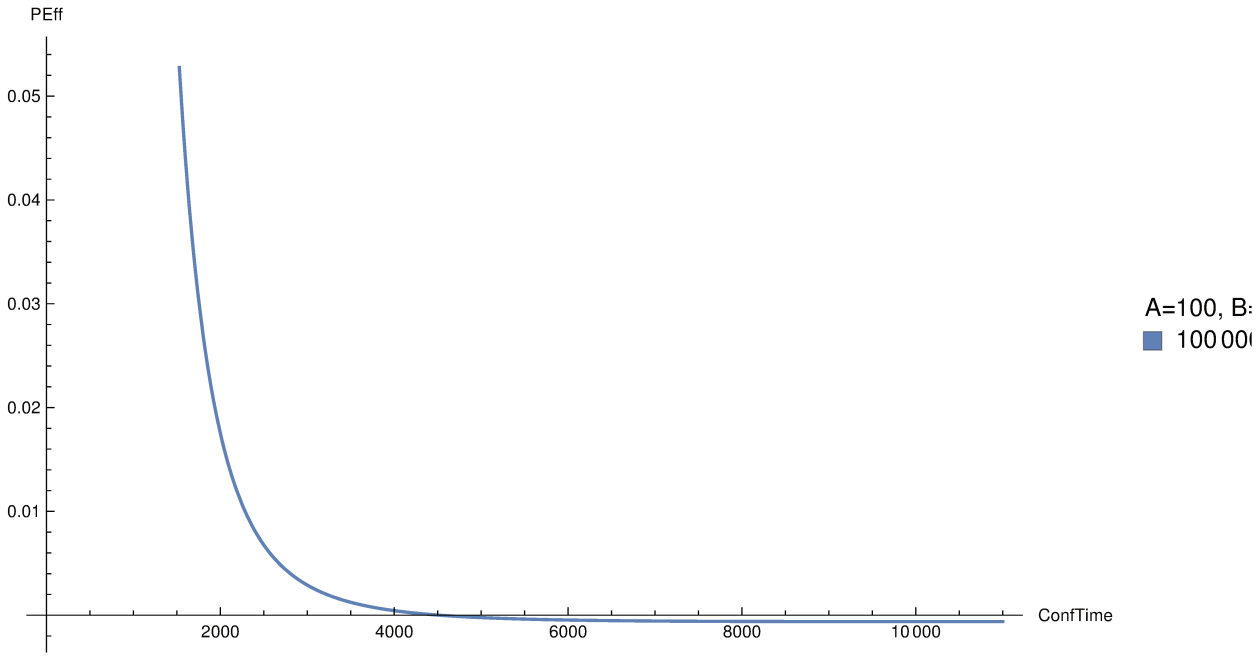

```
(*Export["peffIIa.PDF",%]*)
```

```
peff6[e6_, f26_] :=
 pym[e6] - 3 * g6[e6] * f26 * Sqrt[2 * cn * e6 / (f26^2 + k)] * (e6^(3 / 4)) + e6 / 3
diff6[e6_, f26_] := (e6 - 3 * peff6[e6, f26]) * ((f26^2 + k) / (2 * e6)) - k - f26^2
diffe6[e6_, f26_] := -3 * (e6 + peff6[e6, f26]) * f26
```

```
g6[e_] := C1 * Exp[-C26 * (e / ec - 1)^2 / 2]
```

```
C26 = 10^0;
```

```
ClearAll[a6, e6, f26, s6]
```

```
s6 = NDSolve[{f26'[conf2] == diff6[e6[conf2], f26[conf2]],
    e6'[conf2] == diffe6[e6[conf2], f26[conf2]], f26[conf2] == a6'[conf2] / a6[conf2],
    a6[conf1] == a01, f26[conf1] == f01, e6[conf1] == er1},
  {f26[conf2], e6[conf2], a6[conf2]}, {conf2, conf1, confmax}, Method → {Shooting}]
```

NDSolve::ndsz :
At conf2 == 2.248860607177961`*^-19, step size is effectively zero; singularity or stiff system suspected. >>

```
{{f26[conf2] → InterpolatingFunction[ ⟨Domain: {{1.×10^-20, 2.25×10^-19}}, Output: scalar⟩ ][conf2],
  e6[conf2] → InterpolatingFunction[ ⟨Domain: {{1.×10^-20, 2.25×10^-19}}, Output: scalar⟩ ][conf2],
  a6[conf2] → InterpolatingFunction[ ⟨Domain: {{1.×10^-20, 2.25×10^-19}}, Output: scalar⟩ ][conf2]}}
```

```
a6[conf2_] = a6[conf2] /. s6[[1]]
```

```
InterpolatingFunction[ ⟨Domain: {{1.×10^-20, 2.25×10^-19}}, Output: scalar⟩ ][conf2]
```

```
e6[conf2_] = e6[conf2] /. s6[[1]]
```

```
InterpolatingFunction[ ⟨Domain: {{1.×10^-20, 2.25×10^-19}}, Output: scalar⟩ ][conf2]
```

```
f26[conf2_] = f26[conf2] /. s6[[1]]
```

```
InterpolatingFunction[ ⟨Domain: {{1.×10^-20, 2.25×10^-19}}, Output: scalar⟩ ][conf2]
```

```
peff7[e7_, f27_] :=
 pym[e7] - 3 * g7[e7] * f27 * Sqrt[2 * cn * e7 / (f27^2 + k)] * (e7^(3 / 4)) + e7 / 3
diff7[e7_, f27_] := (e7 - 3 * peff7[e7, f27]) * ((f27^2 + k) / (2 * e7)) - k - f27^2
diffe7[e7_, f27_] := -3 * (e7 + peff7[e7, f27]) * f27
```

```
g7[e_] := C1 * Exp[-C27 * (e / ec - 1)^2 / 2]
```

```
C27 = 10^(-1);

ClearAll[a7, e7, f27, s7]

s7 = NDSolve[{f27'[conf2] == diff7[e7[conf2], f27[conf2]],
    e7'[conf2] == diffe7[e7[conf2], f27[conf2]], f27[conf2] == a7'[conf2] / a7[conf2],
    a7[conf1] == a01, f27[conf1] == f01, e7[conf1] == er1},
  {f27[conf2], e7[conf2], a7[conf2]}, {conf2, conf1, confmax}, Method → {Shooting}]
```

NDSolve::ndsz :
At conf2 == 1.7240538015877827`*^-19, step size is effectively zero; singularity or stiff system suspected. >>

```
{{f27[conf2] → InterpolatingFunction[ ⟨Domain: {{1.×10^-20, 1.72×10^-19}}, Output: scalar⟩ ][conf2],
  e7[conf2] → InterpolatingFunction[ ⟨Domain: {{1.×10^-20, 1.72×10^-19}}, Output: scalar⟩ ][conf2],
  a7[conf2] → InterpolatingFunction[ ⟨Domain: {{1.×10^-20, 1.72×10^-19}}, Output: scalar⟩ ][conf2]}}
```

```
a7[conf2_] = a7[conf2] /. s7[[1]]
```

```
InterpolatingFunction[ ⟨Domain: {{1.×10^-20, 1.72×10^-19}}, Output: scalar⟩ ][conf2]
```

```
e7[conf2_] = e7[conf2] /. s7[[1]]
```

```
InterpolatingFunction[ ⟨Domain: {{1.×10^-20, 1.72×10^-19}}, Output: scalar⟩ ][conf2]
```

```
f27[conf2_] = f27[conf2] /. s7[[1]]
```

```
InterpolatingFunction[ ⟨Domain: {{1.×10^-20, 1.72×10^-19}}, Output: scalar⟩ ][conf2]
```

```
ClearAll[a8, e8, f28, s8]

peff8[e8_, f28_] :=
 pym[e8] - 3 * g8[e8] * f28 * Sqrt[2 * cn * e8 / (f28^2 + k)] * (e8^(3 / 4)) + e8 / 3
diff8[e8_, f28_] := (e8 - 3 * peff8[e8, f28]) * ((f28^2 + k) / (2 * e8)) - k - f28^2
diffe8[e8_, f28_] := -3 * (e8 + peff8[e8, f28]) * f28

g8[e_] := C1 * Exp[-C28 * (e / ec - 1)^2 / 2]

C28 = 10^(-2);

confmax2 = 9.2 * 10^(-20);
```

```
s8 = NDSolve[{f28'[conf2] == diff8[e8[conf2], f28[conf2]],
    e8'[conf2] == diffe8[e8[conf2], f28[conf2]], f28[conf2] == a8'[conf2] / a8[conf2],
    a8[conf1] == a01, f28[conf1] == f01, e8[conf1] == er1},
   {f28[conf2], e8[conf2], a8[conf2]}, {conf2, conf1, confmax}, Method → {Shooting}]
```

NDSolve::ndsz :
At conf2 == 1.2770637838439793`*^-19, step size is effectively zero; singularity or stiff system suspected. >>

```
{{f28[conf2] → InterpolatingFunction[ 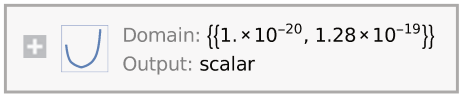 ][conf2],
  e8[conf2] → InterpolatingFunction[ 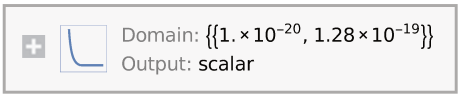 ][conf2],
  a8[conf2] → InterpolatingFunction[ 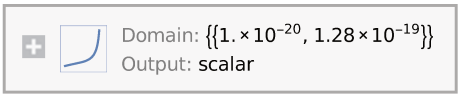 ][conf2]}}
```



```
a8[conf2_] = a8[conf2] /. s8[[1]]
```

```
InterpolatingFunction[ 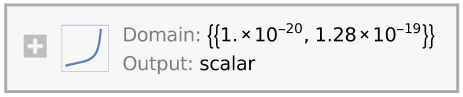 ][conf2]
```



```
e8[conf2_] = e8[conf2] /. s8[[1]]
```

```
InterpolatingFunction[ 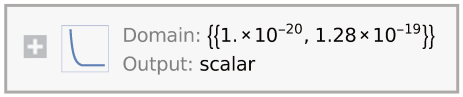 ][conf2]
```



```
f28[conf2_] = f28[conf2] /. s8[[1]]
```

```
InterpolatingFunction[ 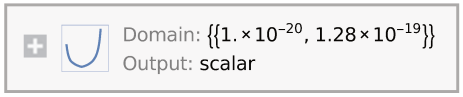 ][conf2]
```



```
ClearAll[a9, e9, f29, s9]

peff9[e9_, f29_] :=
 pym[e9] - 3 * g9[e9] * f29 * Sqrt[2 * cn * e9 / (f29^2 + k)] * (e9^(3 / 4)) + e9 / 3
diff9[e9_, f29_] := (e9 - 3 * peff9[e9, f29]) * ((f29^2 + k) / (2 * e9)) - k - f29^2
diffe9[e9_, f29_] := -3 * (e9 + peff9[e9, f29]) * f29

g9[e_] := C1 * Exp[-C29 * (e / ec - 1)^2 / 2]

C29 = 10^(-3);
```

```
s9 = NDSolve[{f29'[conf2] == diff9[e9[conf2], f29[conf2]],
    e9'[conf2] == diffe9[e9[conf2], f29[conf2]], f29[conf2] == a9'[conf2] / a9[conf2],
    a9[conf1] == a01, f29[conf1] == f01, e9[conf1] == er1},
   {f29[conf2], e9[conf2], a9[conf2]}, {conf2, conf1, confmax}, Method → {Shooting}]
```

NDSolve::ndsz :
At conf2 == 9.285804278075301`*^-20, step size is effectively zero; singularity or stiff system suspected. >>

```
{{f29[conf2] → InterpolatingFunction[ ⟨Domain: {{1.×10^-20, 9.29×10^-20}}, Output: scalar⟩ ][conf2],
  e9[conf2] → InterpolatingFunction[ ⟨Domain: {{1.×10^-20, 9.29×10^-20}}, Output: scalar⟩ ][conf2],
  a9[conf2] → InterpolatingFunction[ ⟨Domain: {{1.×10^-20, 9.29×10^-20}}, Output: scalar⟩ ][conf2]}}
```

```
a9[conf2_] = a9[conf2] /. s9[[1]]
```

```
InterpolatingFunction[ ⟨Domain: {{1.×10^-20, 9.29×10^-20}}, Output: scalar⟩ ][conf2]
```

```
e9[conf2_] = e9[conf2] /. s9[[1]]
```

```
InterpolatingFunction[ ⟨Domain: {{1.×10^-20, 9.29×10^-20}}, Output: scalar⟩ ][conf2]
```

```
f29[conf2_] = f29[conf2] /. s9[[1]]
```

```
InterpolatingFunction[ ⟨Domain: {{1.×10^-20, 9.29×10^-20}}, Output: scalar⟩ ][conf2]
```

```
aux9[e9_, f29_] := -3 * g9[e9] * f29 * Sqrt[2 * cn * e9 / (f29^2 + k)] * (e9^(3 / 4))
```

```
Plot[{peff9[e9[conf2], f29[conf2]],
  pym[e9[conf2]], e9[conf2] / 3, aux9[e9[conf2], f29[conf2]]},
 {conf2, conf1, 9.28 * 10^(-20)}, PlotLegends → "Expressions",
 AxesLabel → {ConfTime, PEff}, AxesStyle → Black, ImageSize → Large]
```

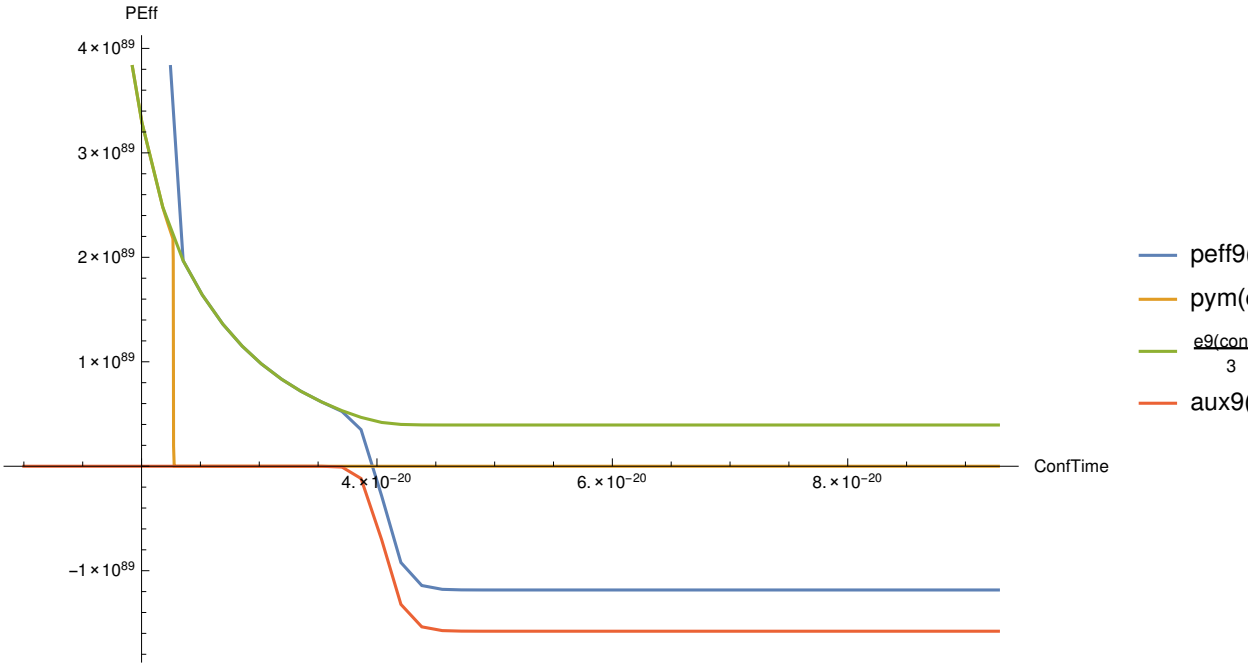


```
LogPlot[{-peff9[e9[conf2], f29[conf2]], -aux9[e9[conf2], f29[conf2]]},
 {conf2, conf1, 9.28 * 10^(-20)}, PlotLegends → "Expressions",
 AxesLabel → {ConfTime, PEff}, AxesStyle → Black, ImageSize → Large]
```

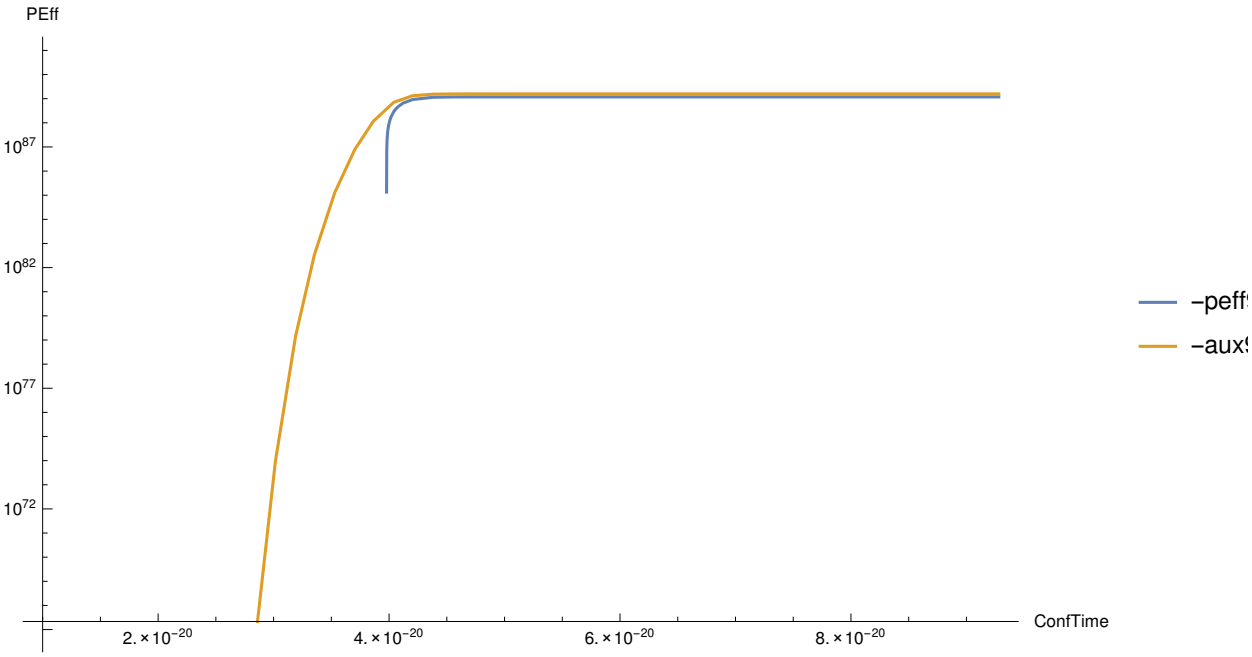

```
Plot[{peff6[e6[conf2], f26[conf2]],
  peff7[e7[conf2], f27[conf2]], peff8[e8[conf2], f28[conf2]],
  peff9[e9[conf2], f29[conf2]]}, {conf2, conf1, 9 * 10^(-20)},
 PlotLegends → SwatchLegend[{C26, C27, C28, C29}, LegendLabel → "A=100, B="],
 AxesLabel → {ConfTime, PEff}, AxesStyle → Black, ImageSize → Large]
```

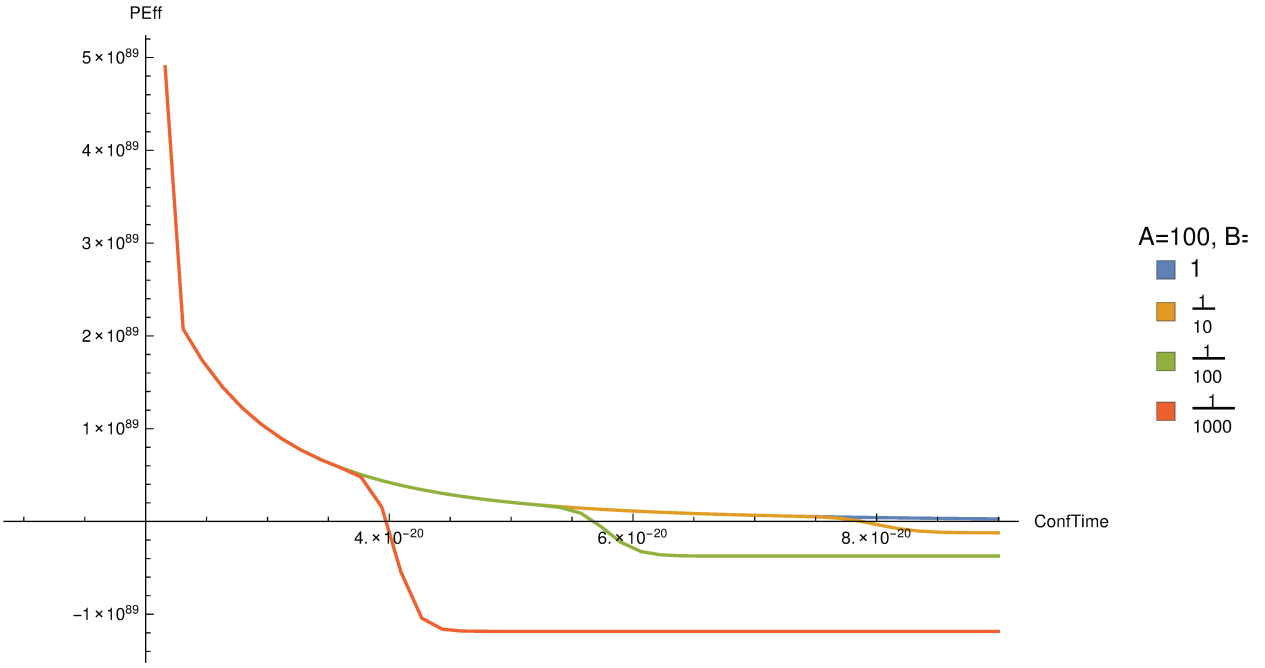


```
(*Export["peffIIb.PDF",%]*)

(*:O*)
```

```
LogPlot[{e5[conf2] / ec, e4[conf2] / ec, e3[conf2] / ec, e2[conf2] / ec, e[conf2] / ec},
 {conf2, conf1, 2.7 * 10^(-19)},
 PlotLegends → SwatchLegend[{C2, C22, C23, C24, C25}, LegendLabel → "A=100, B="],
 AxesLabel → {ConfTime, Log[Energy / Ec]}, AxesStyle → Black, ImageSize → Large]
```

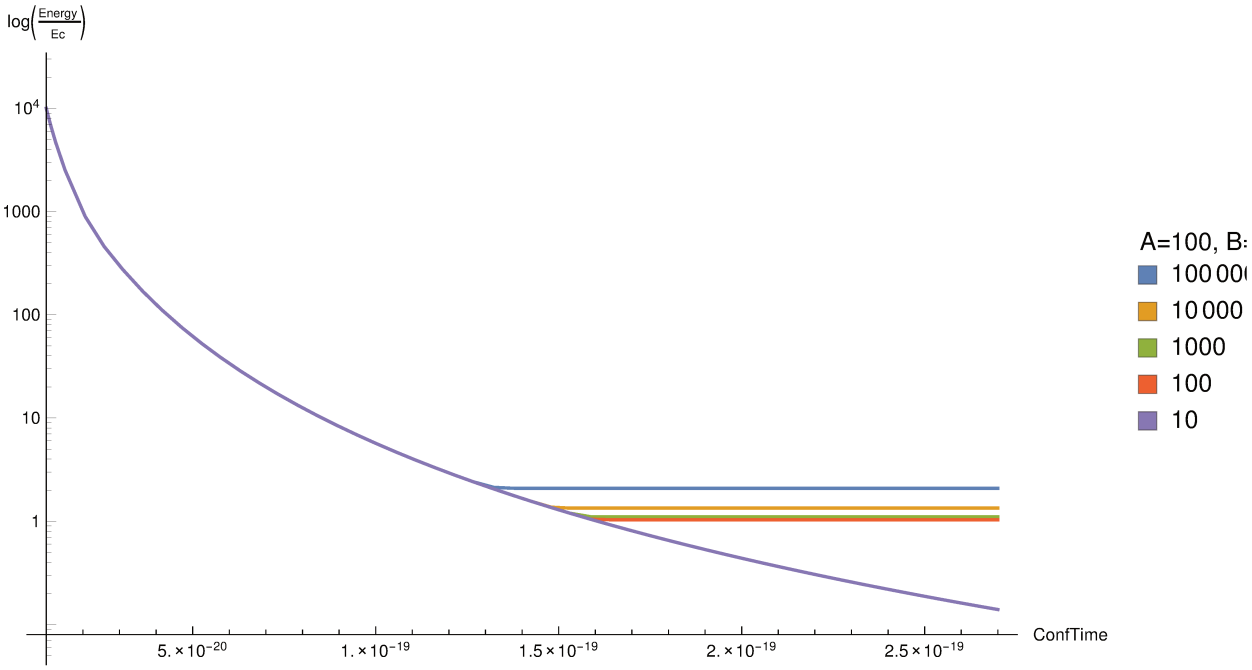


```
(*Export["EnergyIIa.PDF",%]*)
```

```
LogPlot[{e9[conf2] / ec, e8[conf2] / ec, e7[conf2] / ec, e6[conf2] / ec},
 {conf2, conf1, 9 * 10^(-20)},
 PlotLegends → SwatchLegend[{C26, C27, C28, C29}, LegendLabel → "A=100, B="],
 AxesLabel → {ConfTime, Log[Energy / Ec]}, AxesStyle → Black, ImageSize → Large]
```

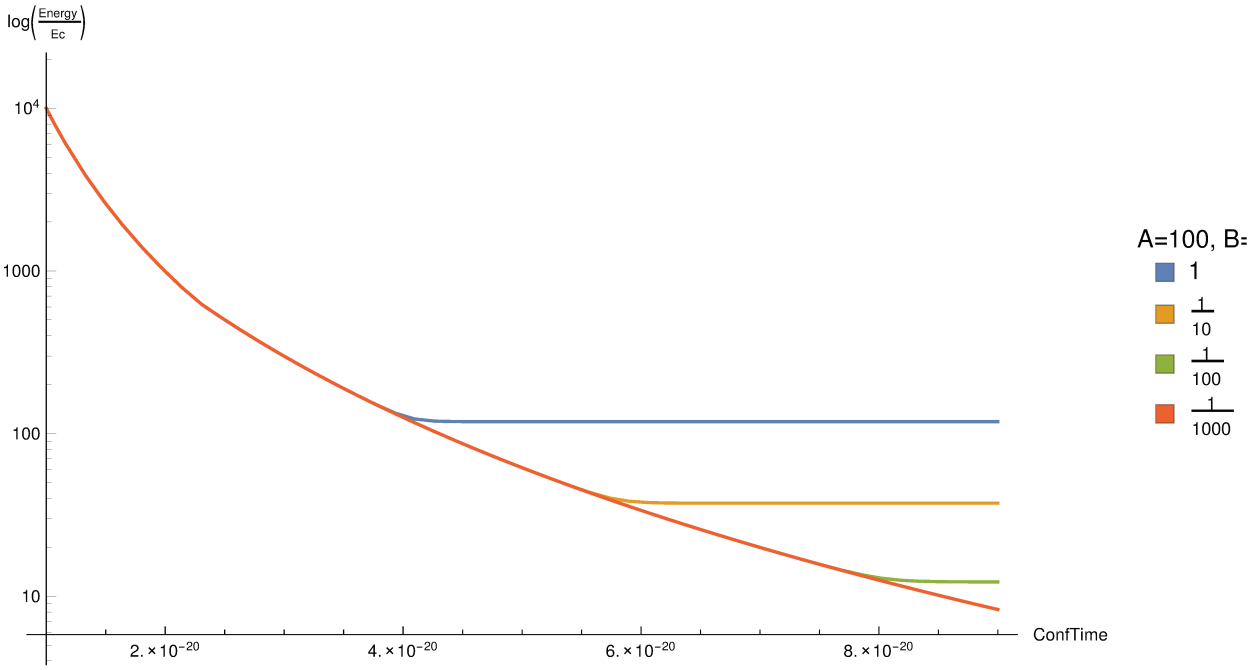


```
(*Export["EnergyIIb.PDF",%]*)
```

```
ParametricPlot[{{Log[peff[e[conf2], f2[conf2]]], Log[e[conf2] / ec]},
  {Log[peff2[e2[conf2], f22[conf2]]], Log[e2[conf2] / ec]},
  {Log[peff3[e3[conf2], f23[conf2]]], Log[e3[conf2] / ec]},
  {Log[peff4[e4[conf2], f24[conf2]]], Log[e4[conf2] / ec]},
  {Log[peff5[e5[conf2], f25[conf2]]], Log[e5[conf2] / ec]}},
 {conf2, conf1, 2.7 * 10^(-19)}, PlotRange → All,
 AxesLabel → {Log[peff], Log[Energy / Ec]},
 PlotLegends → SwatchLegend[{C2, C22, C23, C24, C25}, LegendLabel → "A=100, B="],
 AxesStyle → Black, ImageSize → Large]
```

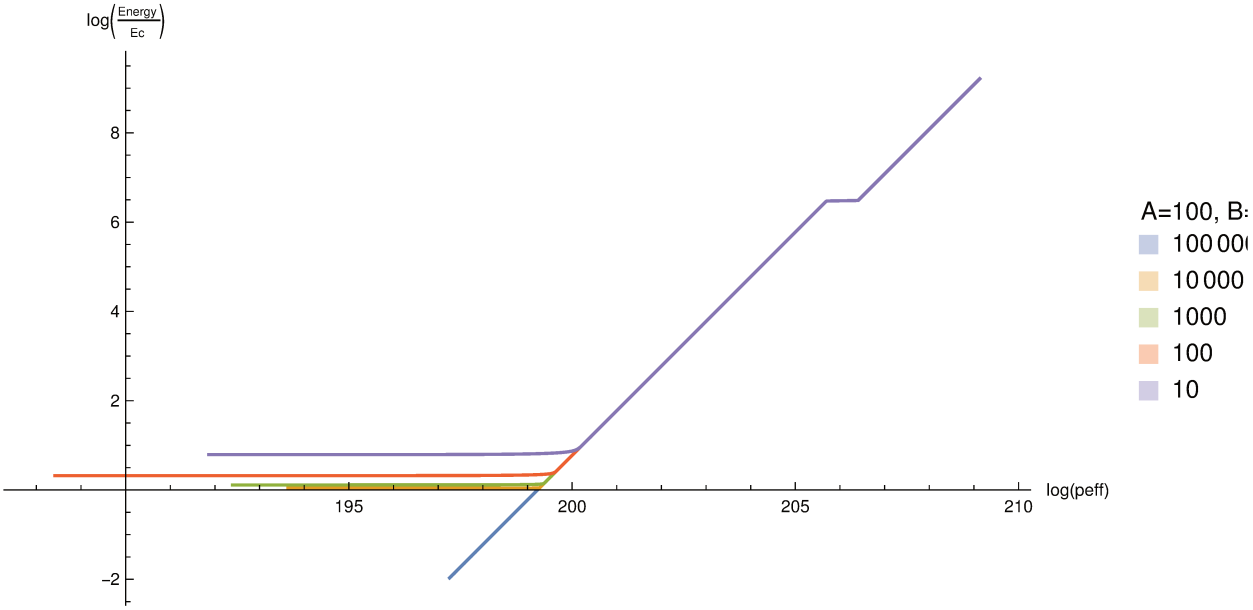


```
(*Export["ExPeffIIa.PDF",%]*)
```

```
ParametricPlot[{{Log[peff6[e6[conf2], f26[conf2]]], Log[e6[conf2] / ec]},
  {Log[peff7[e7[conf2], f27[conf2]]], Log[e7[conf2] / ec]},
  {Log[peff8[e8[conf2], f28[conf2]]], Log[e8[conf2] / ec]},
  {Log[peff9[e9[conf2], f29[conf2]]], Log[e9[conf2] / ec]}},
 {conf2, conf1, 9 * 10^(-20)}, PlotRange → All,
 AxesLabel → {Log[peff], Log[Energy / Ec]},
 PlotLegends → SwatchLegend[{C16, C17, C18, C19}, LegendLabel → "B=100, A="],
 AxesStyle → Black, ImageSize → Large]
```

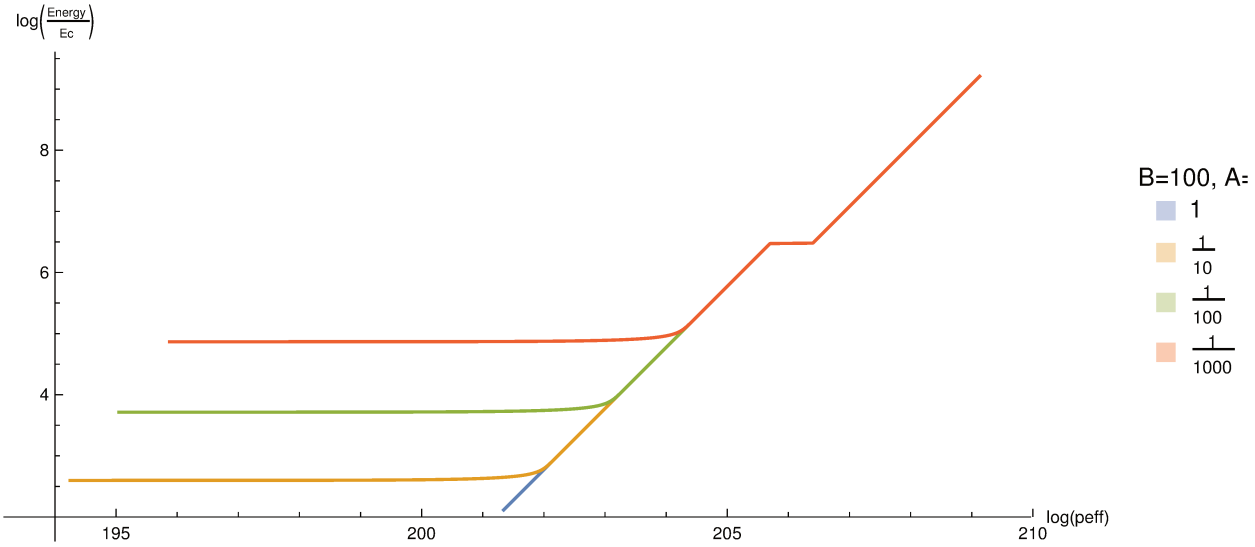


```
(*Export["ExPeffIIb.PDF",%]*)
```

```
N1 = Log[a[10^(4)] / a[conf1]]
```

```
55.5999
```

```
N2 = Log[a2[3.2 * 10^(-19)] / a2[conf1]]
```

```
5.02062
```

```
N3 = Log[a3[3.2 * 10^(-19)] / a3[conf1]]
```

```
5.88909
```

```
N4 = Log[a4[3 * 10^(-19)] / a4[conf1]]
```

```
5.04944
```

```
N5 = Log[a5[2.7 * 10^(-19)] / a5[conf1]]
```

```
5.37331
```

```
N6 = Log[a6[2.2 * 10^(-19)] / a6[conf1]]
```

```
4.97626
```

```
N7 = Log[a7[1.7 * 10^(-19)] / a7[conf1]]
```

```
5.18268
```

```
N8 = Log[a8[1.2 * 10^(-19)] / a8[conf1]]
```

```
3.46093
```

```
N9 = Log[a9[9.2 * 10^(-20)] / a9[conf1]]
```

```
5.07908
```

```
Nym = {N1, N2, N3, N4, N5, N6, N7, N8, N9};
Amp = {C2, C22, C23, C24, C25, C26, C27, C28, C29};
LAmp = Log10[Amp];
Do[
    Sow[
     Flatten[ReplacePart[{a, b}, {1 → Take[LAmp, {u}], 2 → Take[Nym, {u}]
       }]

     ]],
    {u, 1, Length[Nym], 1}
   ] // Reap // Last;
merged = %[[1]];
```

```
ListPlot[merged, AxesLabel → {Log[Ampl], NEfolds},
 AxesStyle → Black, ImageSize → Large, PlotRange → All]
```

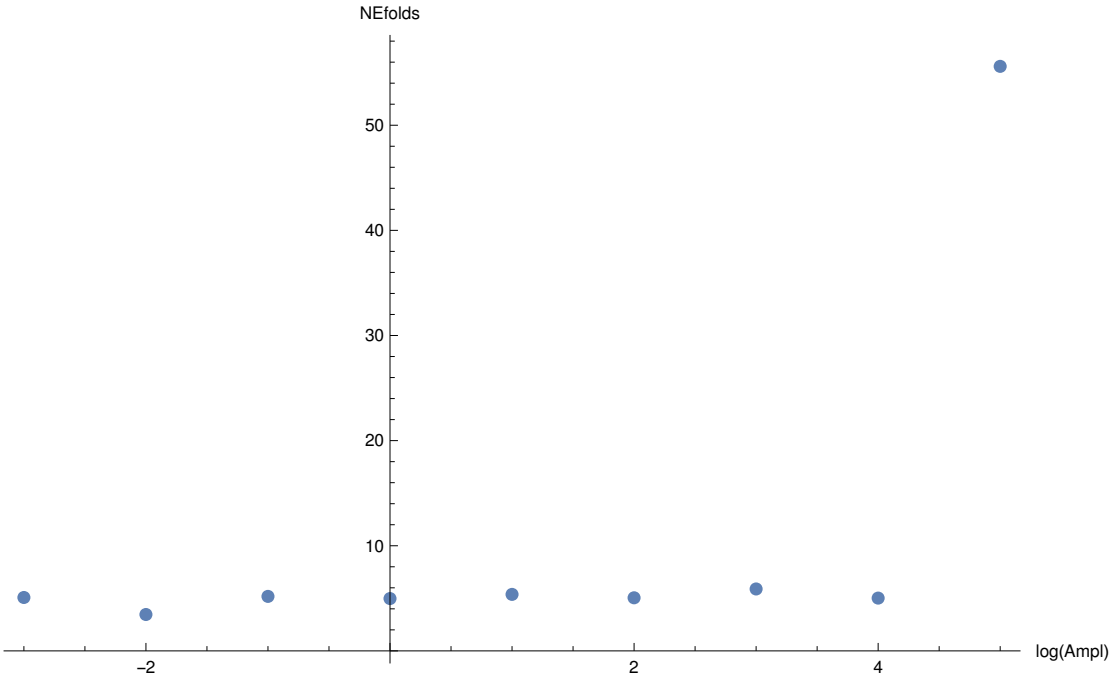


```
(*but no graceful exit*)
```

```
g10[e_] := C1 * Exp[-C210 * (e / ec - 1)^2 / 2]
```

```
peff10[e10_, f210_] :=
 pym[e10] - 3 * g10[e10] * f210 * Sqrt[2 * cn * e10 / (f210^2 + k)] * (e10^(3 / 4)) + e10 / 3
diff10[e10_, f210_] :=
 (e10 - 3 * peff10[e10, f210]) * ((f210^2 + k) / (2 * e10)) - k - f210^2
diffe10[e10_, f210_] := -3 * (e10 + peff10[e10, f210]) * f210
```

```
C210 = 10^6;
```

```
ClearAll[a10, e10, f210, s10]
```

```
s10 = NDSolve[{f210'[conf2] == diff10[e10[conf2], f210[conf2]],
    e10'[conf2] == diffe10[e10[conf2], f210[conf2]], f210[conf2] ==
     a10'[conf2] / a10[conf2], a10[conf1] == a01, f210[conf1] == f01, e10[conf1] == er1},
  {f210[conf2], e10[conf2], a10[conf2]}, {conf2, conf1, confmax}, Method → {Shooting}]
```

NDSolve::ndsz :
At conf2 == 11357.123406873614`, step size is effectively zero; singularity or stiff system suspected. ≫

```
{{f210[conf2] → InterpolatingFunction[ 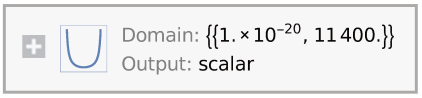 [conf2],
   e10[conf2] → InterpolatingFunction[ 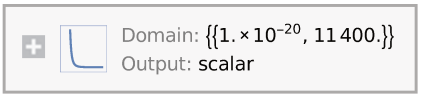 [conf2],
   a10[conf2] → InterpolatingFunction[ 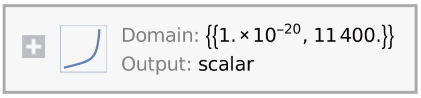 [conf2]}}
```



```
a10[conf2_] = a10[conf2] /. s10[[1]]
```

```
InterpolatingFunction[ 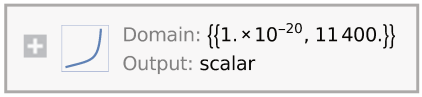 [conf2]
```



```
e10[conf2_] = e10[conf2] /. s10[[1]]
```

```
InterpolatingFunction[ 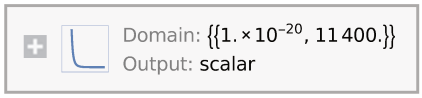 [conf2]
```



```
f210[conf2_] = f210[conf2] /. s10[[1]]
```

```
InterpolatingFunction[ 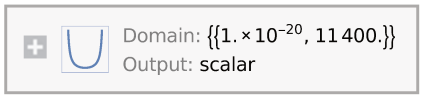 [conf2]
```

```
Plot[{pym[e10[conf2]], peff10[e10[conf2], f210[conf2]], e10[conf2] / 3},
 {conf2, conf1, 3.2 * 10^(-5)}, PlotLegends → "Expressions",
 AxesLabel → {ConfTime, pym}, AxesStyle → Black, ImageSize → Large]
```